

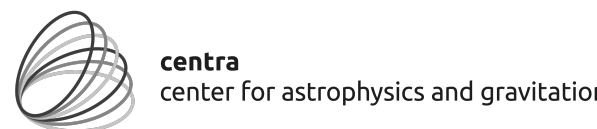


High-redshift simulations of IFS low-redshift galaxies

Status report within the CRISP WP5

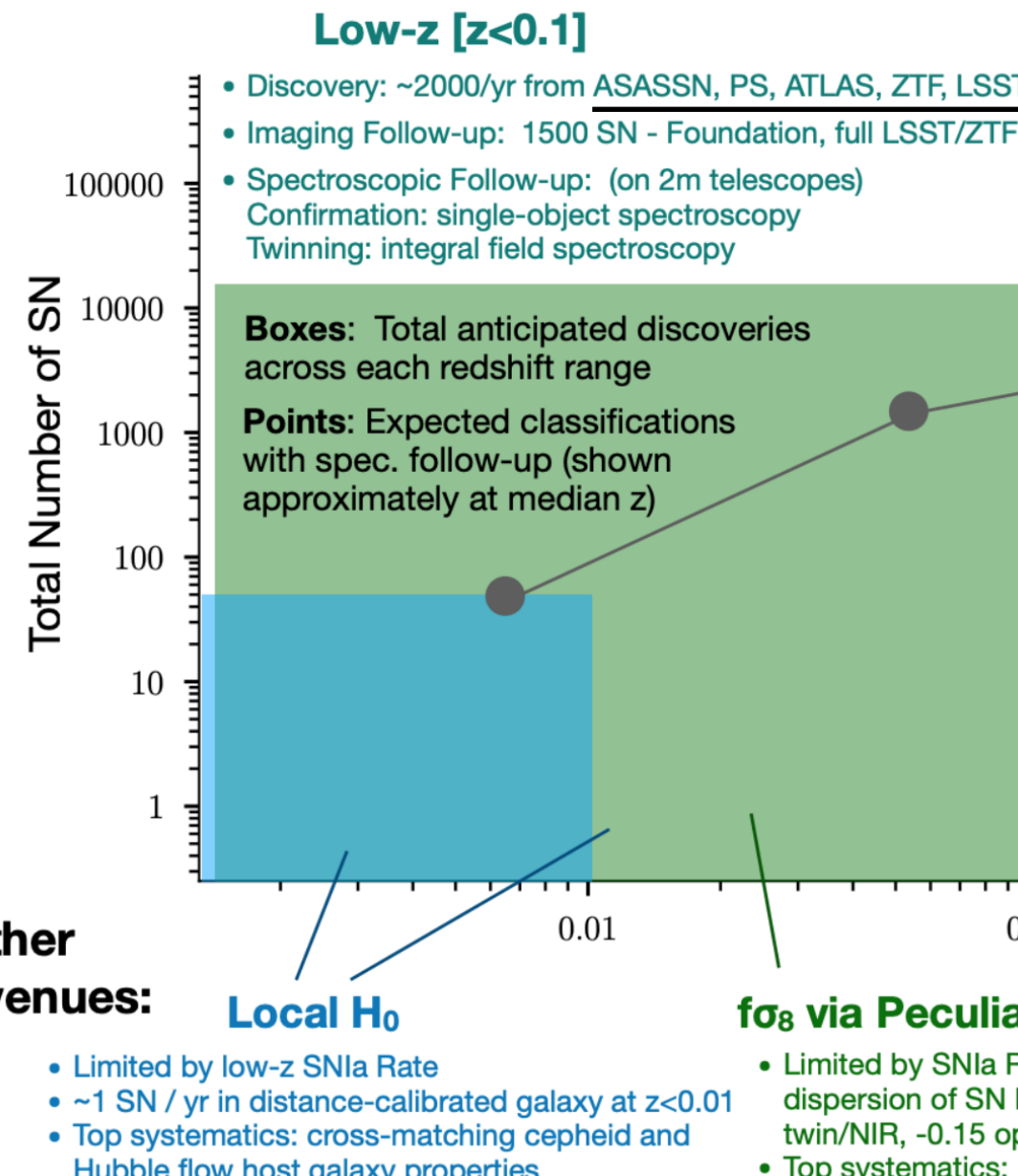
Ana Paulino-Afonso

Granada | January 29, 2020



SN Ia Cosmology

The next 10 years at a glance



Mid-z [$0.1 < z < 1$]

- Discovery + Imaging: >300,000 photometric, 6,000 spectroscopic from SDSS, SNLS, PS1, DES, LSST, WFIRST
- Spectroscopic Follow-up: multi-object spec. on 4-8m telescopes

H2030

High-z [$z > 1$]

- Discovery + Imaging: ~6,000 photometric, 1,000 spectroscopic from HST, JWST, WFIRST
- Spectroscopic Follow-up: JWST, WFIRST, 8m+, ELTs

Constraints on $w(z)$ from the SNIa Hubble diagram

- Top Systematics for measuring w:
- Calibration across wavelength range
 - Intrinsic scatter, Population Drifts
 - Classification

σ_8 via Weak Lensing

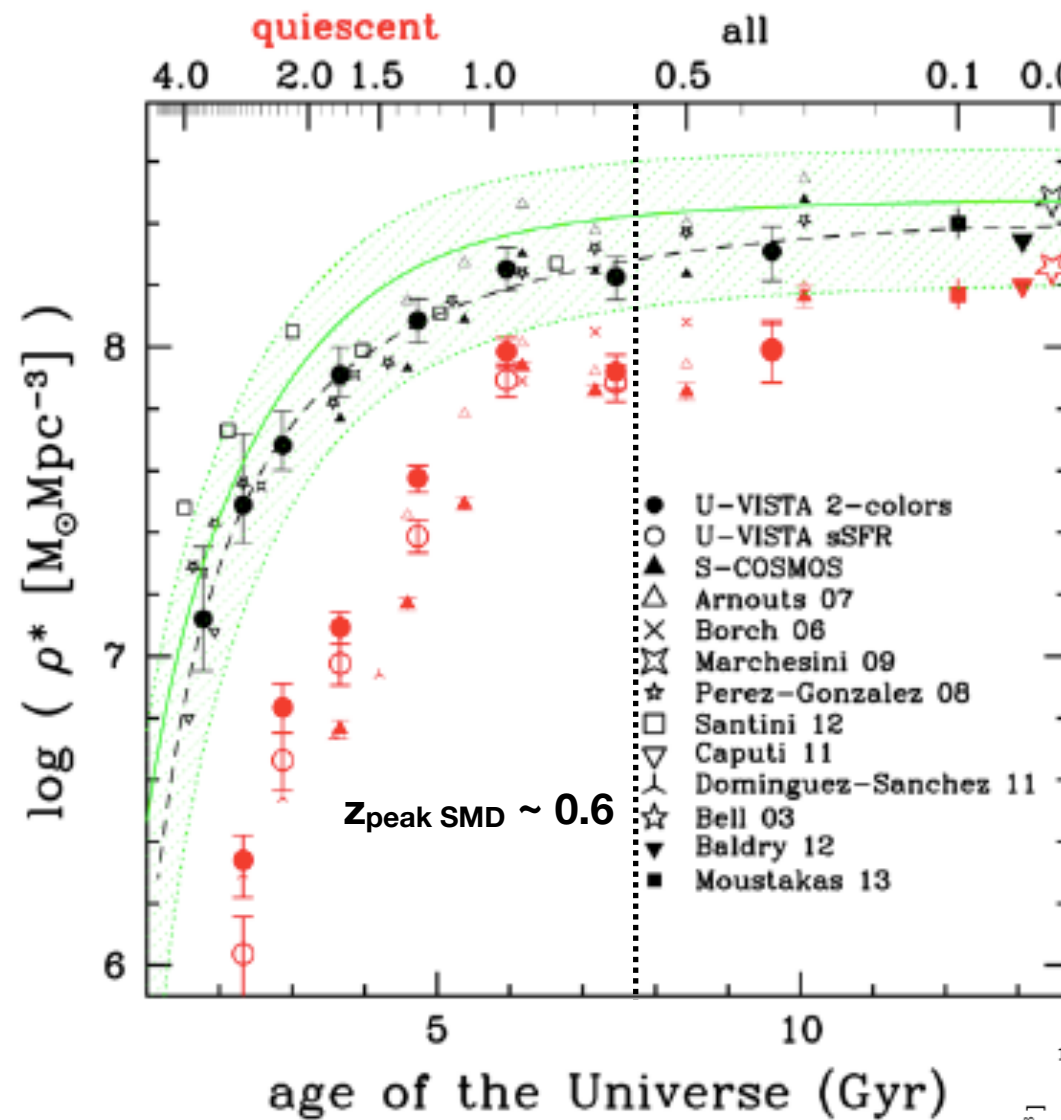
- Limited by max redshift of survey
- Signal goes with $\sim 0.05z$
- Top systematics: population drift, selection effects

Strong Lensing Time Delay Cosmography

- Limited by lensed SN discovery rates and follow-up
- Dedicated follow-up necessary
- Top systematics: microlensing, lens model systematics

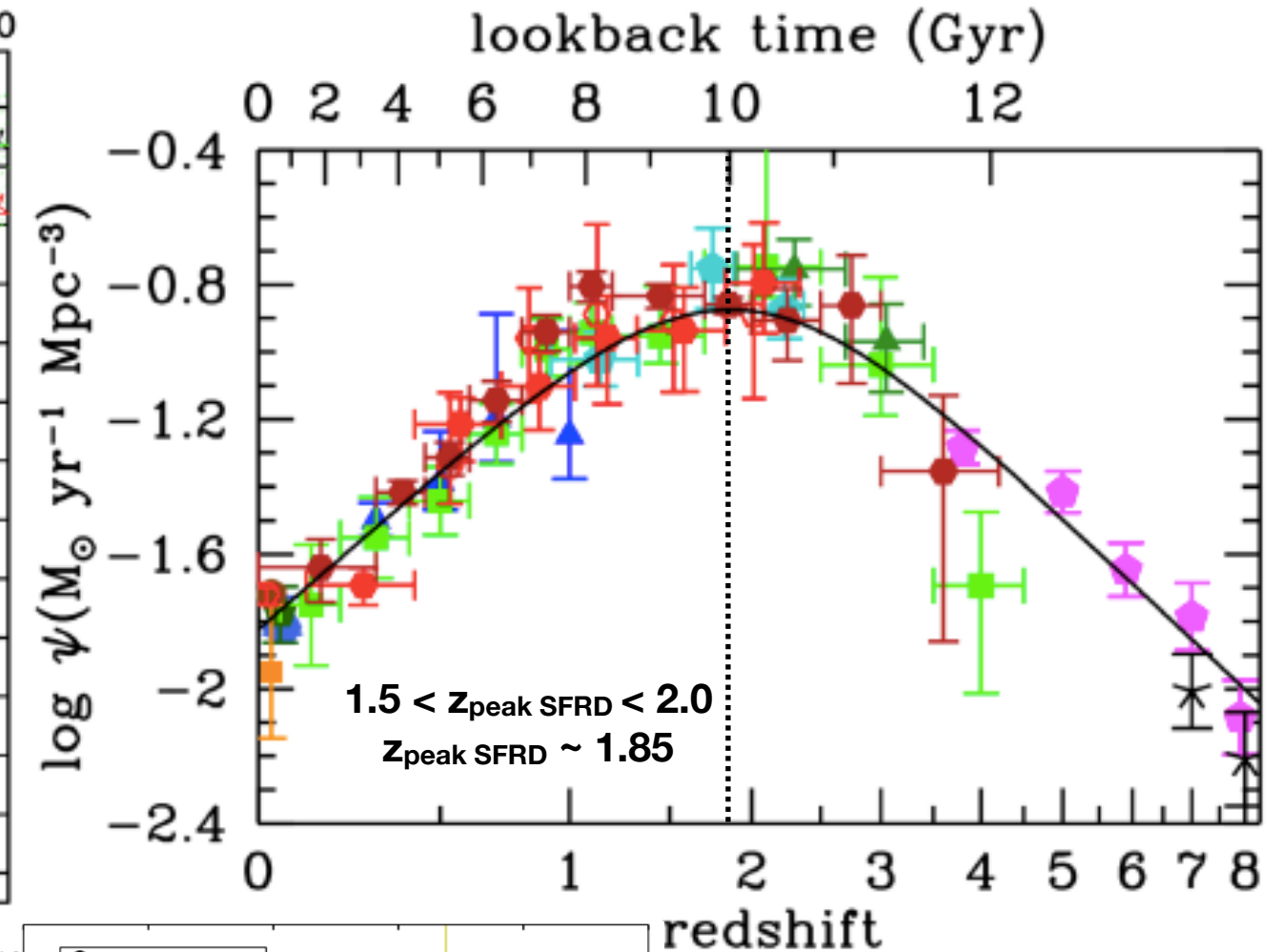
Additional avenues include isotropy tests and galaxy survey correlations

Looking back in time...

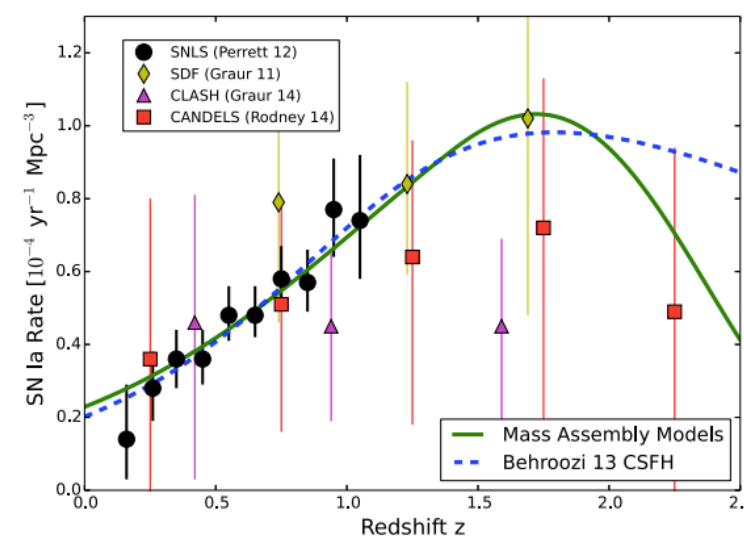


see Ilbert et al., A&A, 2013, 556, A55 (arXiv: 1301.3157)

do SN Ia magnitudes evolve with time
and, if so, are they being properly
accounted in SN Ia cosmology analysis?



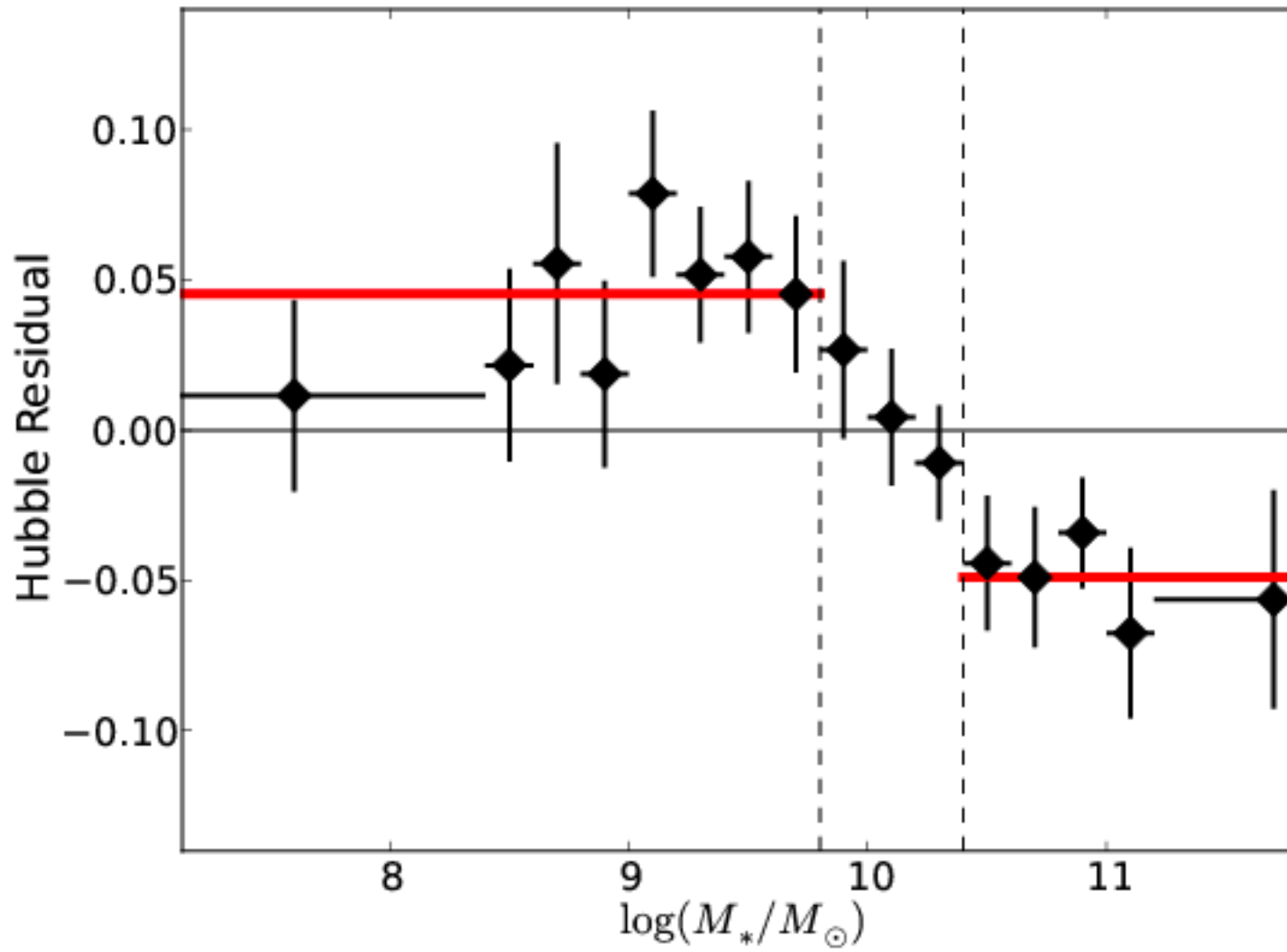
see Madau & Dickinson,
ARA&A, 2014, 52, 415-486 (arXiv: 1403.0007)



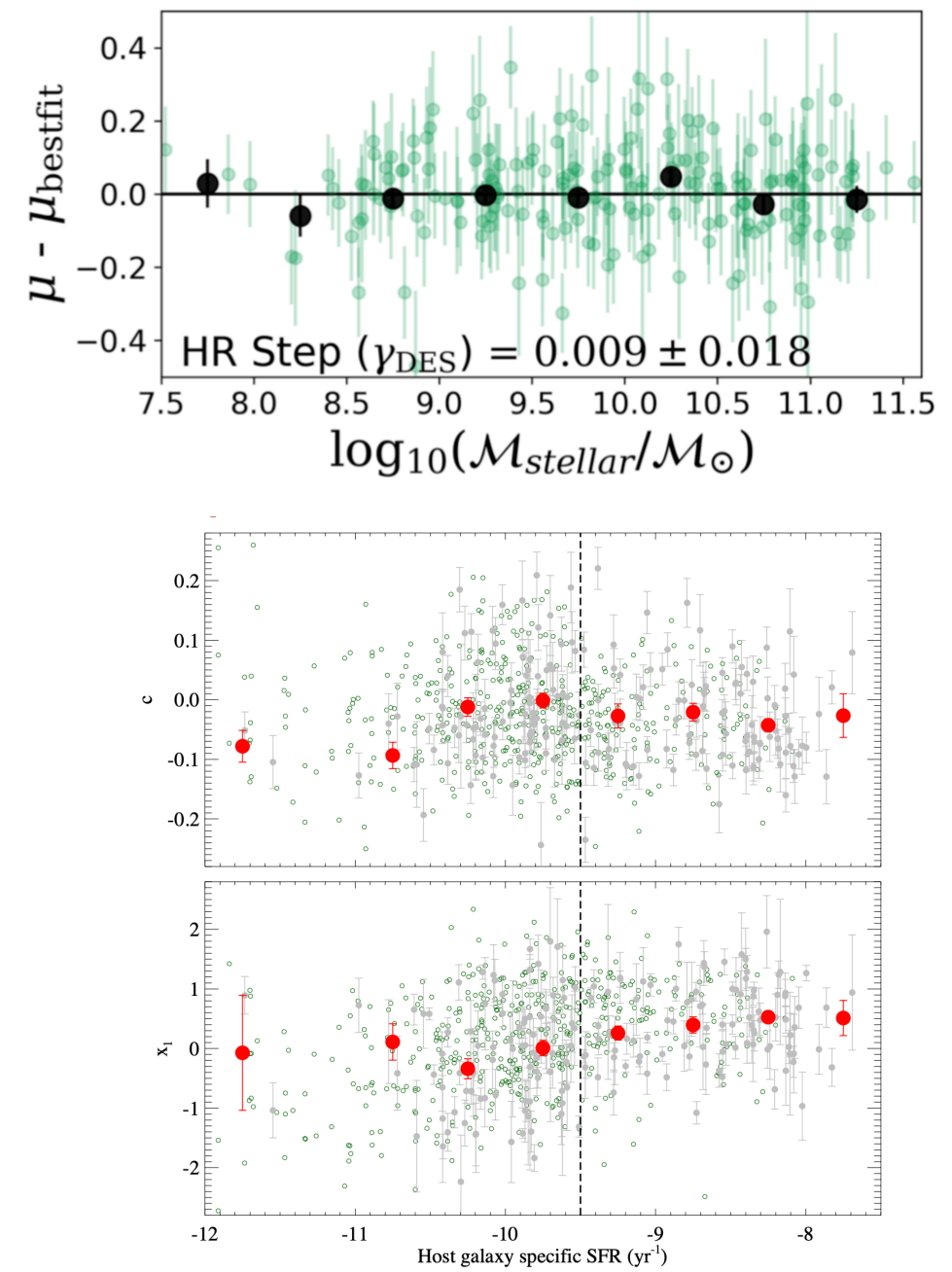
see Childress et al., MNRAS, 2014,
445, 1898-1911 (arXiv: 1409.2951)

“Mass-Step”

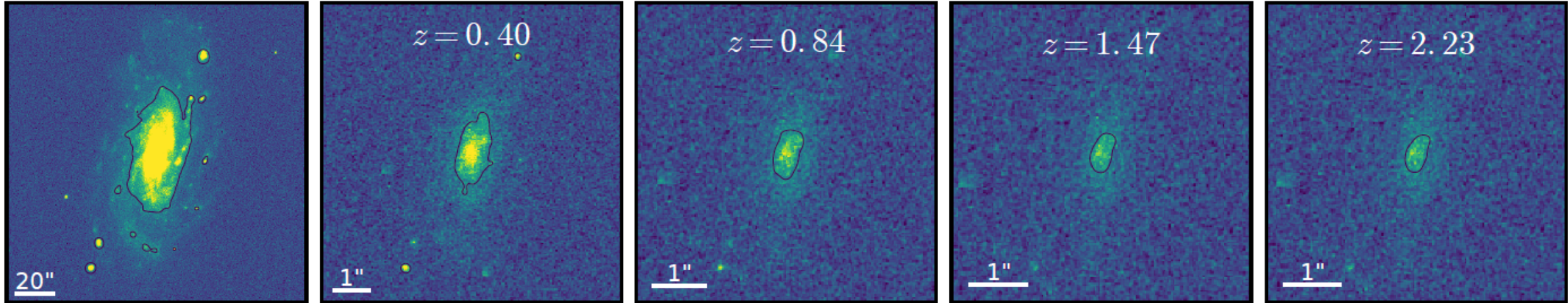
$$\mu = m_B - M + \alpha \times x_1 - \beta \times c + \gamma + \mu_{\text{bias}}$$



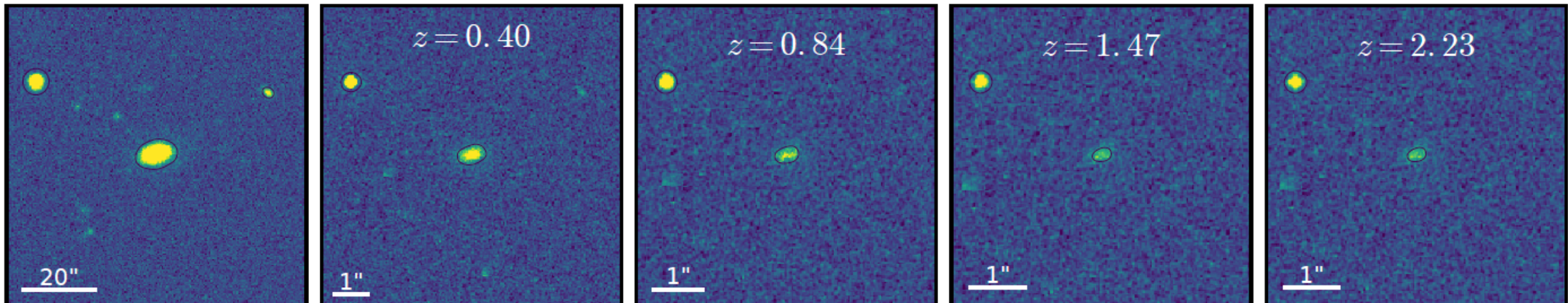
$$\text{HR} = \Delta\mu = \mu_{\text{obs}} - \mu_{\text{theory}}$$



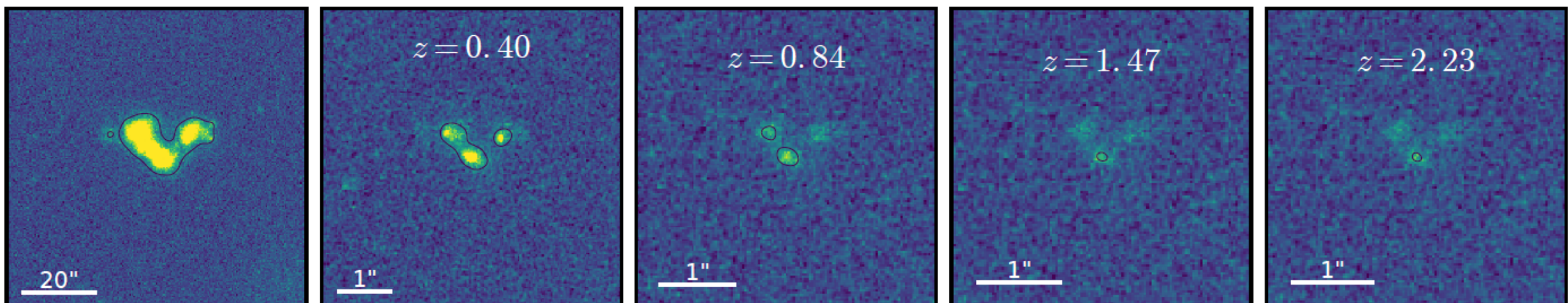
CALIFA



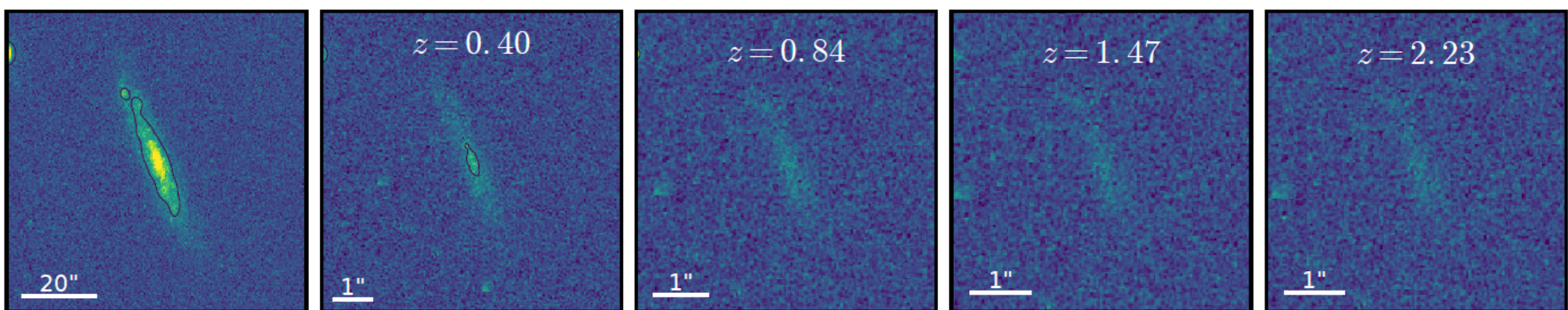
SAM I



MANGA

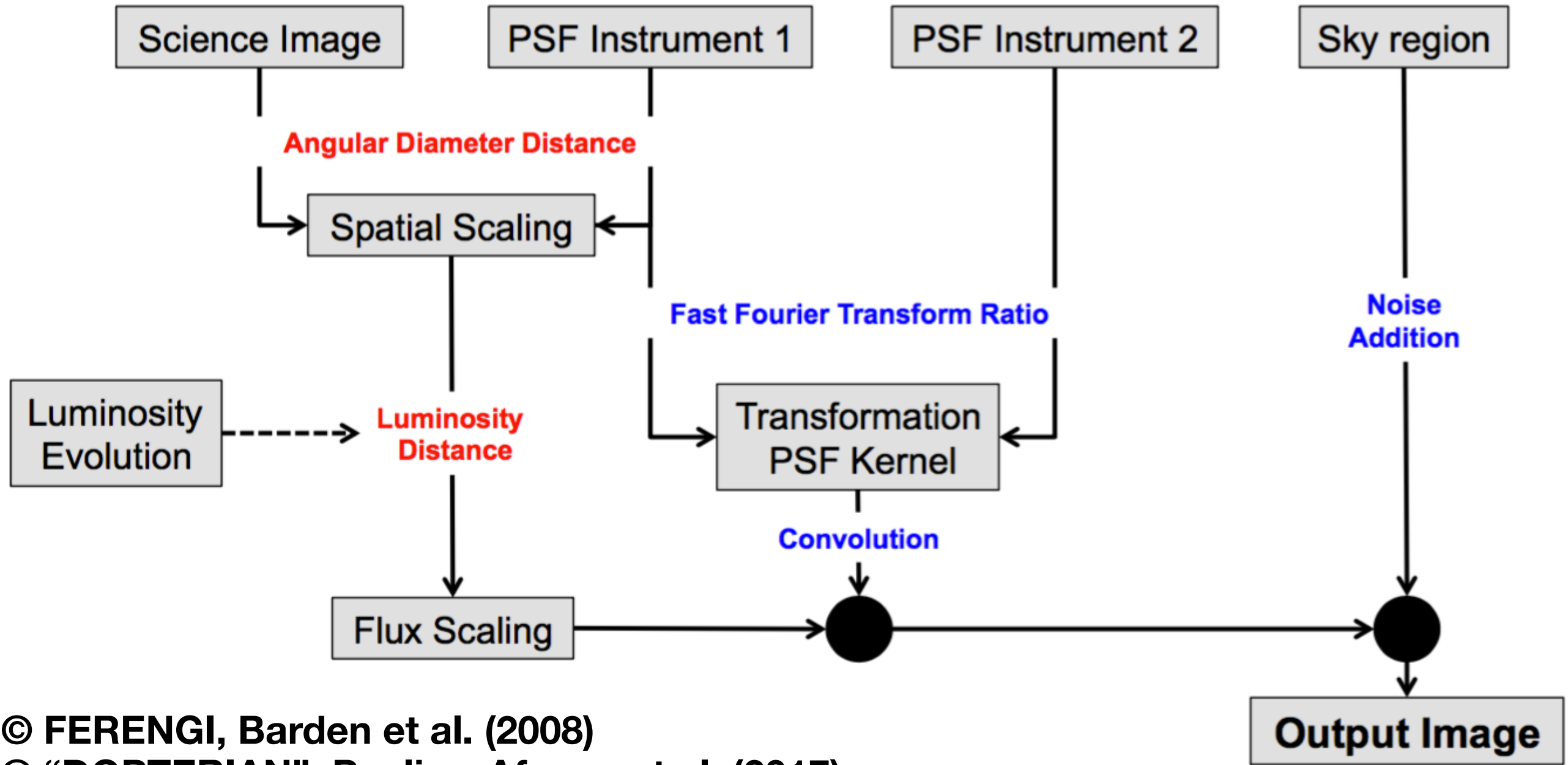


NYU-VAGC



Artificial Redshifting Galaxies

This is the general scheme that describes how to transform a source observed in one instrument into an higher redshift image observed with a different instrument.

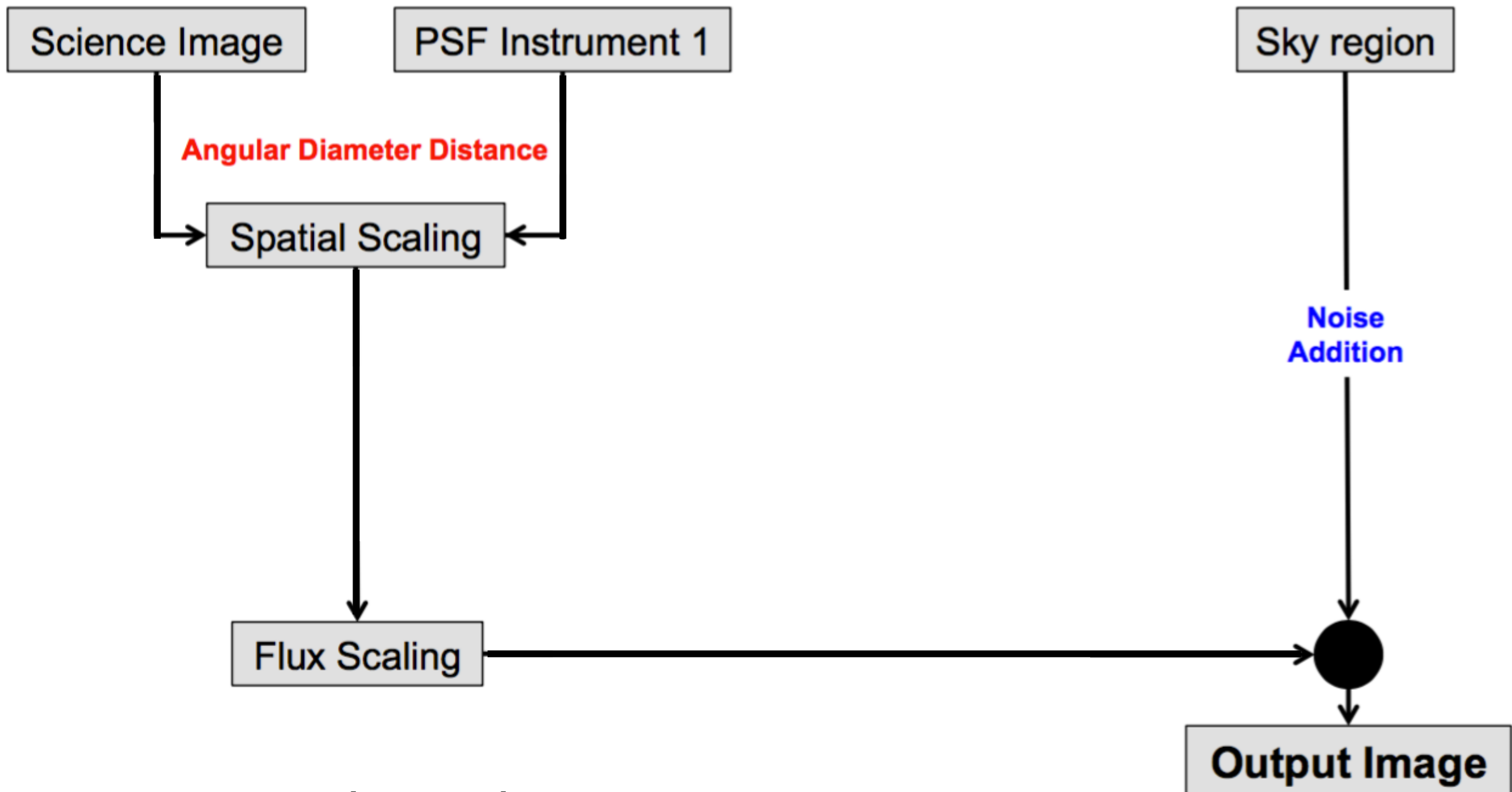


© FERENGI, Barden et al. (2008)

© “DOPTERIAN”, Paulino-Afonso et al. (2017)

Artificial Redshifting Galaxies

This is the scheme that describes the test that we are performing. I.e. we assume that we can observe a local source at higher redshift using the same instrument.



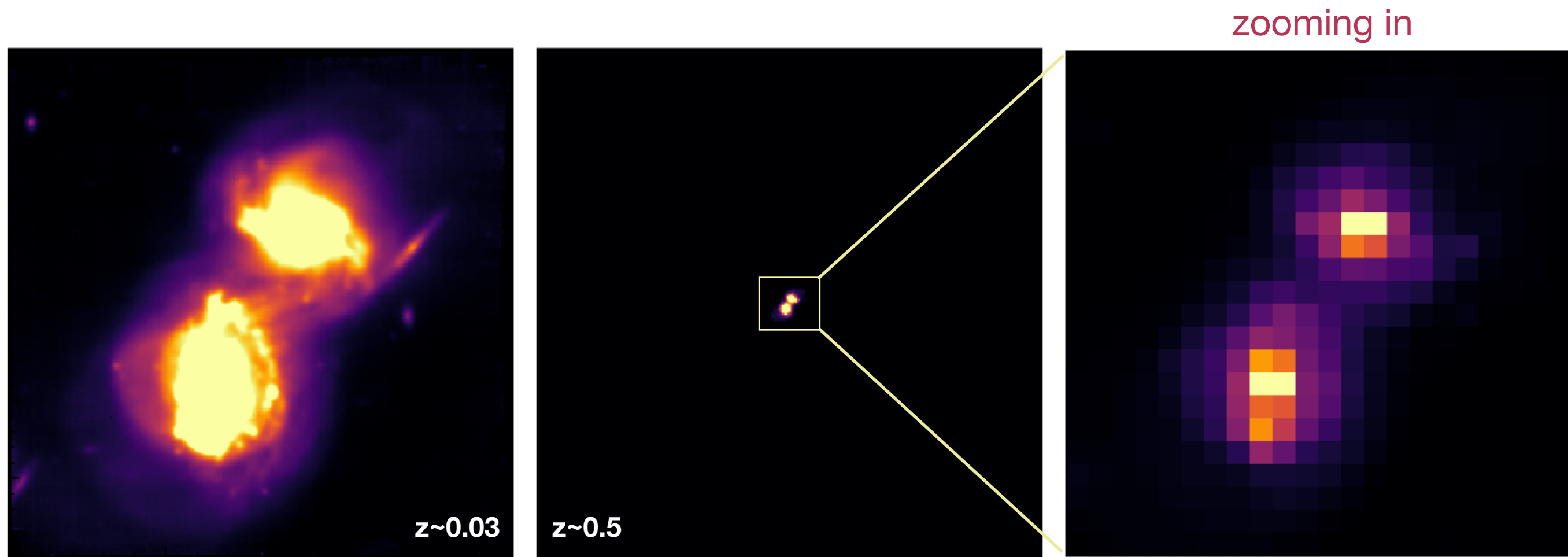
© Paulino-Afonso et al. (in prep.)

Object selection



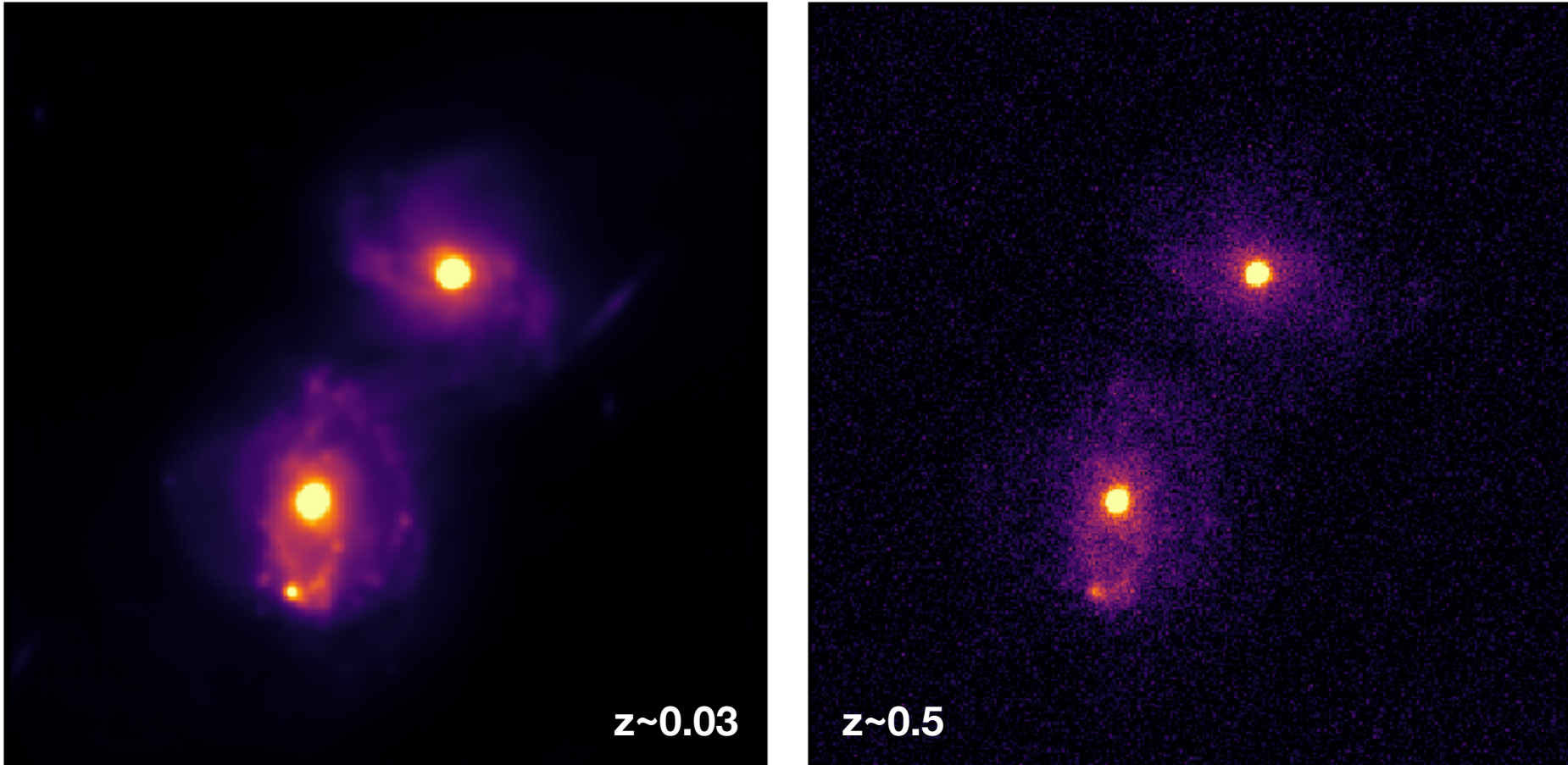
select pixels belonging to object for artificial redshifting

Scaling effect



the galaxy being more distant will occupy a smaller angular section of the sky, which translates into a smaller number of pixels (as the pixel-scale is constant)

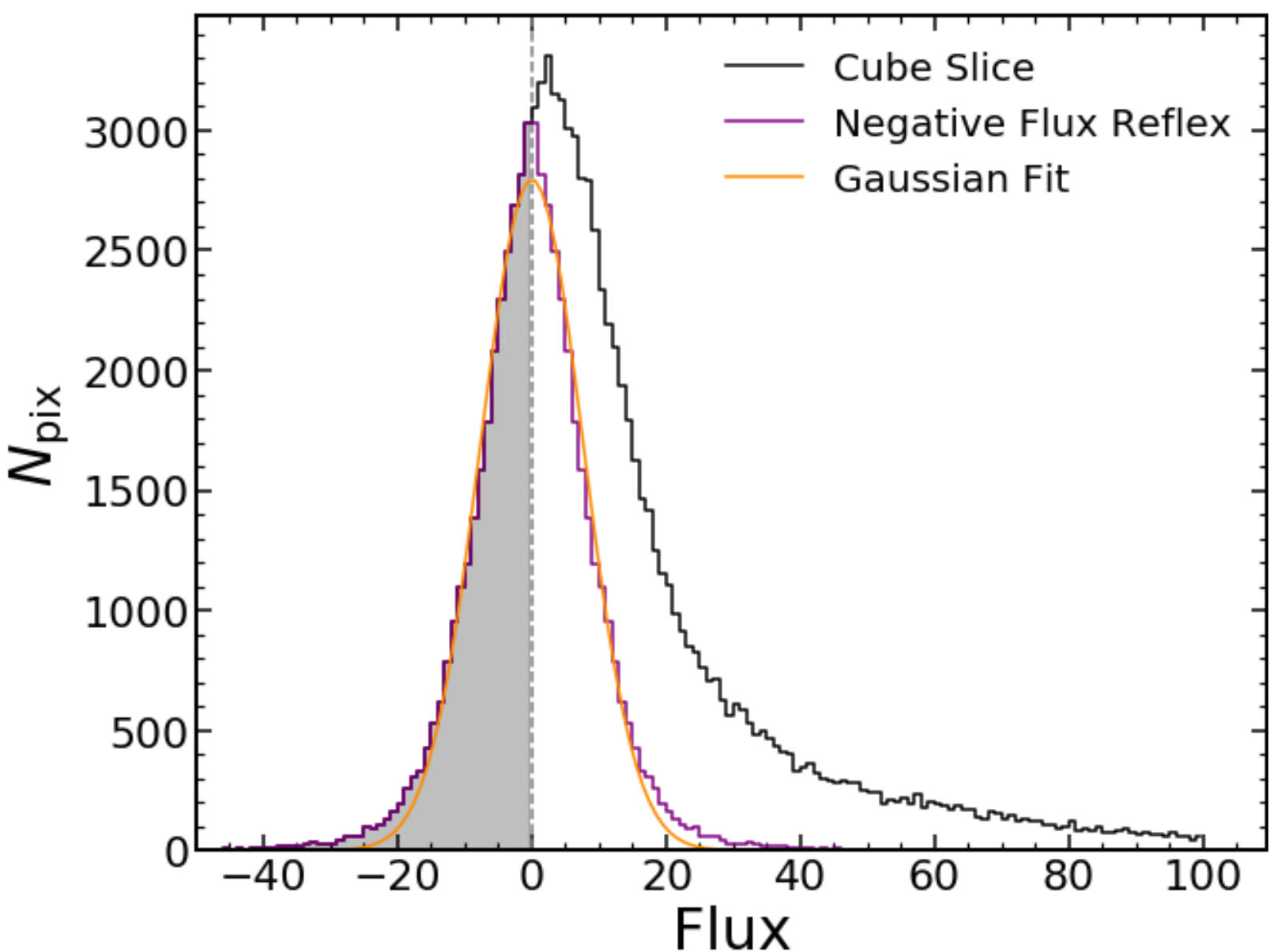
Just dimming



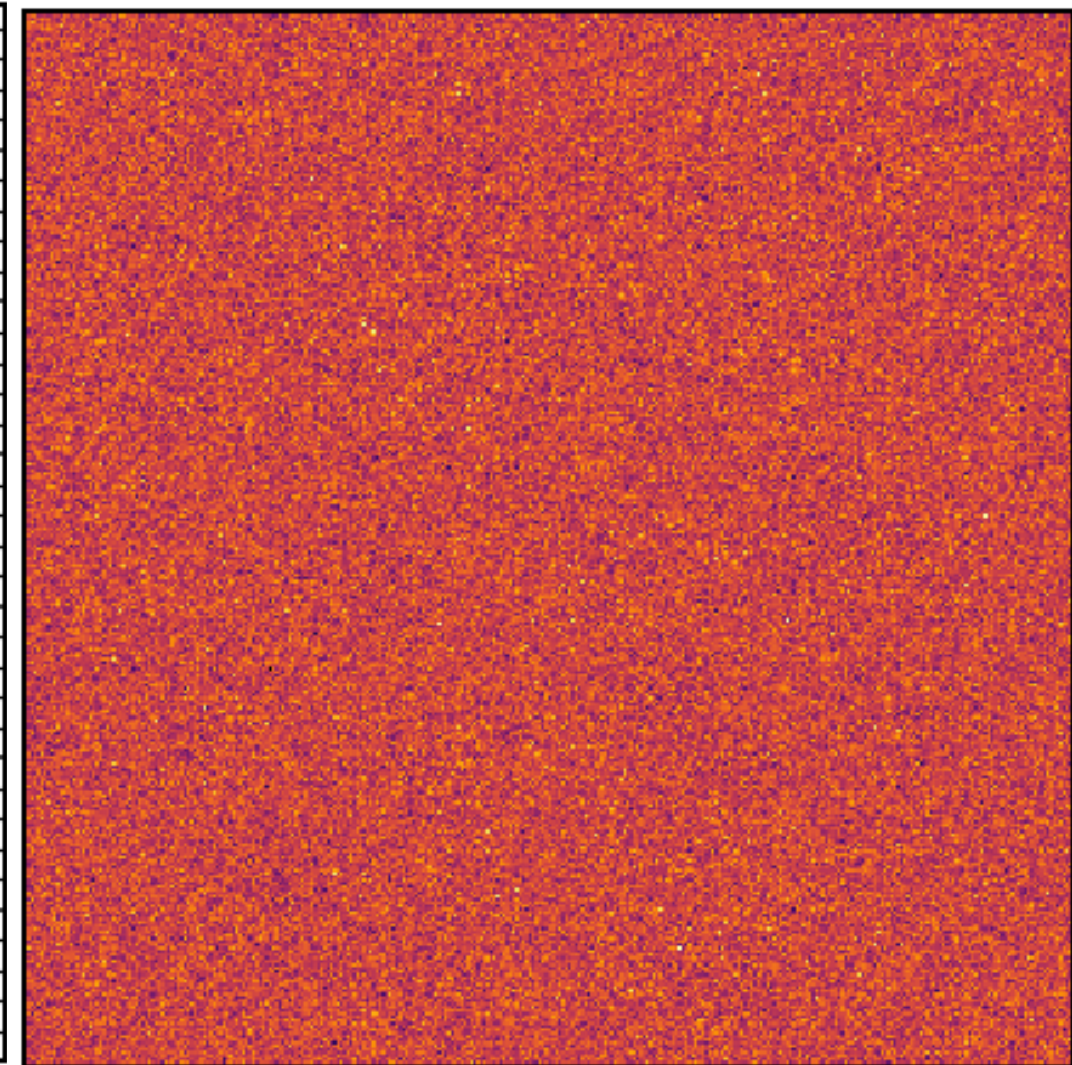
the flux in each pixel of the galaxy will diminish by a $(1+z)^3$ factor due to cosmological surface brightness dimming.

Noise estimation

Noise is assumed to be gaussian.

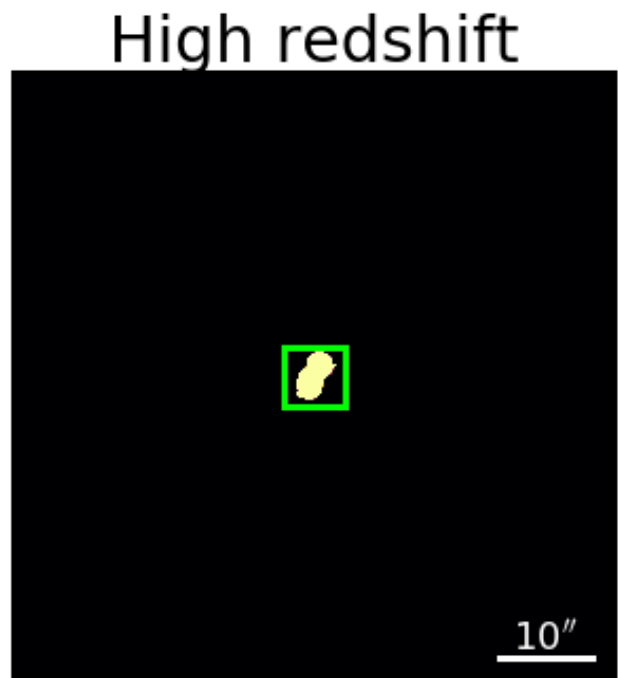
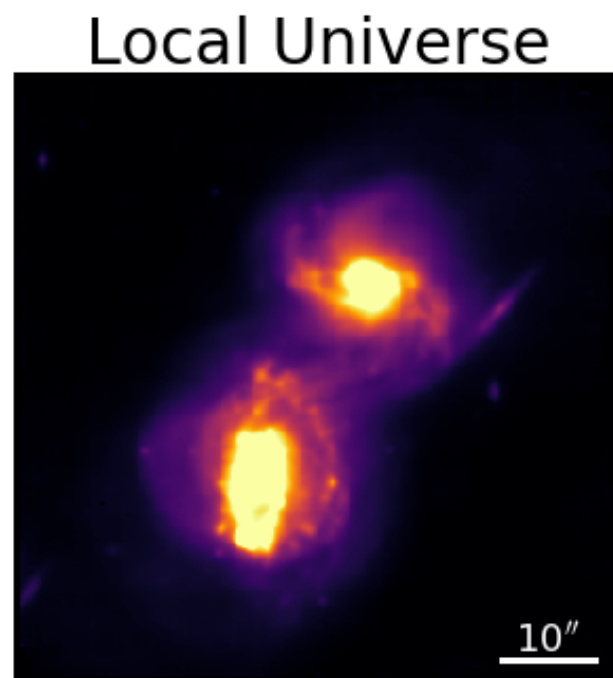


Generate image based on best-fit Gaussian noise.

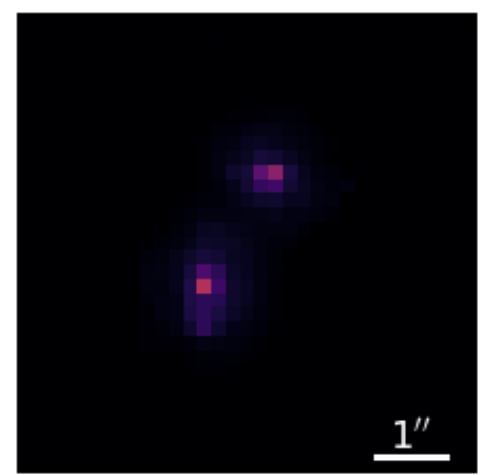
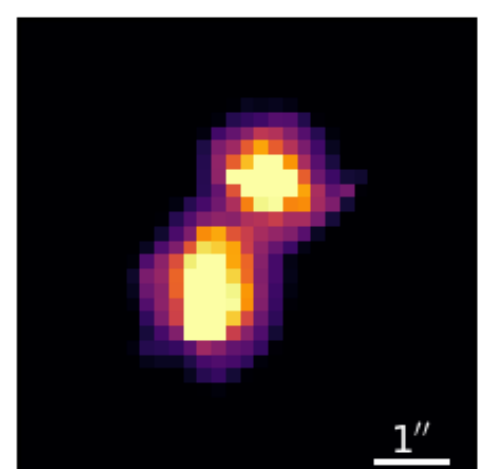
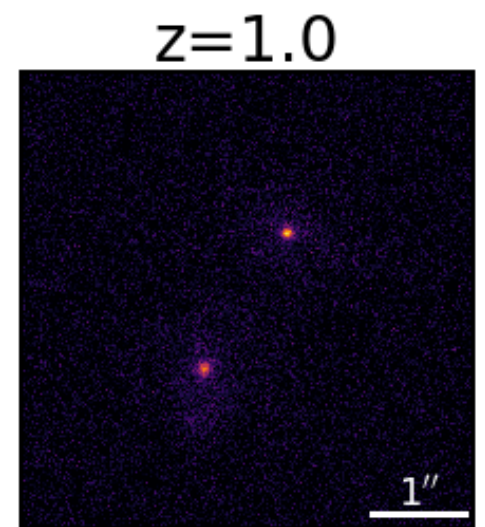
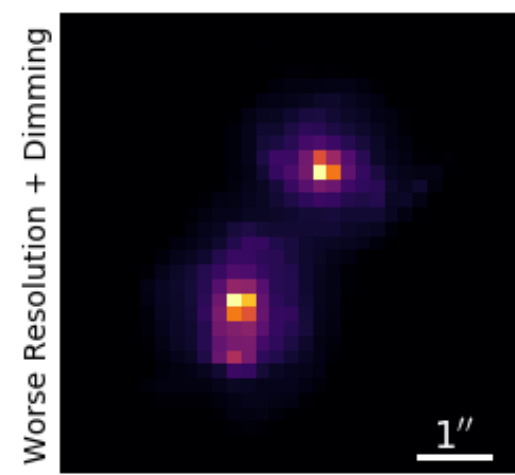
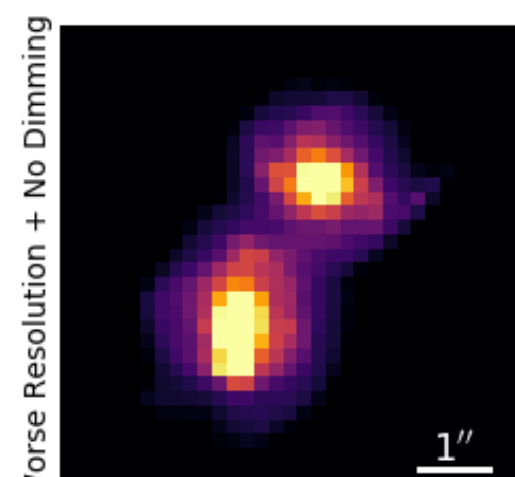
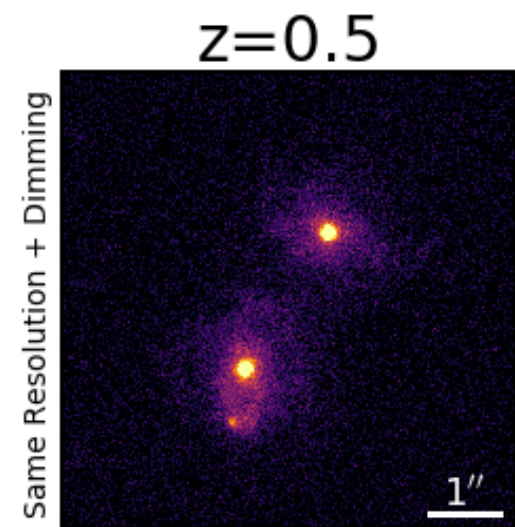


Gaussian parameters are estimated from reflected flux histogram of negative values

Artificial redshifted data

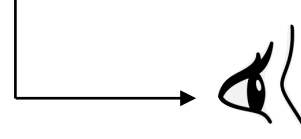


SN2014dm

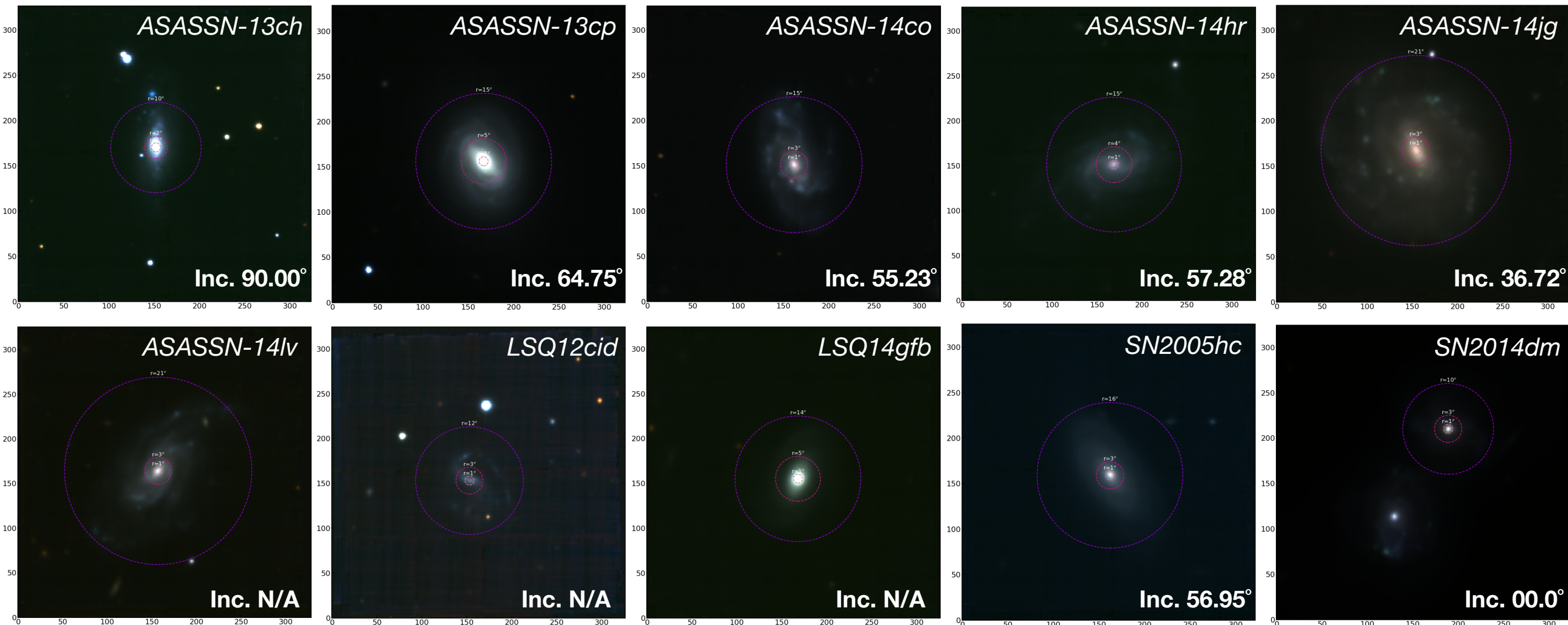


Data sample

a non-representative test sample of the Amusing survey (PIs: J. Anderson & L. Galbany)



RGB images made from the MUSE data cube

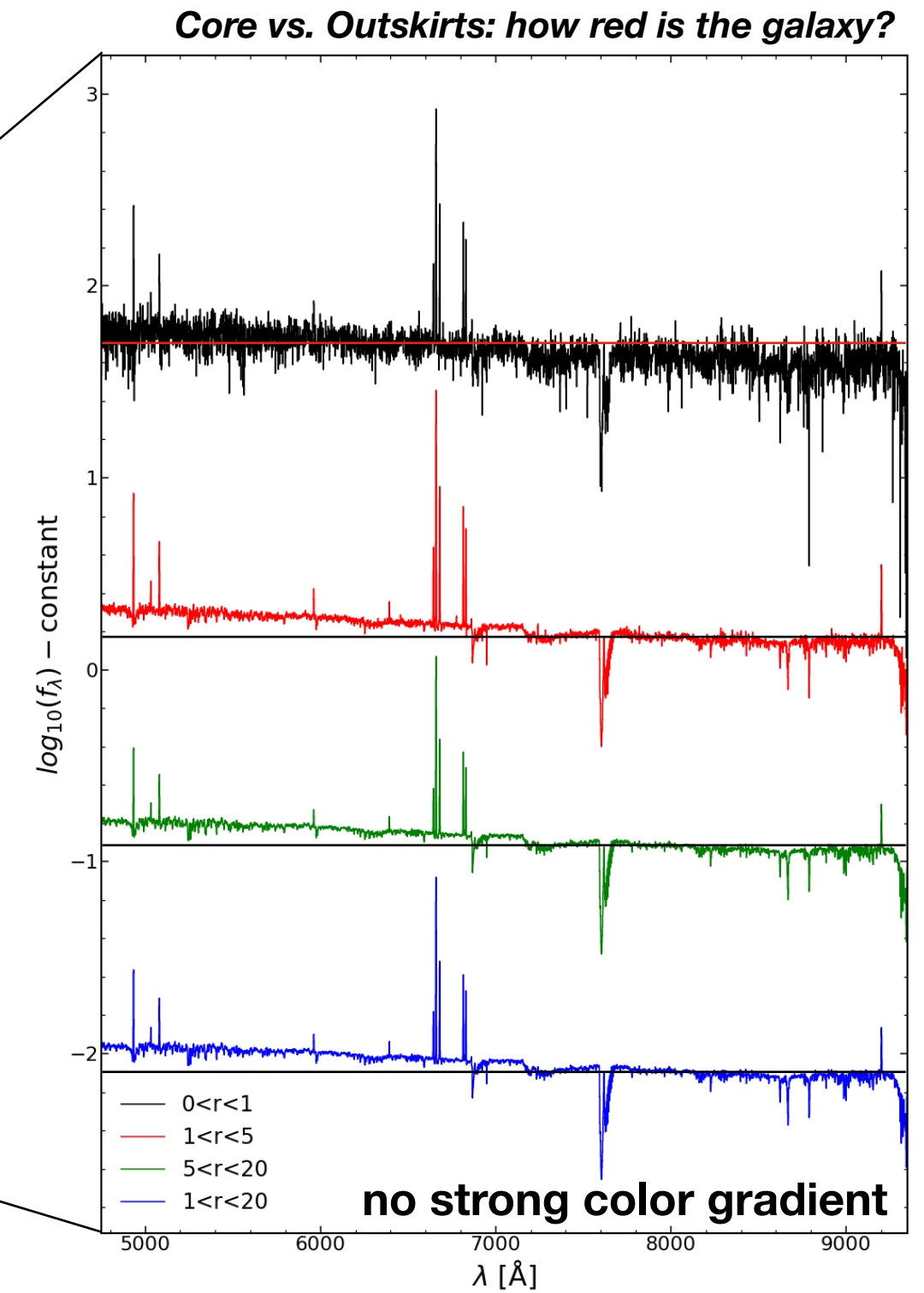
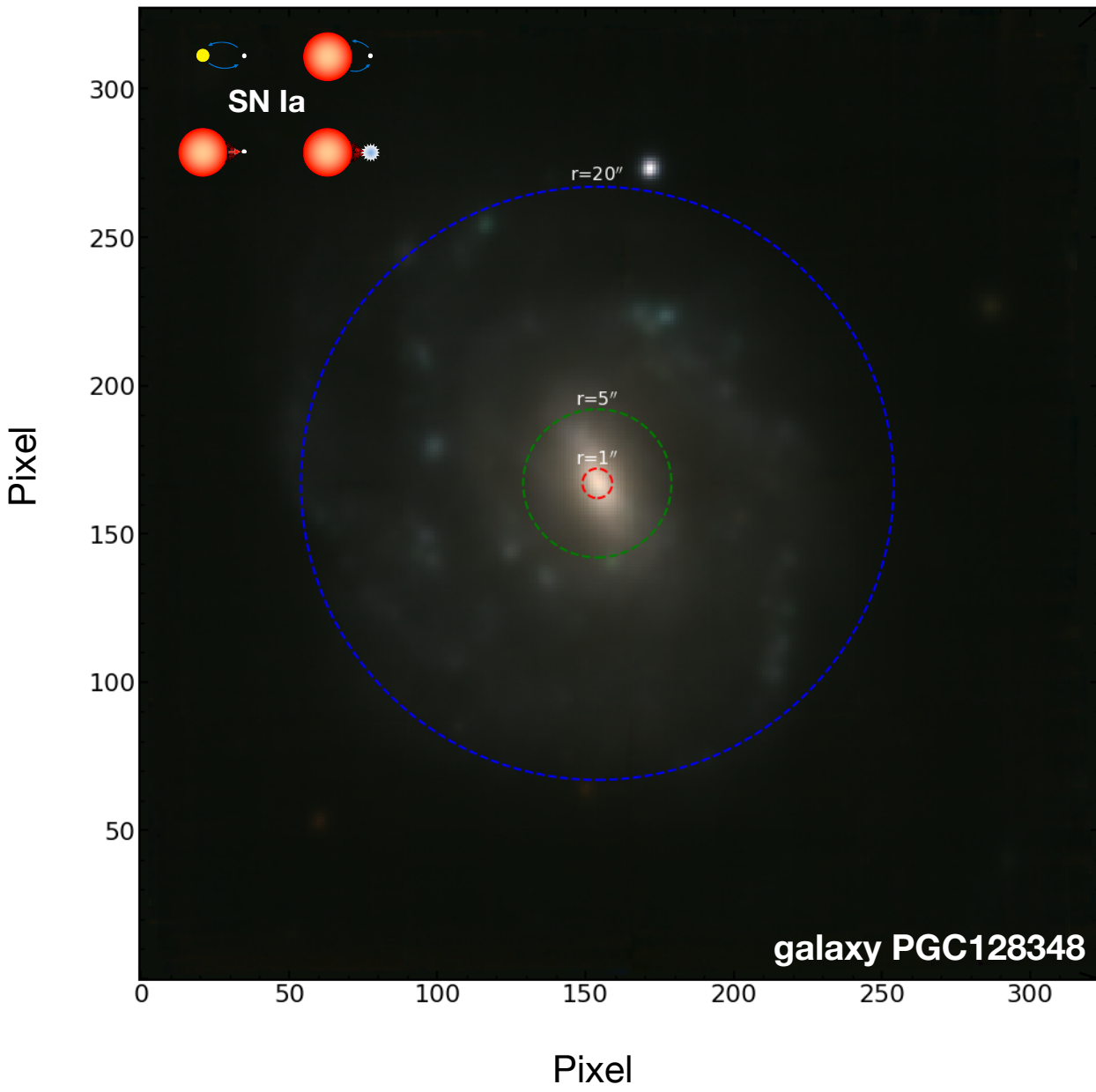


see https://github.com/amusing-muse/Characterization/blob/master/Sample_char/amusing_sample_char.csv

see also eg. Galbany et al., MNRAS, 2016, 455, 4087-4099 (arXiv: 1511.01495)

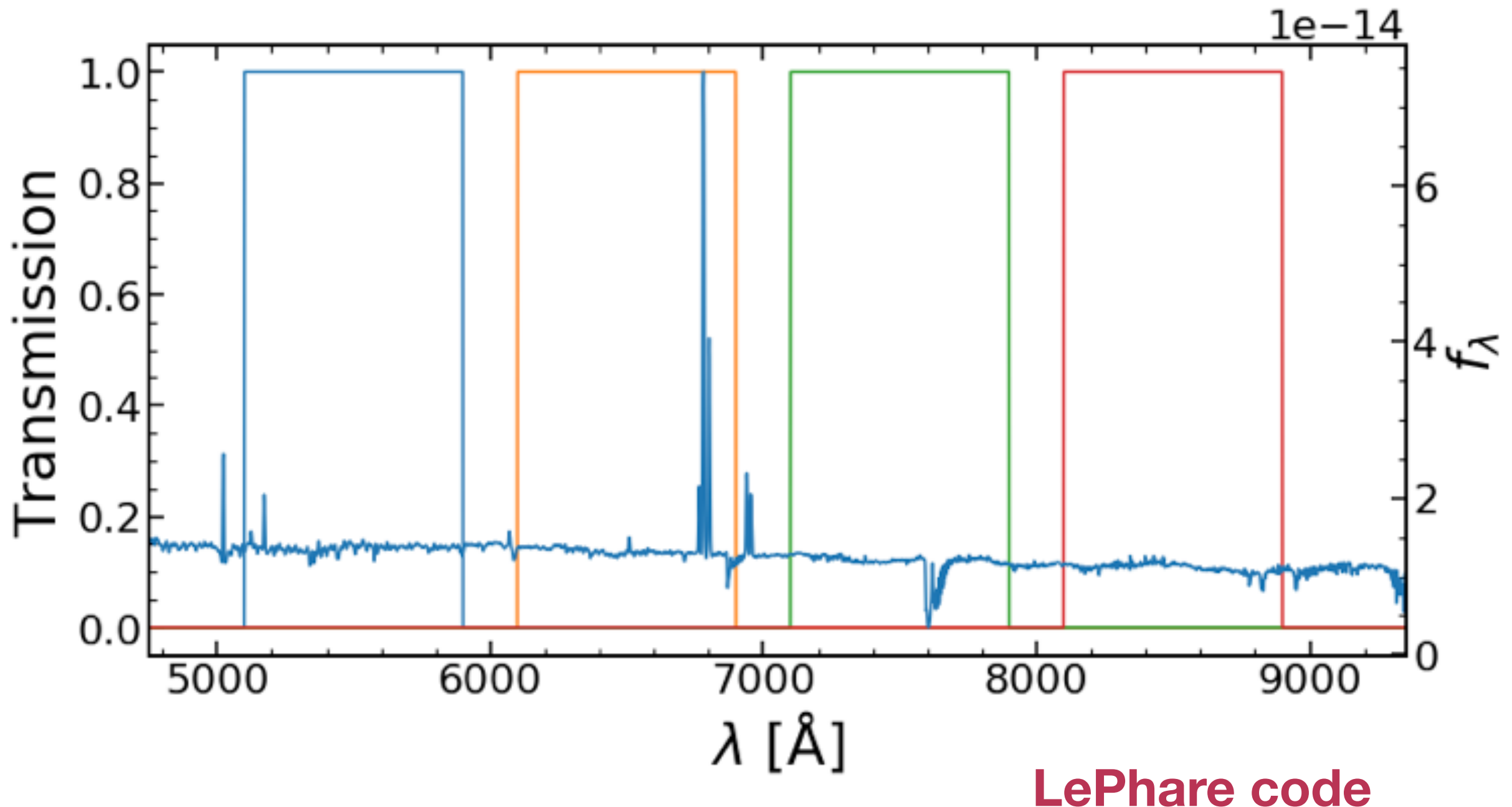
ASASSN-14jg host

aperture effects and limitations on the accuracy
of MUSE spectrophotometry analysis



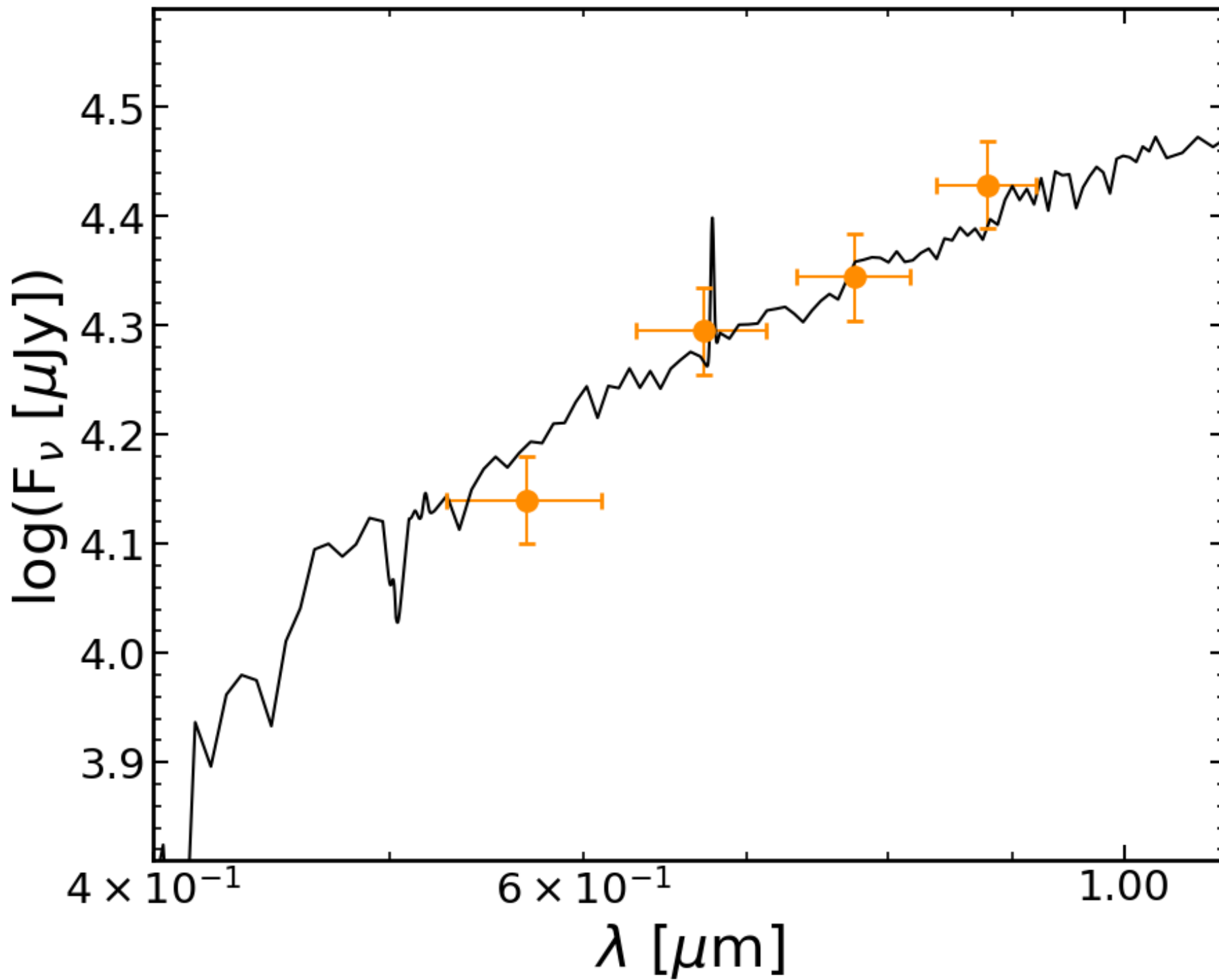
Stellar mass estimation

to transform the spectral information into photometric data,
four perfect top-hat filters were created



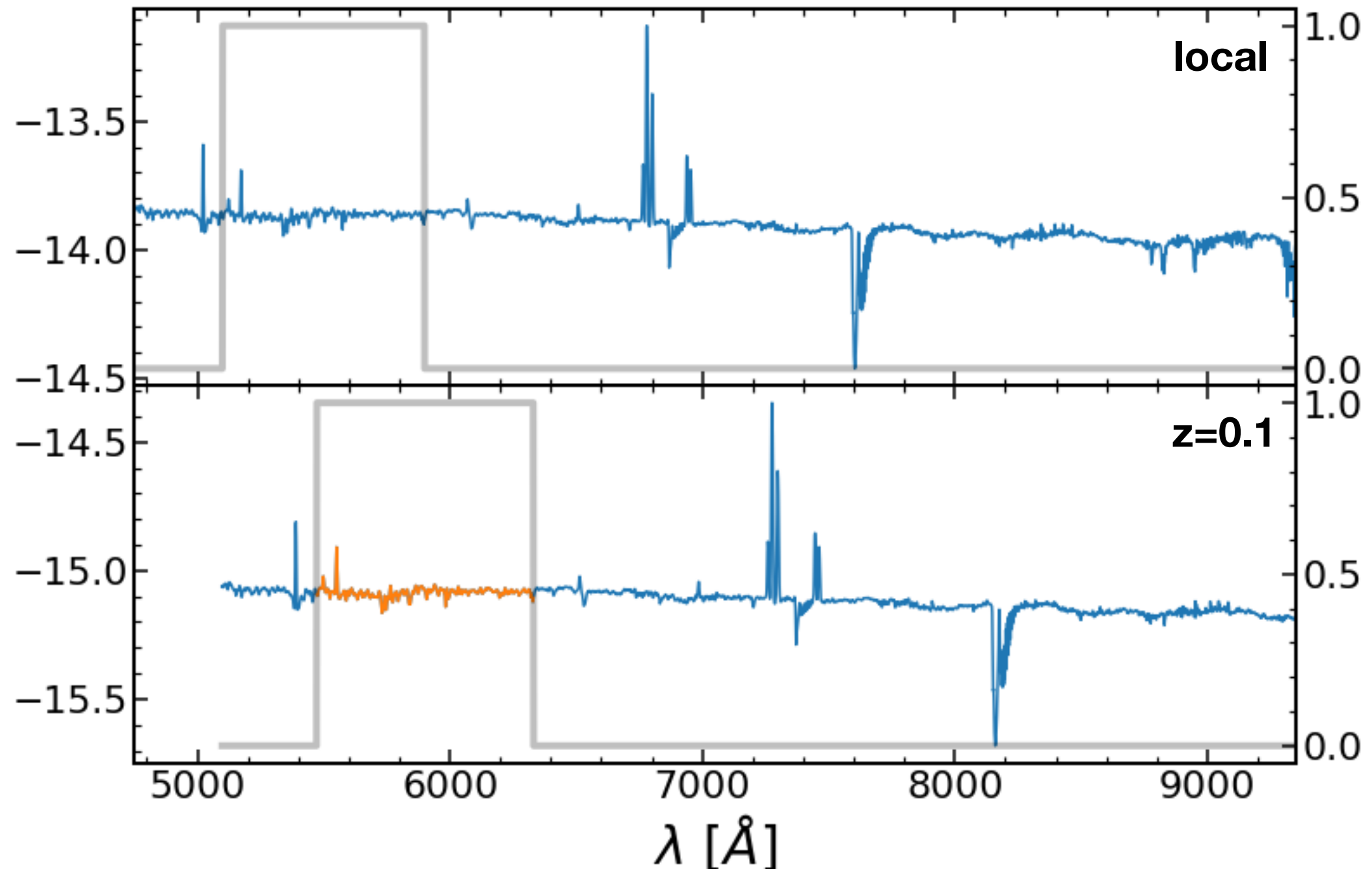
SN2014dm host galaxy SED

the photometric data is fed into a SED fitting code to estimate the stellar mass of the object



Synthetic filters

To test the algorithm on a perfect scenario, a set of 4 identical filters (800 Å width) covering the entire region of the MUSE cube data is defined. Then, to each simulated redshift both the center and the width of the filter is multiplied by $(1+z)$ so that it exactly matched the same rest-frame coverage as in the input local Galaxy.



Testing LePhare stellar masses estimation

The artificial redshifting part of the algorithm is stable, but we need to make sure that the stellar mass estimates computed from LePhare are well estimated. To do so we devised a test that compares stellar masses at different redshifts without applying any artificial redshifting technique to the cube data:

This test has three steps:

- 1 - compute the magnitudes in each of the 4 filters on the original cube data;
- 2 - compute the apparent magnitudes at a given redshift, z , applying the formula
$$m(z) = m(z=0) + (5 \cdot \log_{10}(dL(z=z)/(dL(z=0)))) - (2.5 \cdot \log_{10}((1+z)/(1+z_0)))$$
- 3 - feed the simulated magnitudes to LePhare to obtain stellar masses;

Since the input magnitudes are computed by fixing the absolute magnitude at all redshifts (for all filters), the stellar mass should be exactly the same, and so the $\Delta \log_{10}(M)=0$ for all redshifts. Any differences in stellar masses must indicate any internal problems with how LePhare estimates the mass.

Note on LePhare

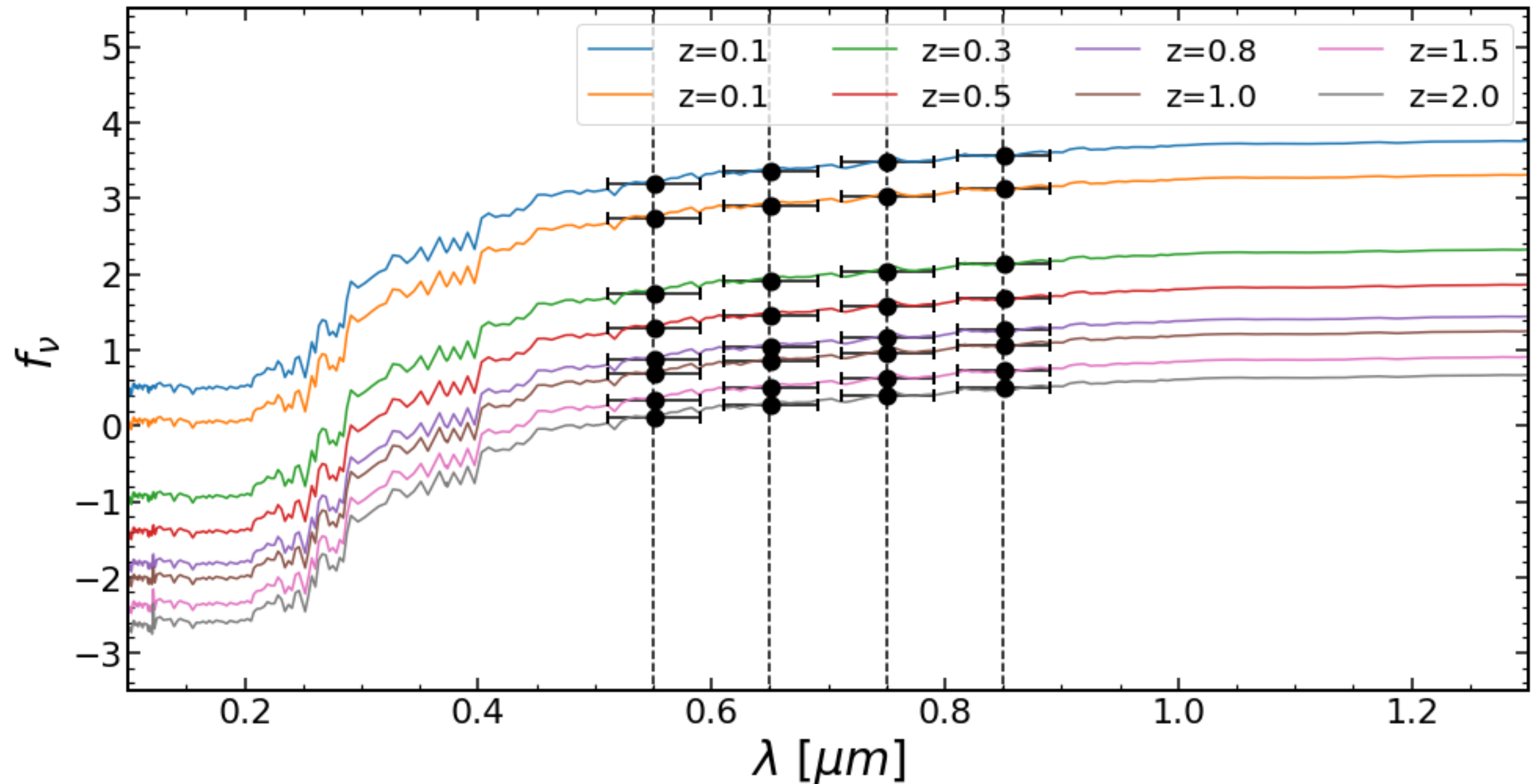
To run LePhare it is necessary to establish the grid of models that will be used to compare to the input data. This implies a number of choices that include:

- Star formation histories (SFH)
- Dust attenuation curves
- Metallicities
- Initial Mass Functions (IMF)
- Stellar Models

To limit the number of models (and greatly reduce the computing time, as it scales with the number of individual choices, multiplicatively), we choose to fit BC03 models with a Chabrier IMF and solar metallicity. We chose a single attenuation curve (Calzetti+ 2000) with three different normalizations, and 9 SFH (exponentially declining star formation rates, with a characteristic timescale, τ , of 0.1,0.3,1,2,3,5,10,15, 30 Gyrs). This set of models is typically used to derive stellar masses in the high redshift universe, as this is the variable that is most stable. Nevertheless, a change in the grid of used models can introduce a systematic difference of 0.2-0.3 dex (also seen when using different codes with different assumptions).

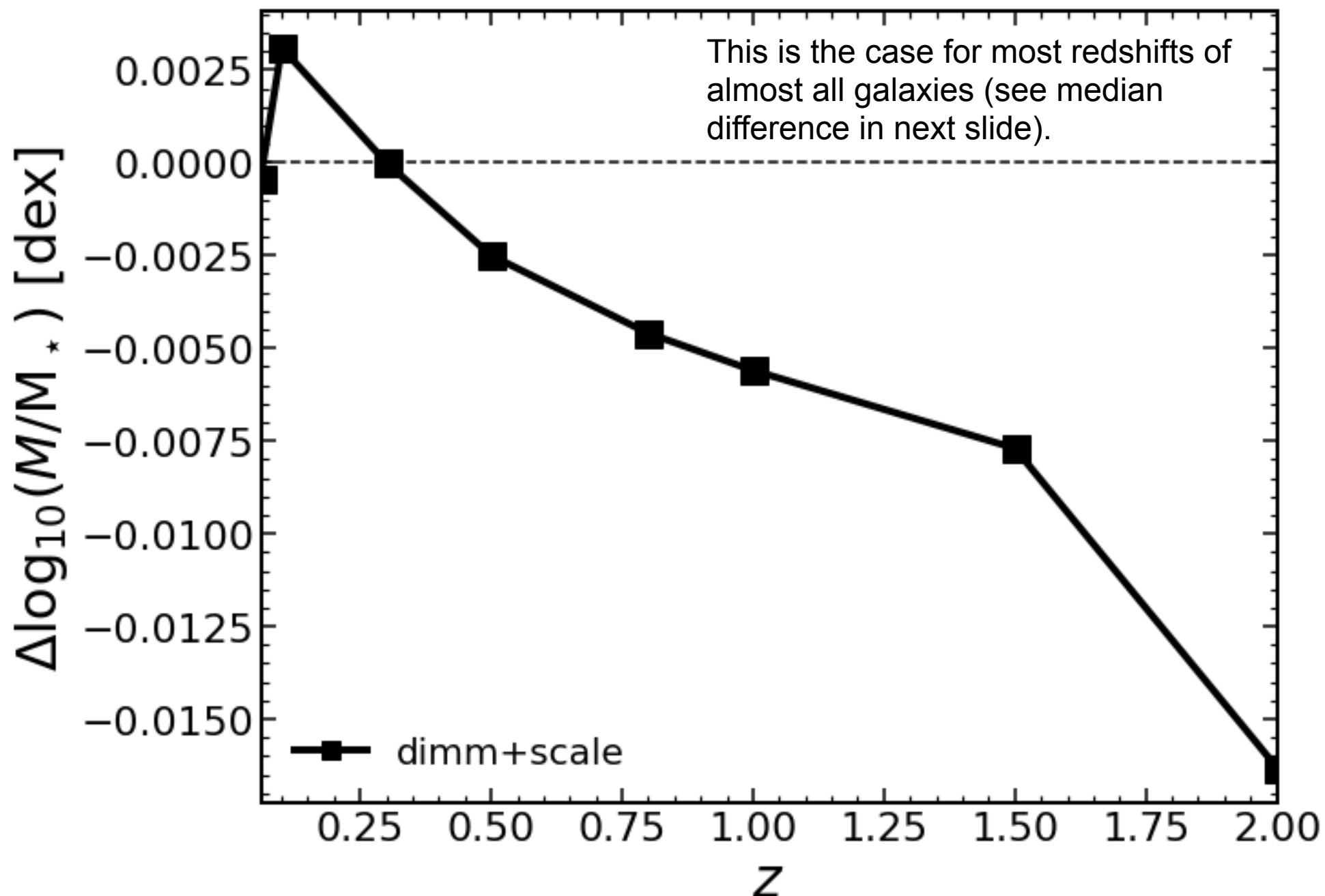
Results for LSQ14gfb

The example below illustrates the issue, with all SEDs aligned in rest-frame, and the individual magnitudes (and filter widths) shown by the black circles. The different fluxes reflect the flux change due to the galaxies being at higher redshift. In this scenario the SEDs are similar at all redshifts.



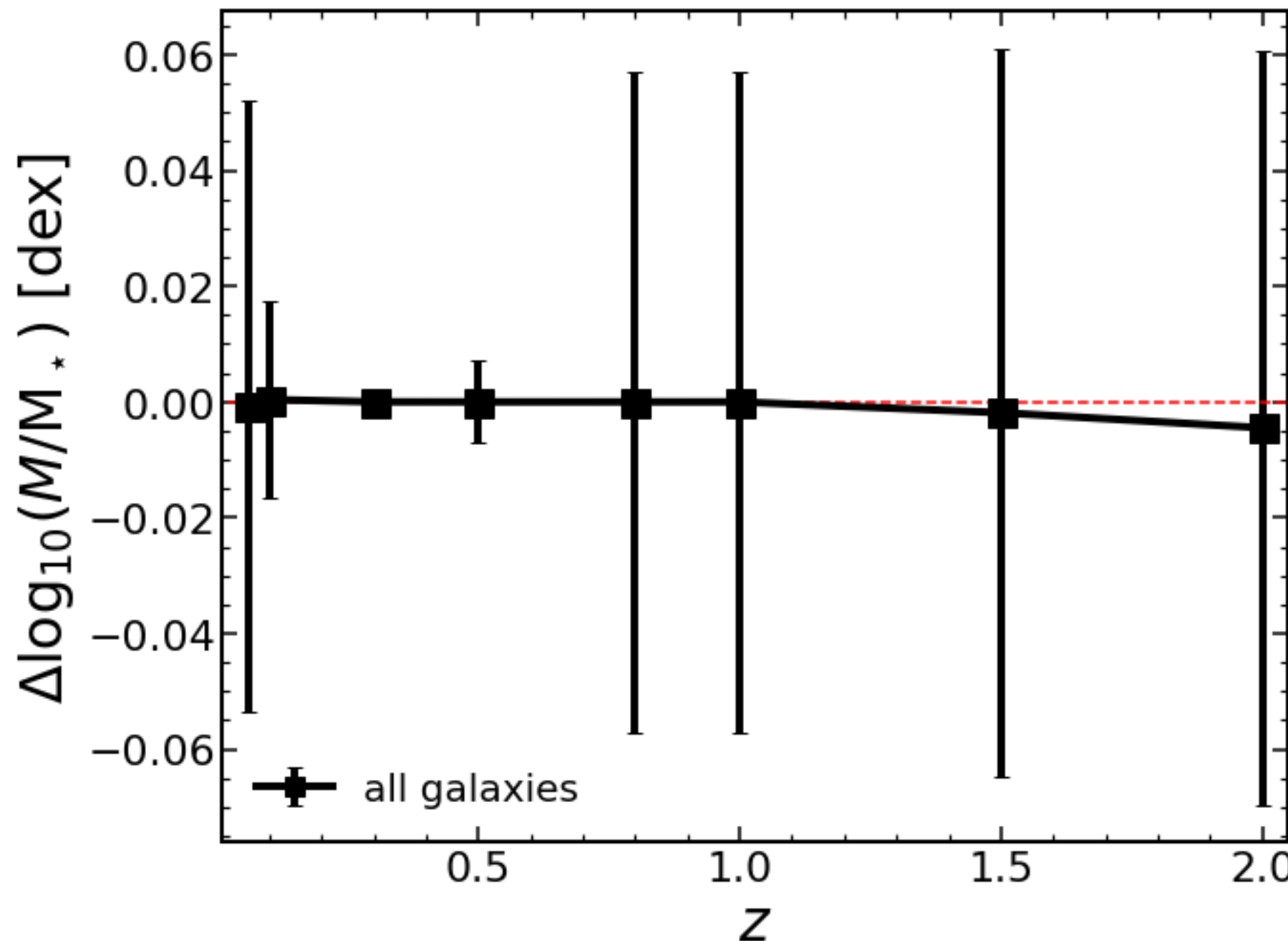
Mass residuals for LSQ14gfb

The absolute differences in stellar mass is well below 0.05 dex (see below).



Median Mass Residuals

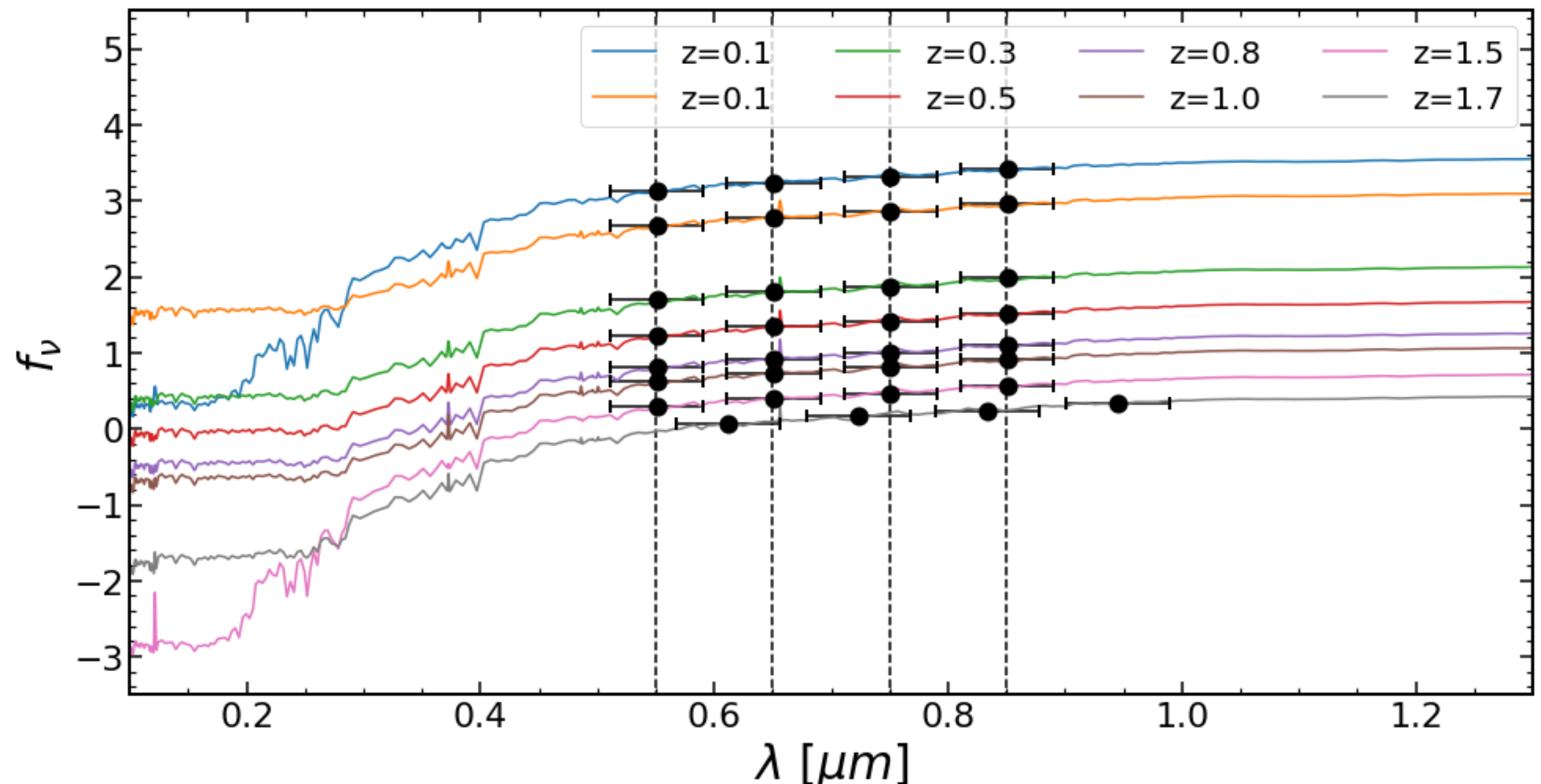
This figure highlights that the median stellar mass difference is very close to 0 (always below 0.01 dex) with some variance due to the “catastrophic” failure of some galaxies (see example in next slide).



Results for LSQ12cid

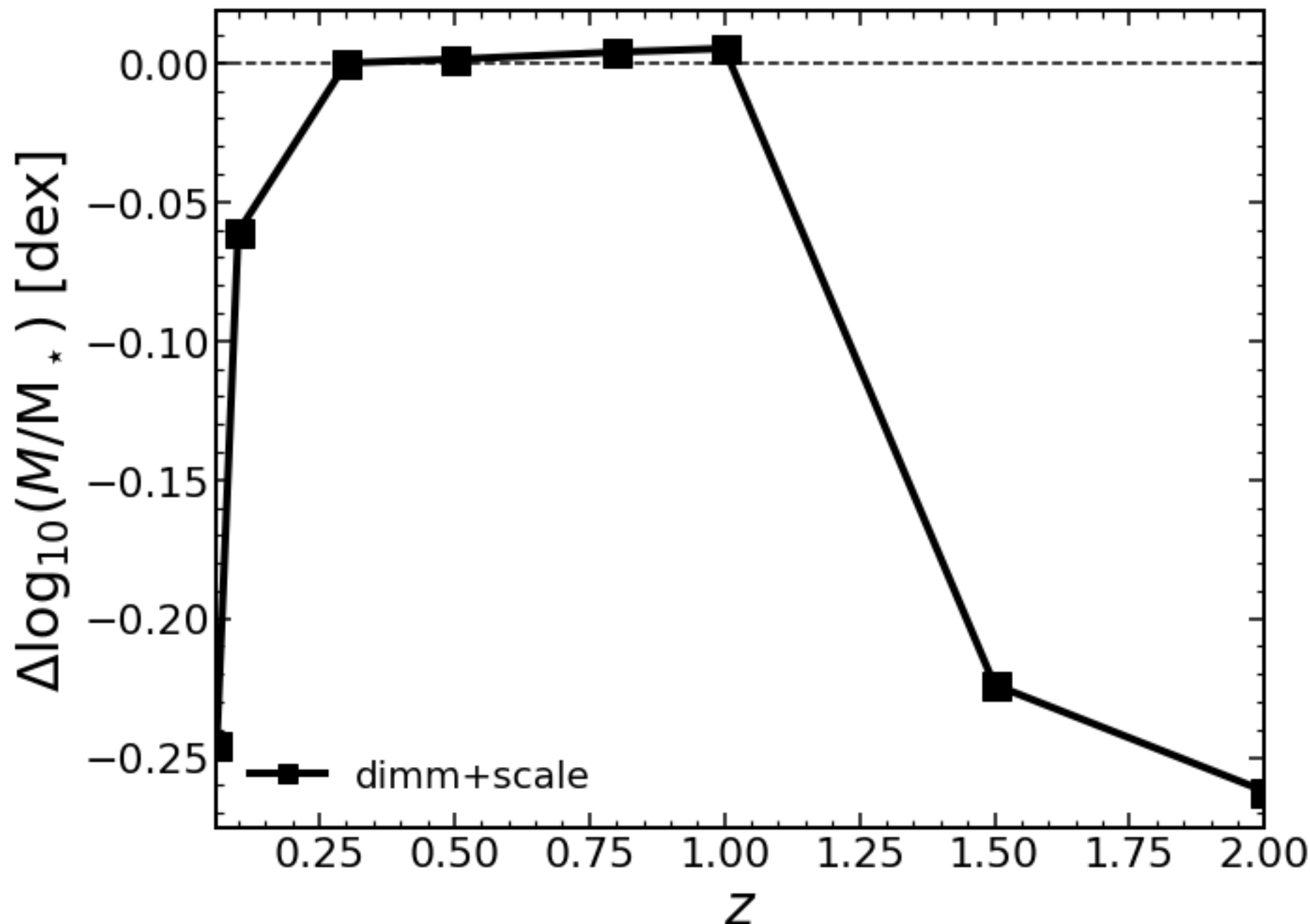
The example above illustrates one problem we encounter with this exercise for some particular examples. In this scenario the SEDs are not similar at all redshifts and the absolute differences in stellar mass can reach large values (up to 0.25 dex, see next slide).

This is a combination of two problems, one is internal to LePhare and is illustrated by the shift in the magnitudes at $z=2$, which reflects a problem with LePhare on fixing the redshift of the galaxy (this affects the visualization, but not much the stellar masses).



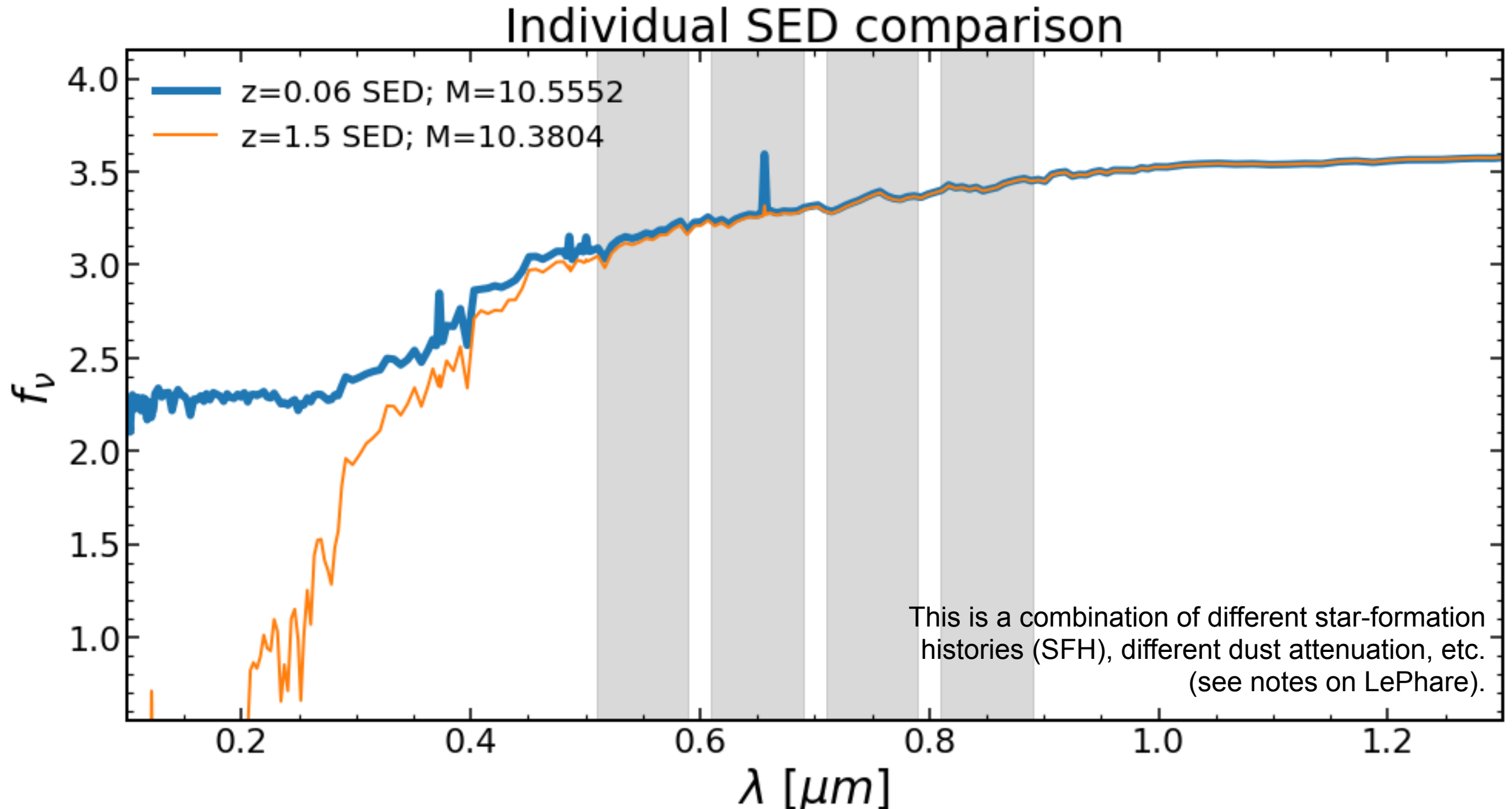
Mass residuals for LSQ12cid

The bigger issue is with the different best-fit SEDs that LePhare provides given the input magnitudes (see next slide).



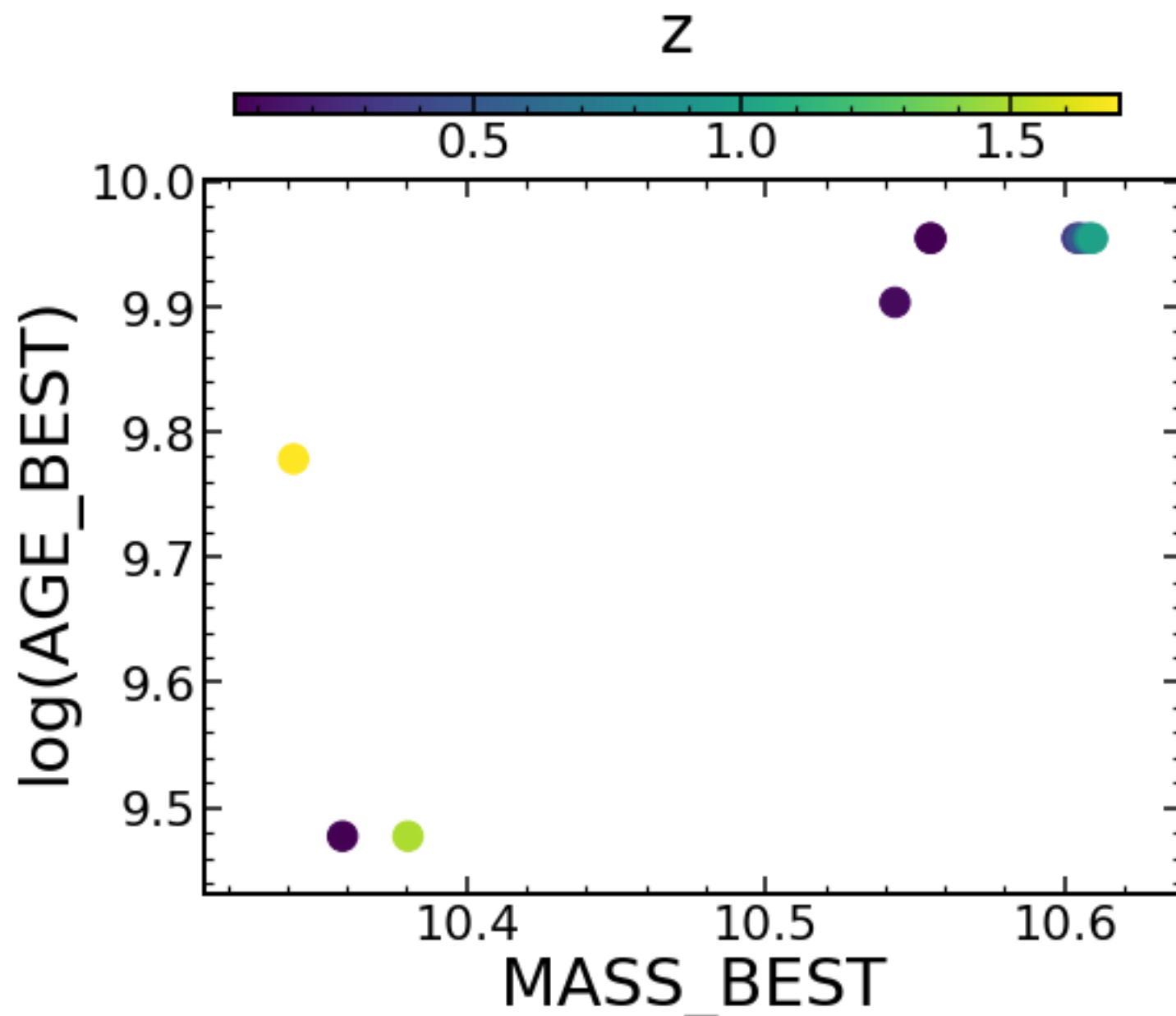
UV “catastrophe” for LSQ12cid

This figure illustrates how an SED can have incredibly similar shape and fluxes in the regions where the filters are computed (black vertical stripes), while being extremely different in the blue-UV region. This different SED is what explains the differences in stellar masses that we find, even in the case of identical optical rest-frame magnitudes.

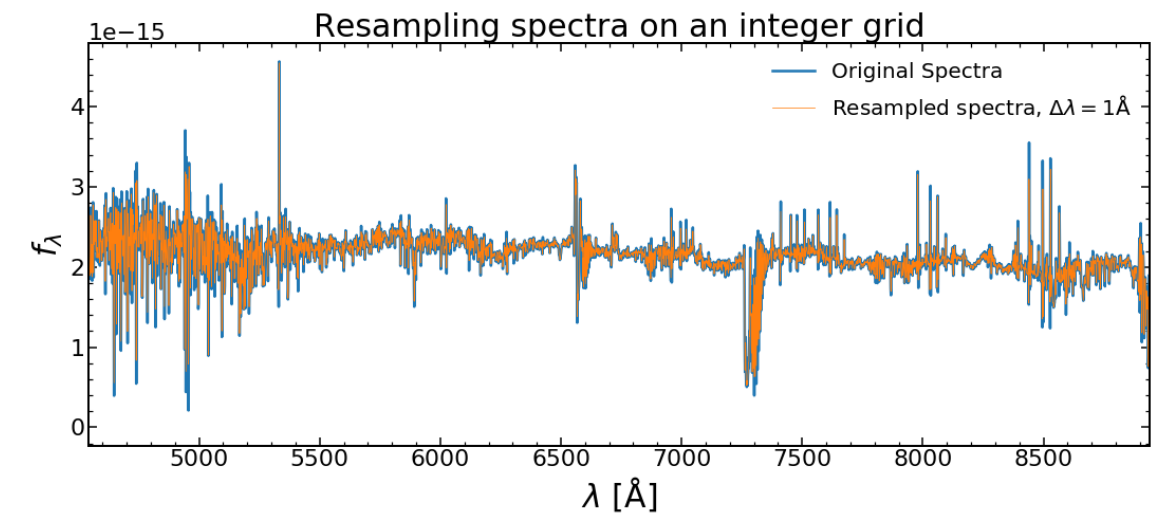
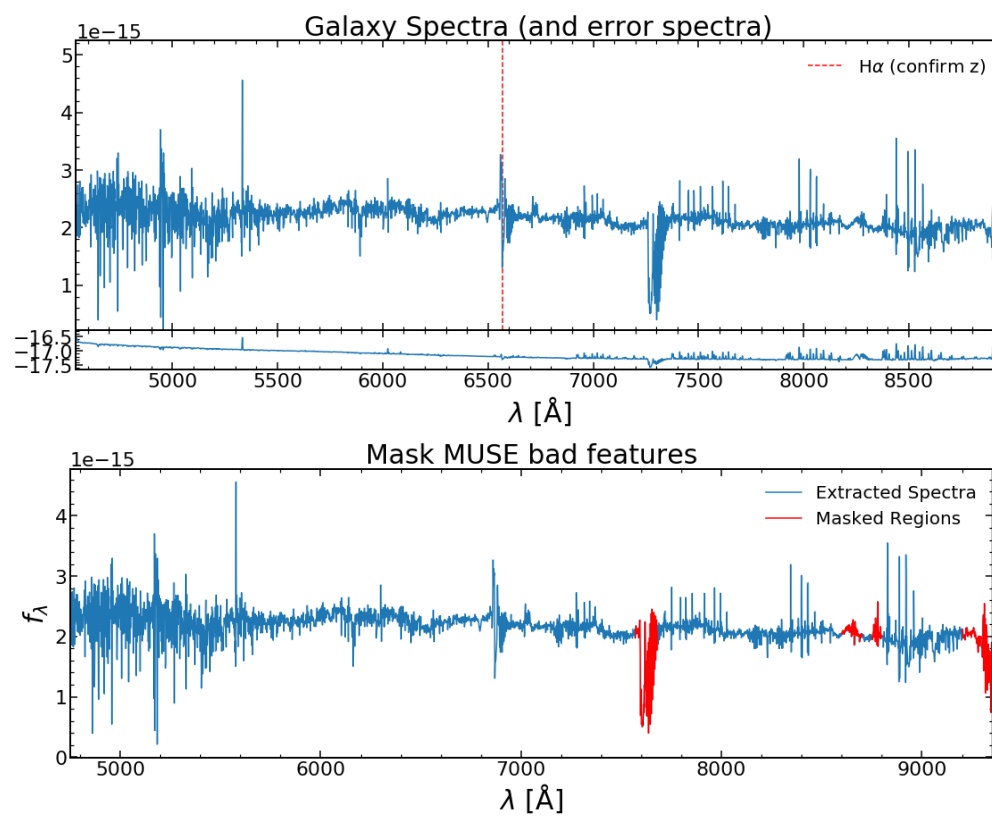
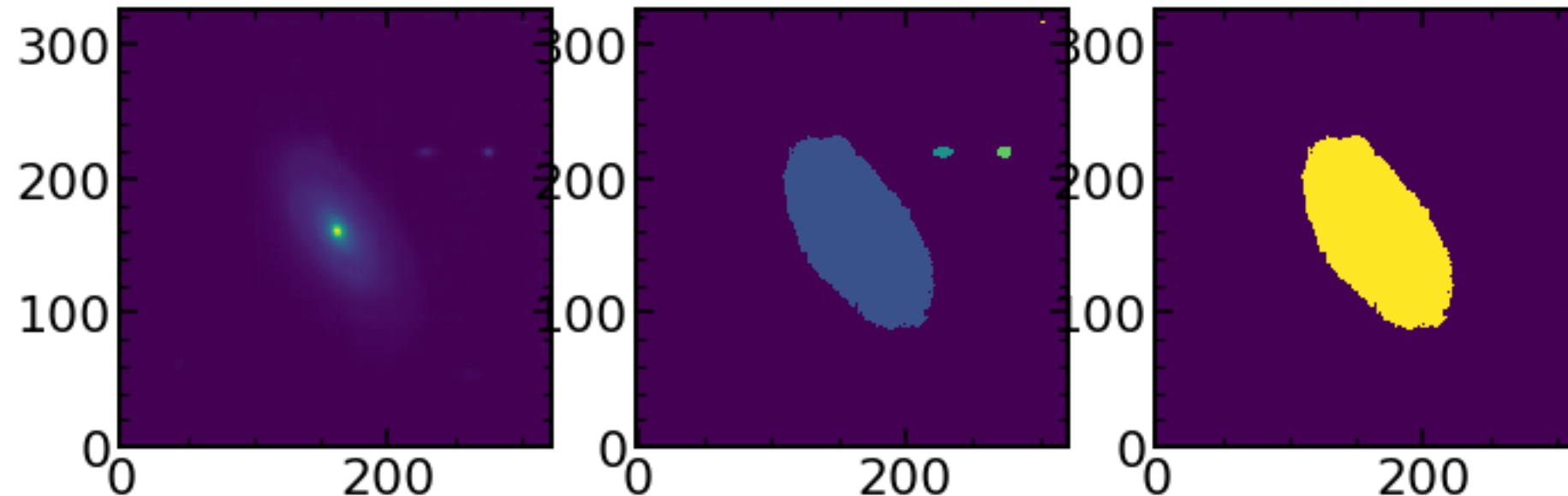


Exploration of the degeneracies for LSQ12cid

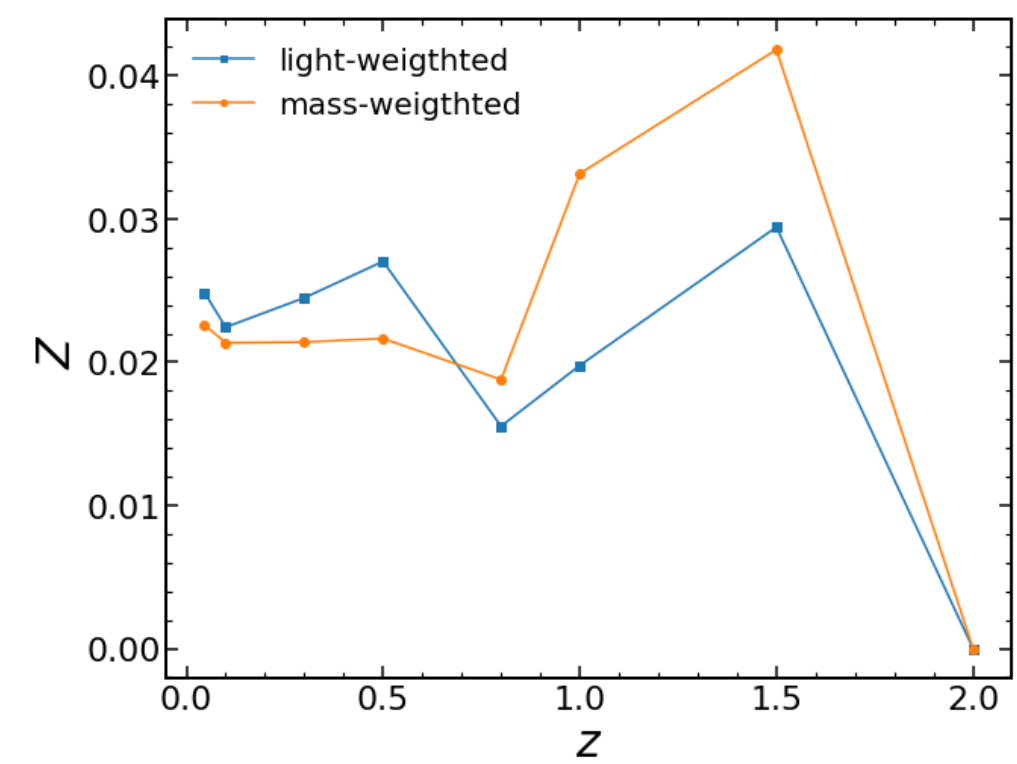
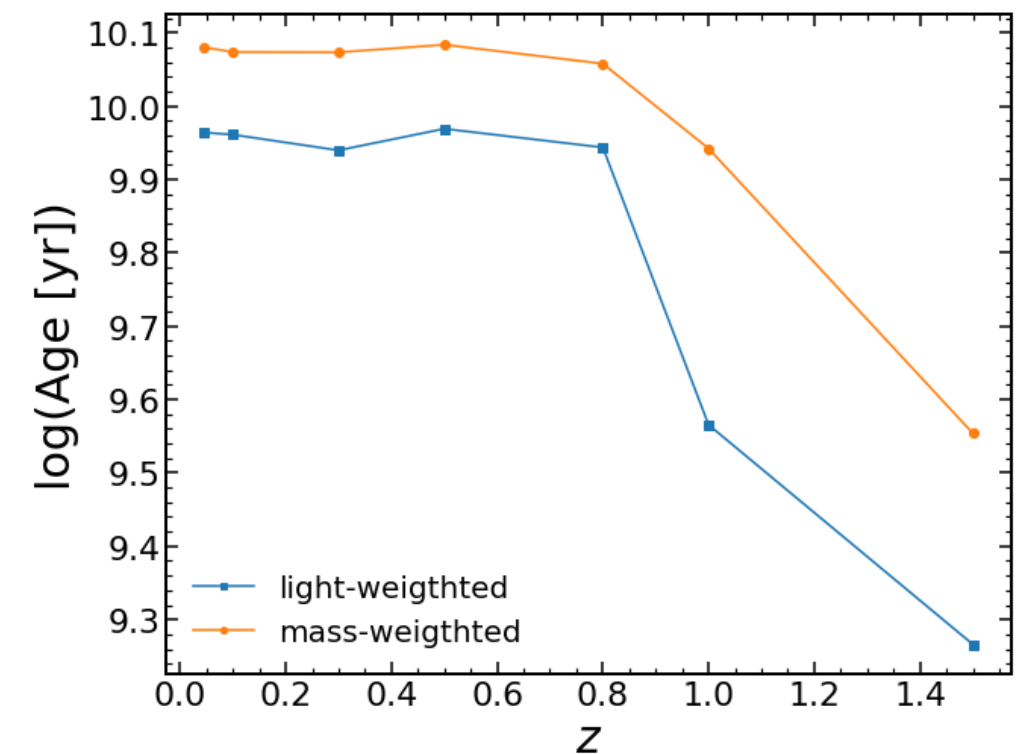
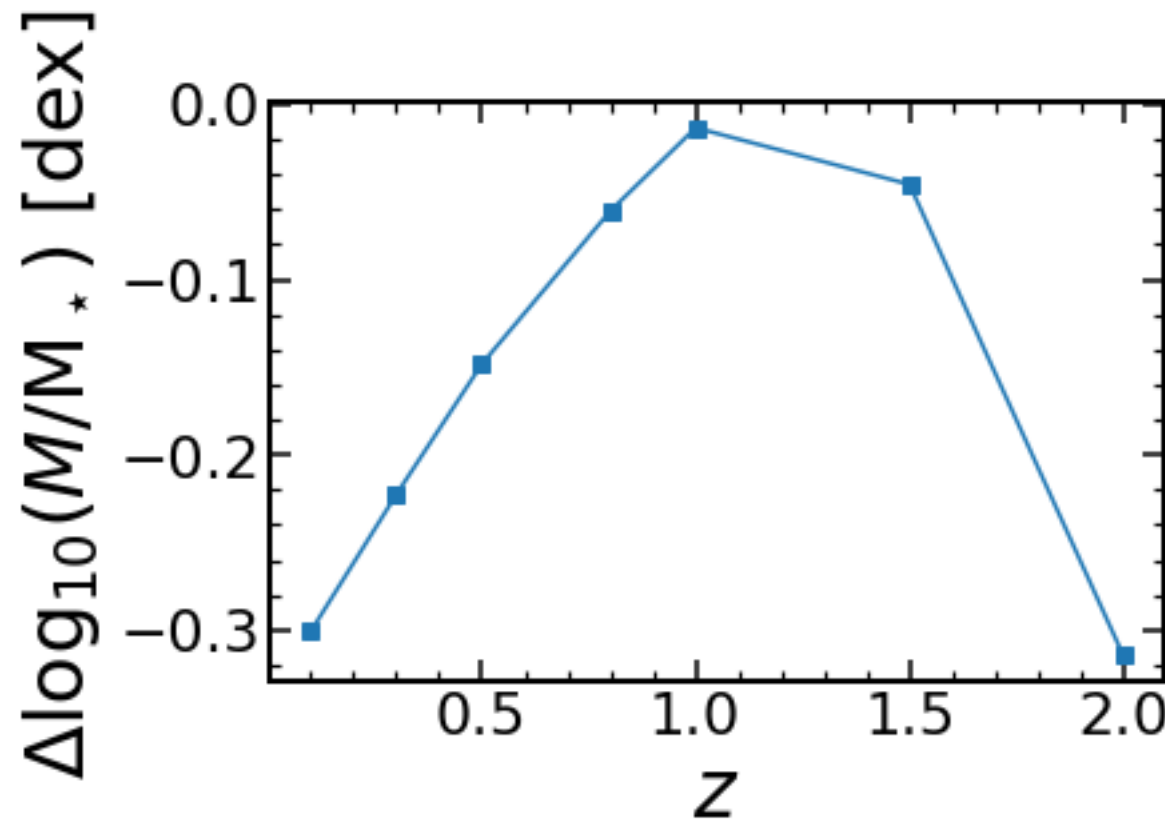
This is the most significant correlation that introduces the systematic biases in the stellar masses and is correlated with the best-fit stellar age (that is coupled to the individual SFH). I.e., the biggest cause of systematic differences in the catastrophic failures is due to the large range of used SFHs, and a degeneracy of the models when using only 4 filters in the optical rest-frame region.



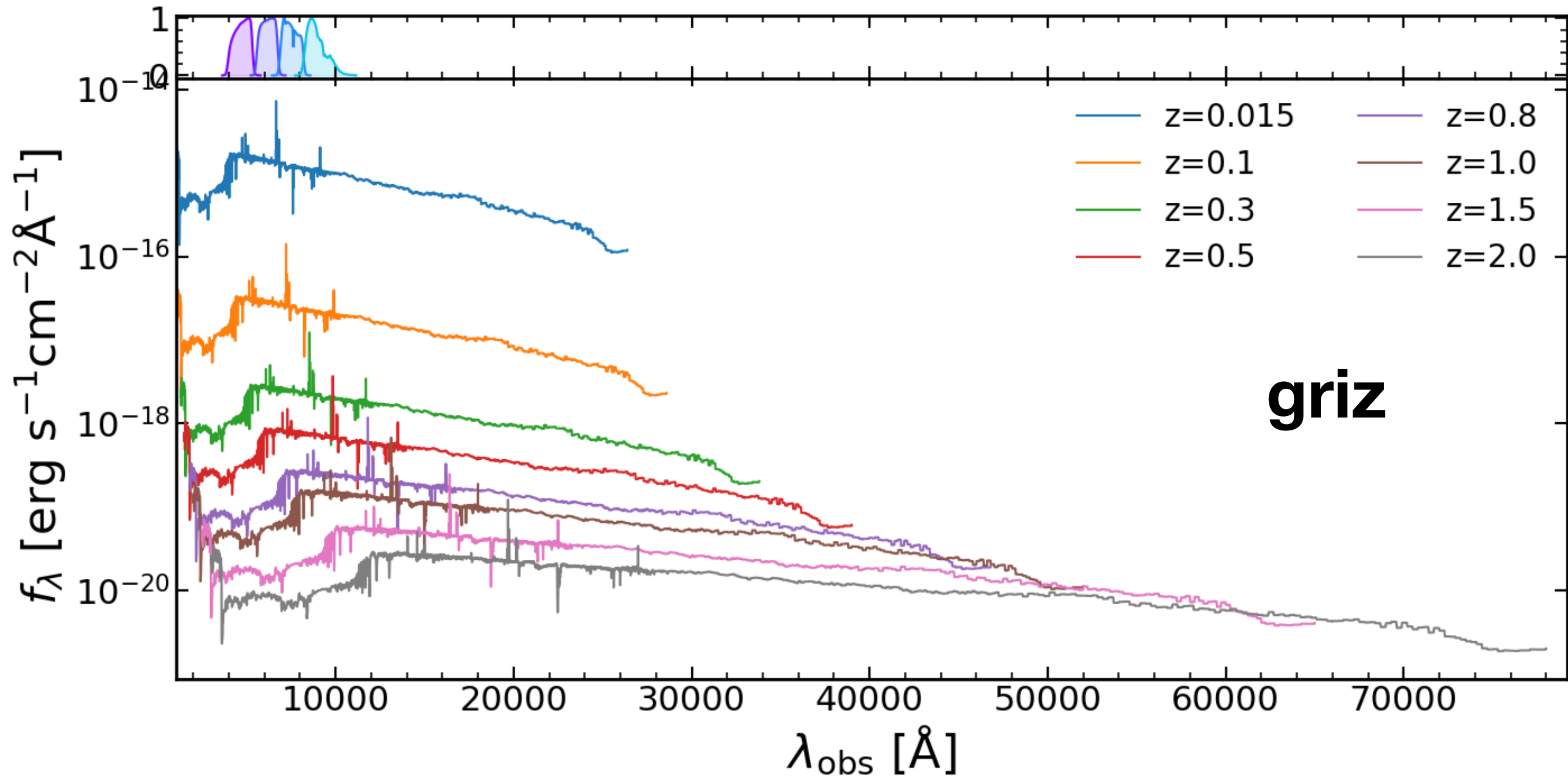
1-D approach



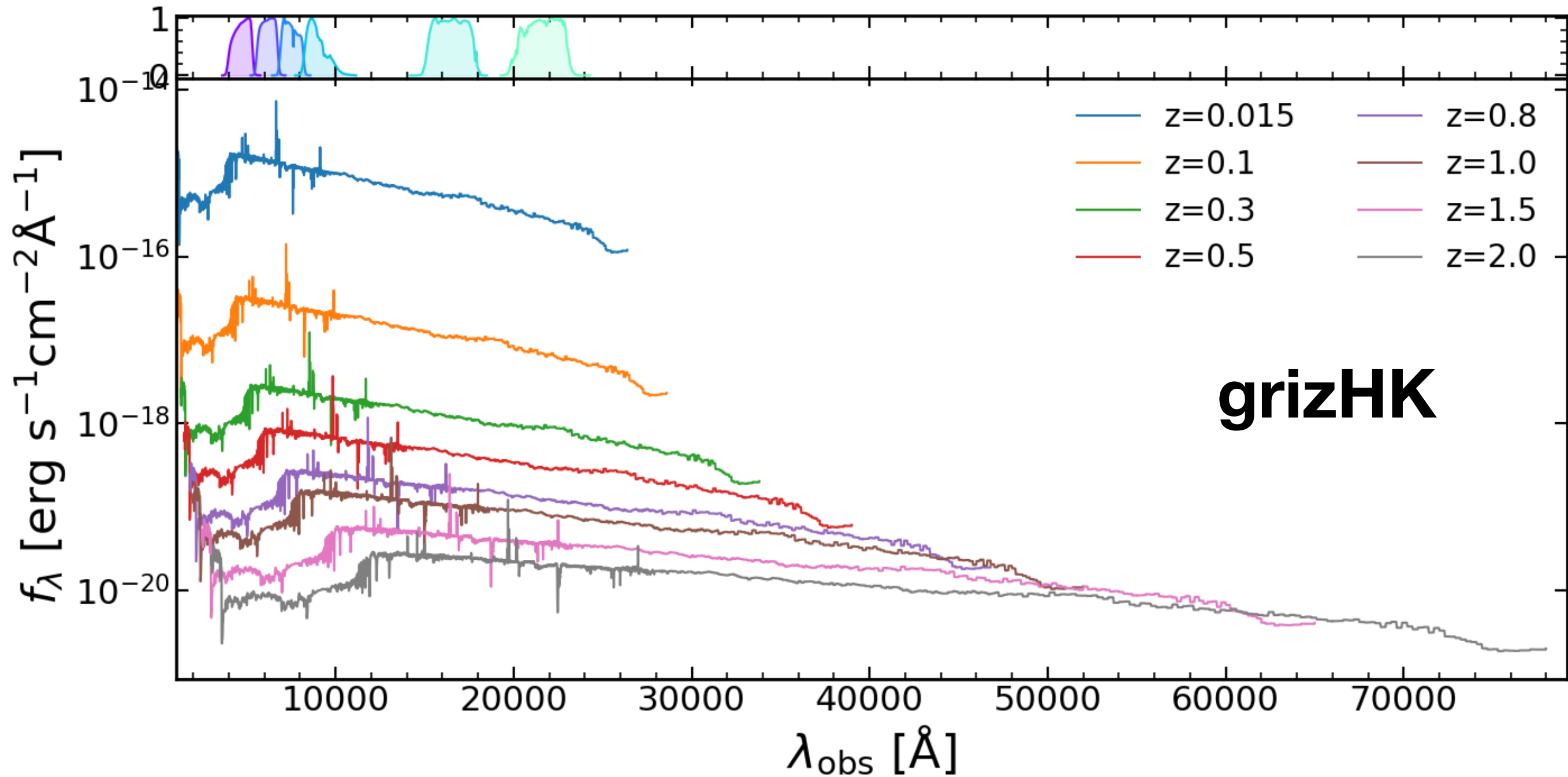
1-D approach



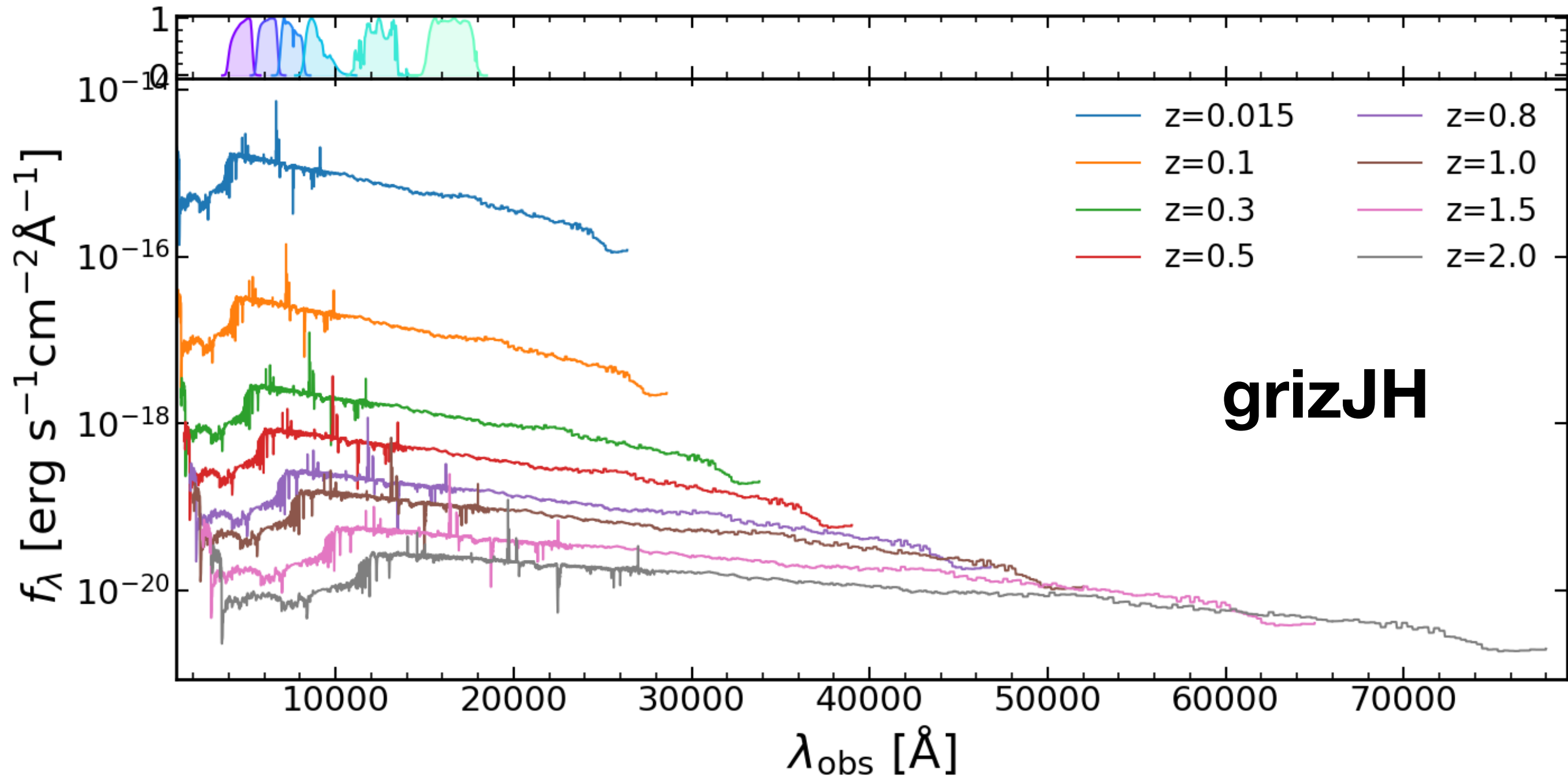
Broad Band Photometry



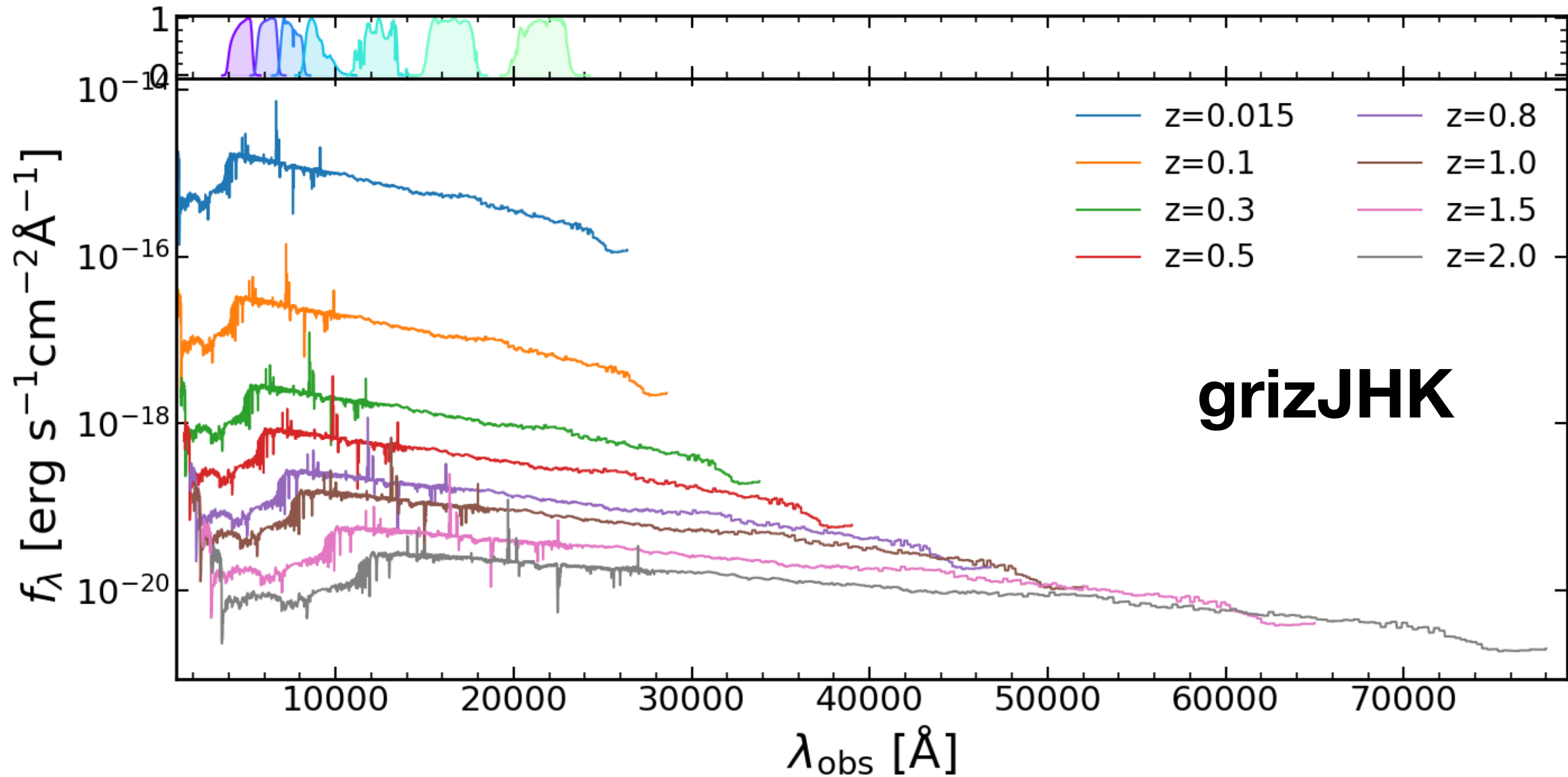
Broad Band Photometry



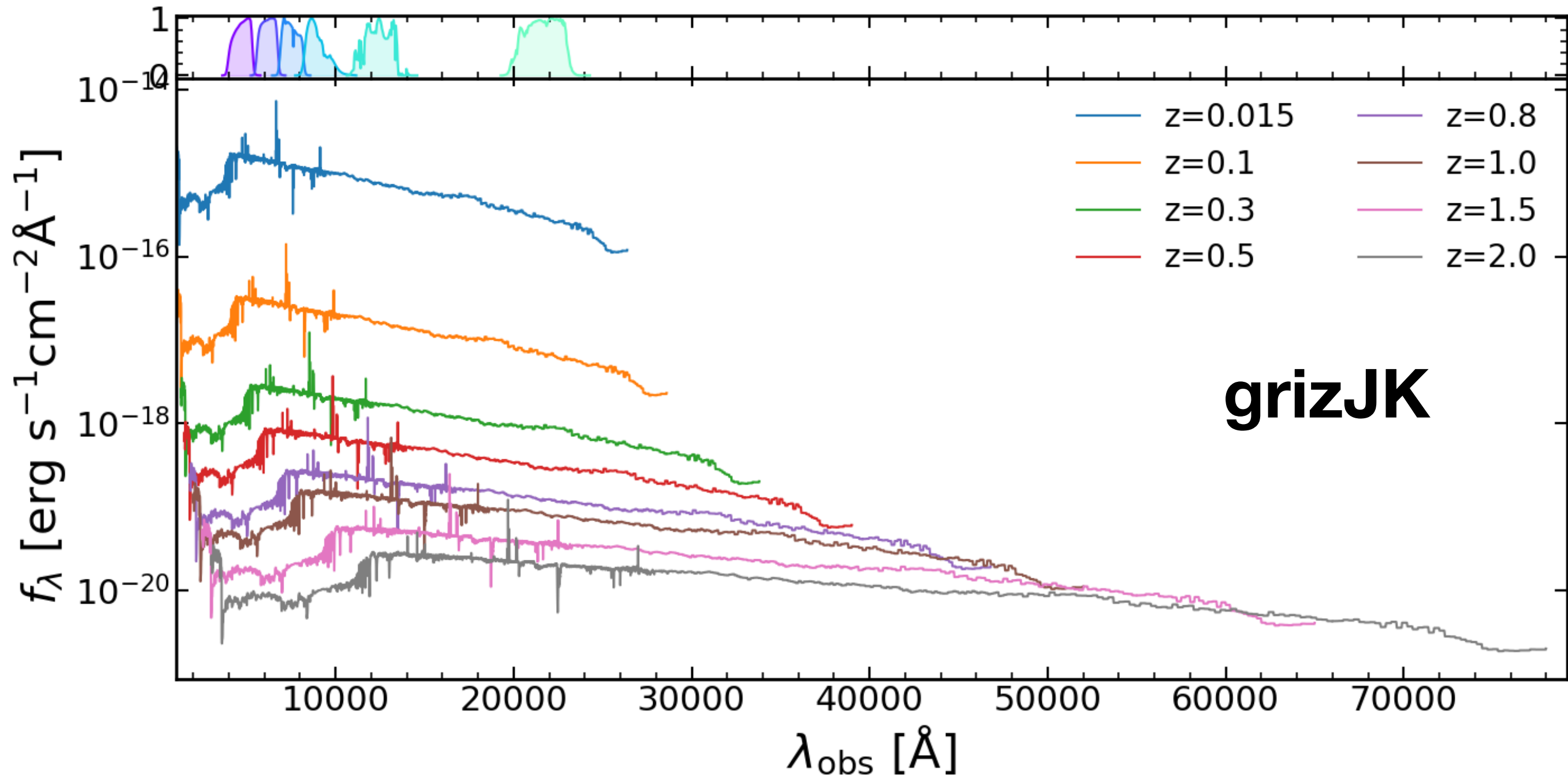
Broad Band Photometry



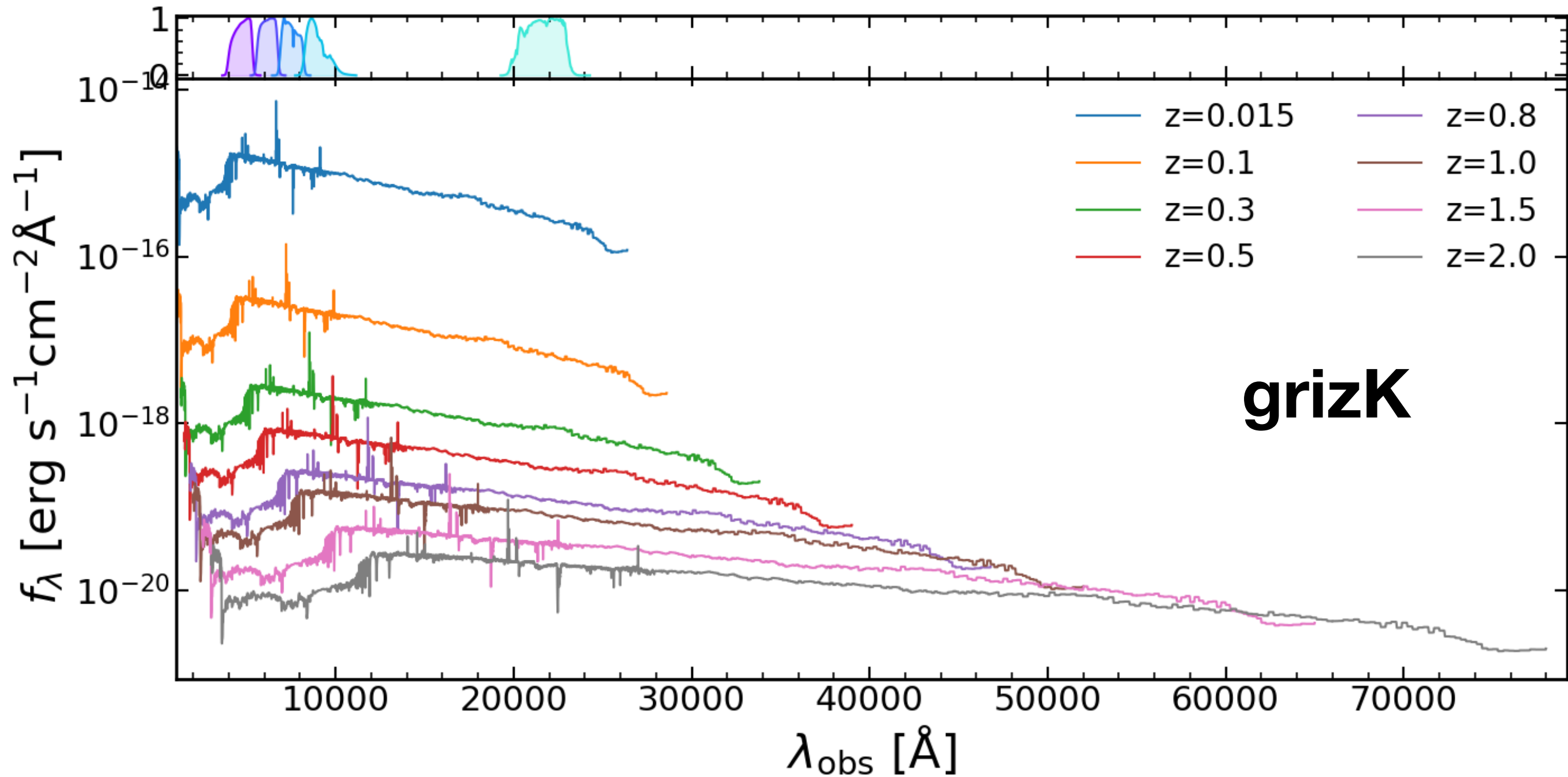
Broad Band Photometry



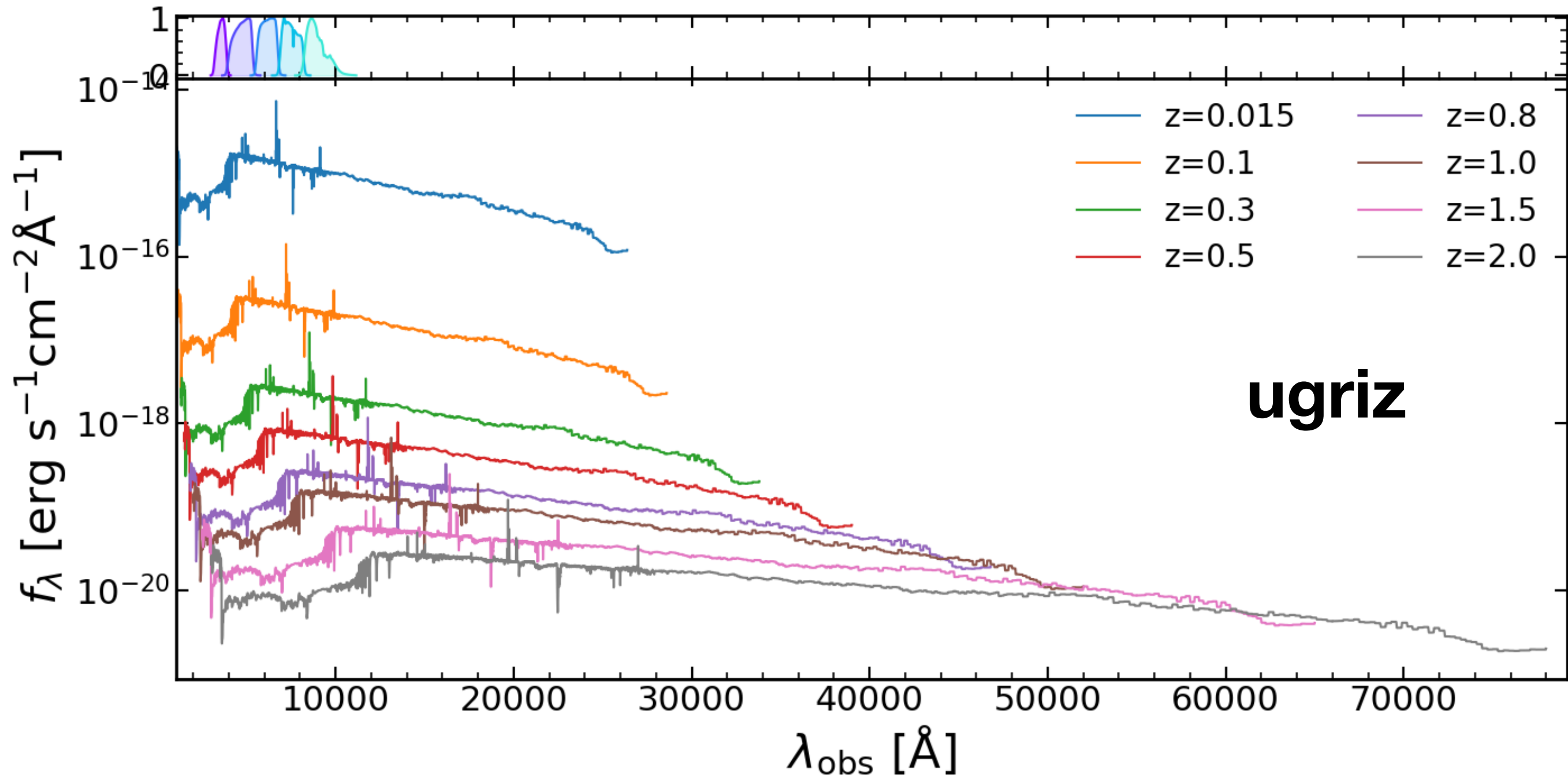
Broad Band Photometry



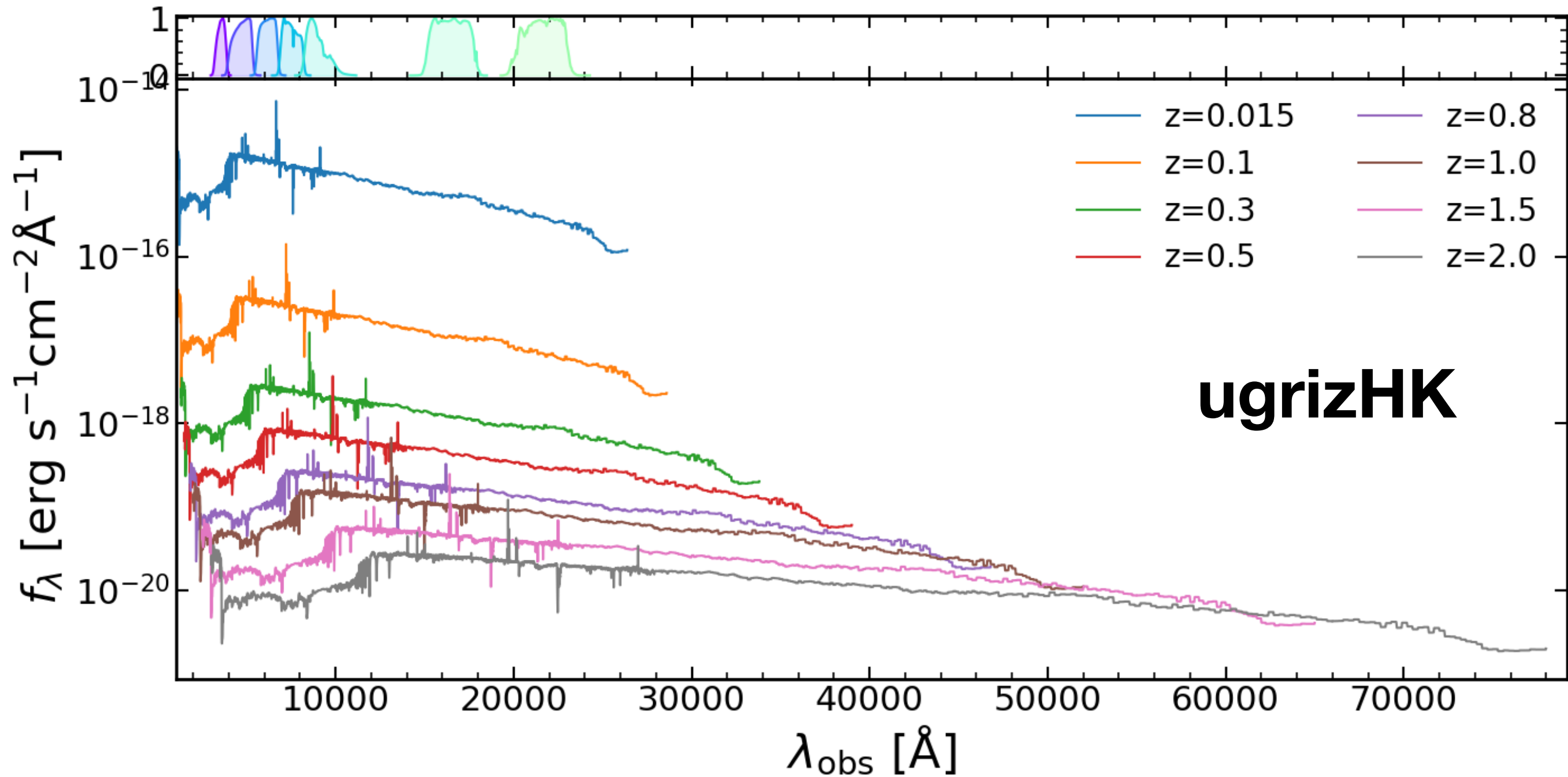
Broad Band Photometry



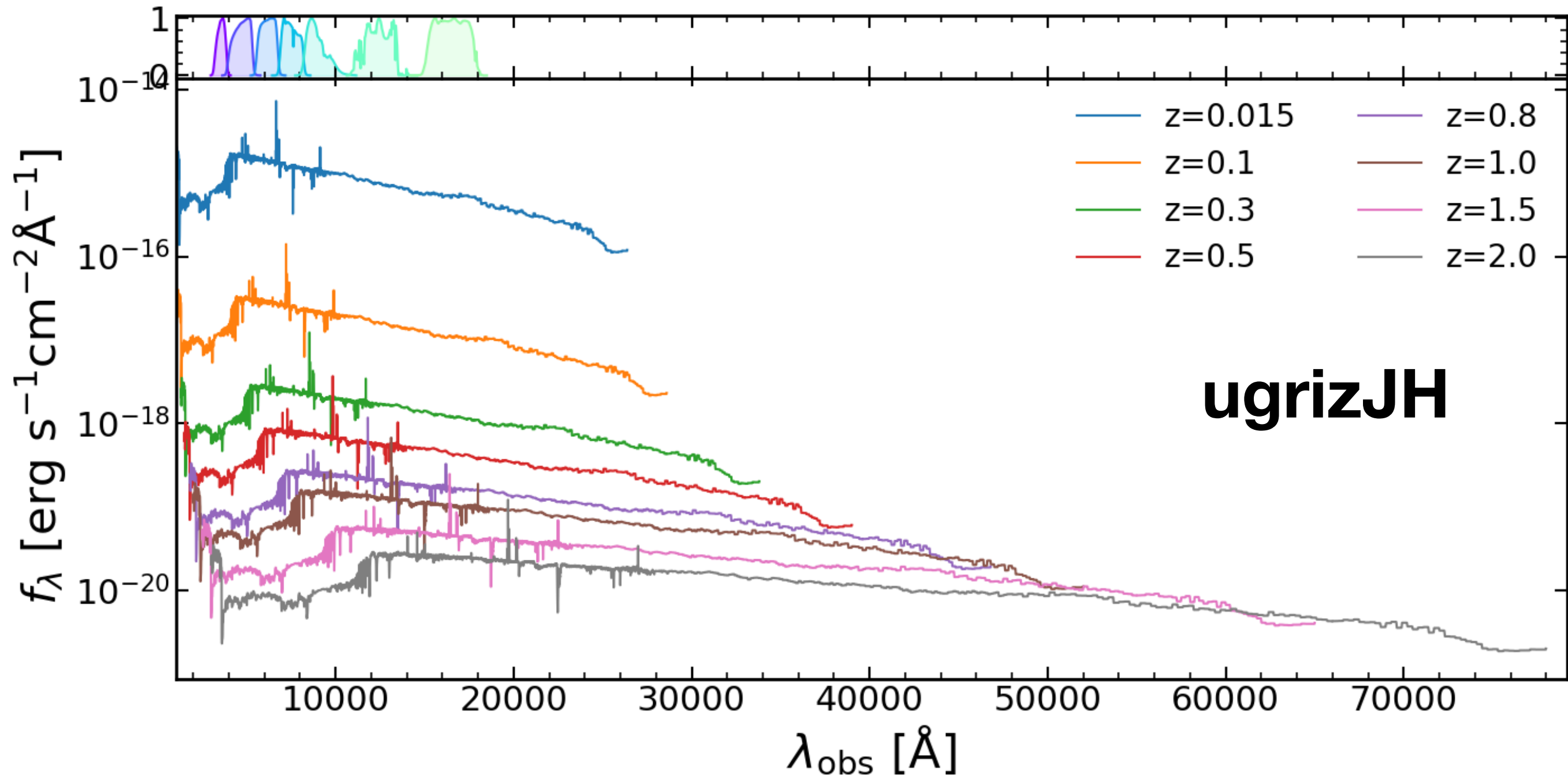
Broad Band Photometry



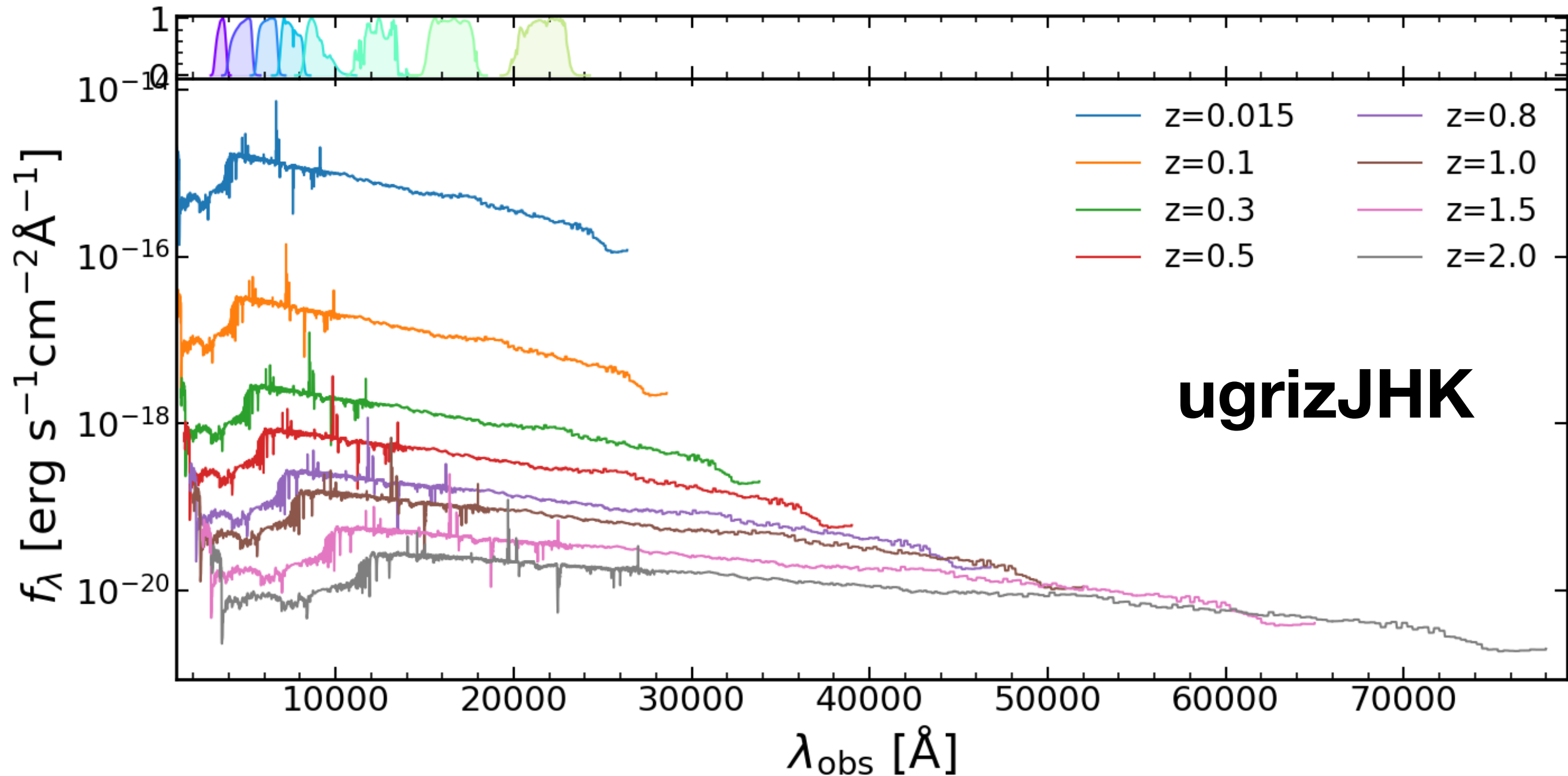
Broad Band Photometry



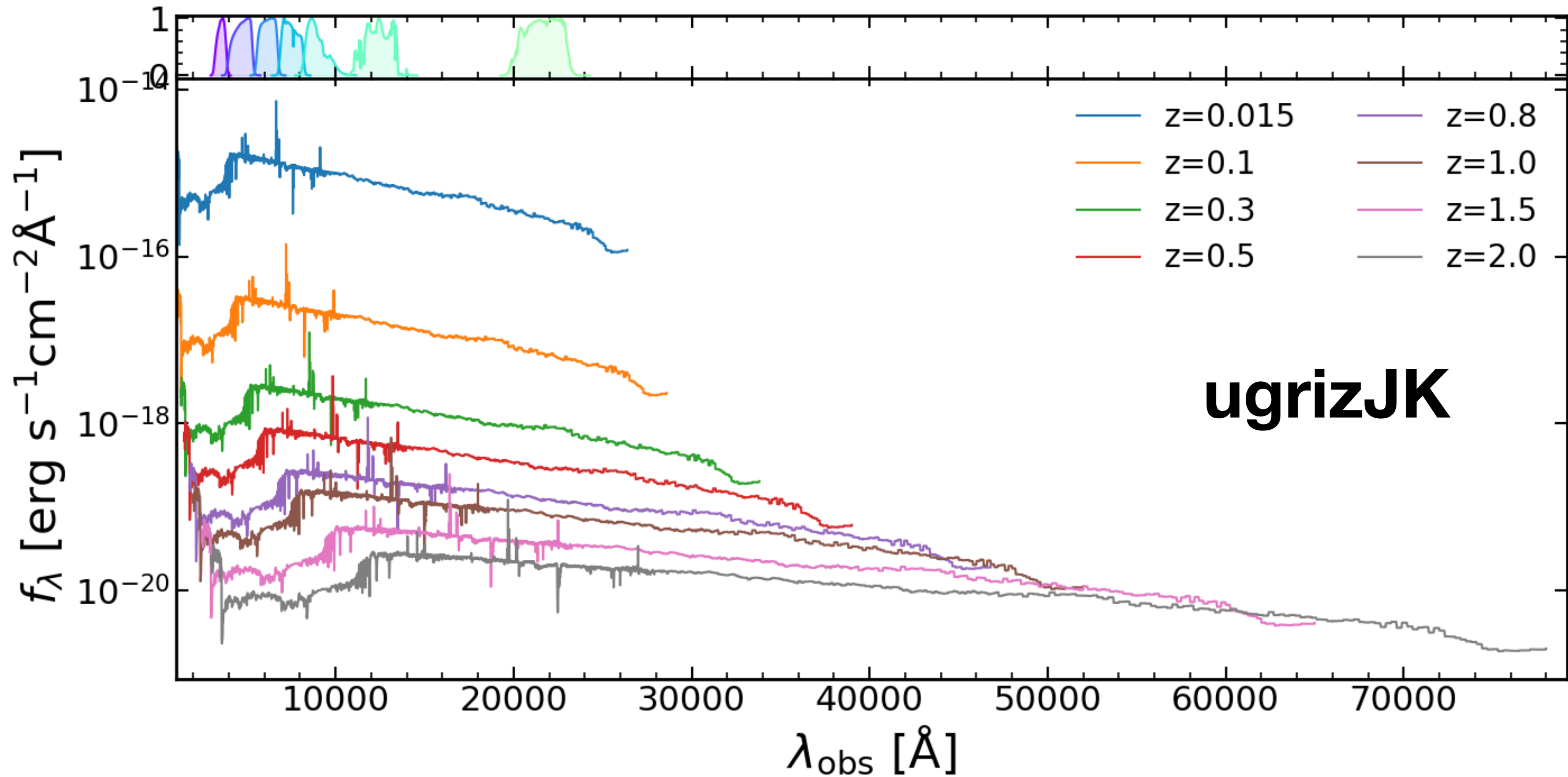
Broad Band Photometry



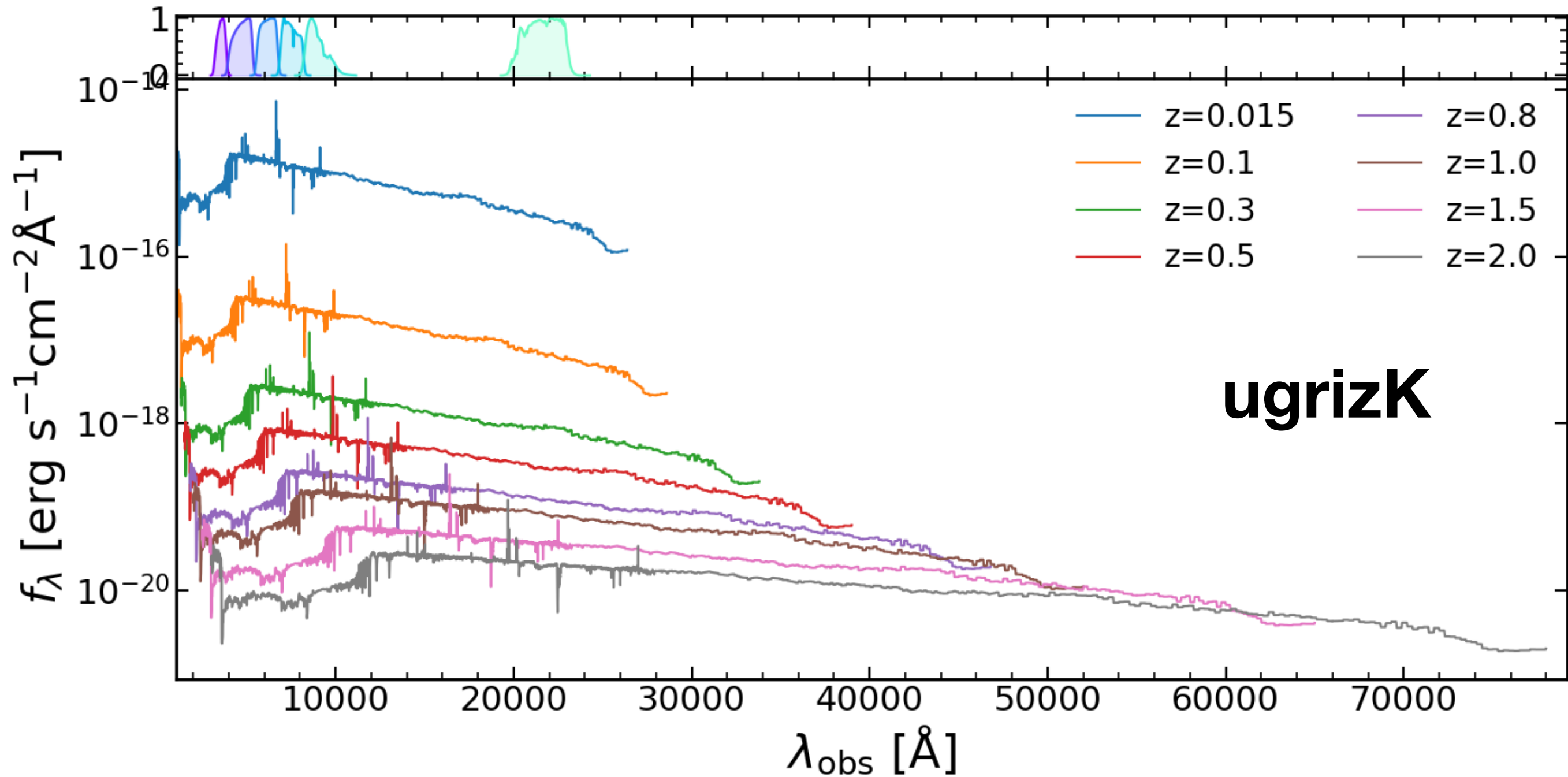
Broad Band Photometry



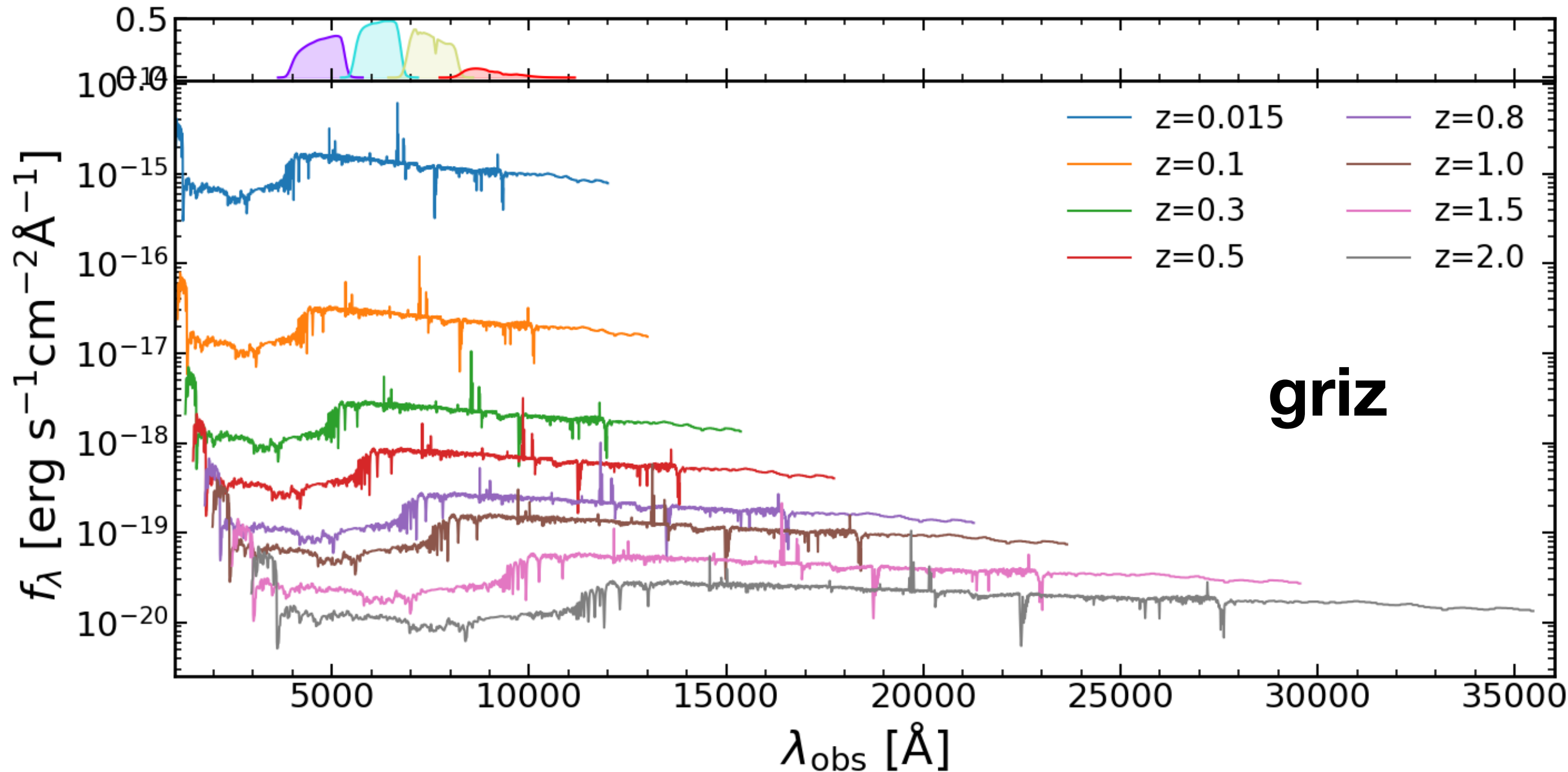
Broad Band Photometry



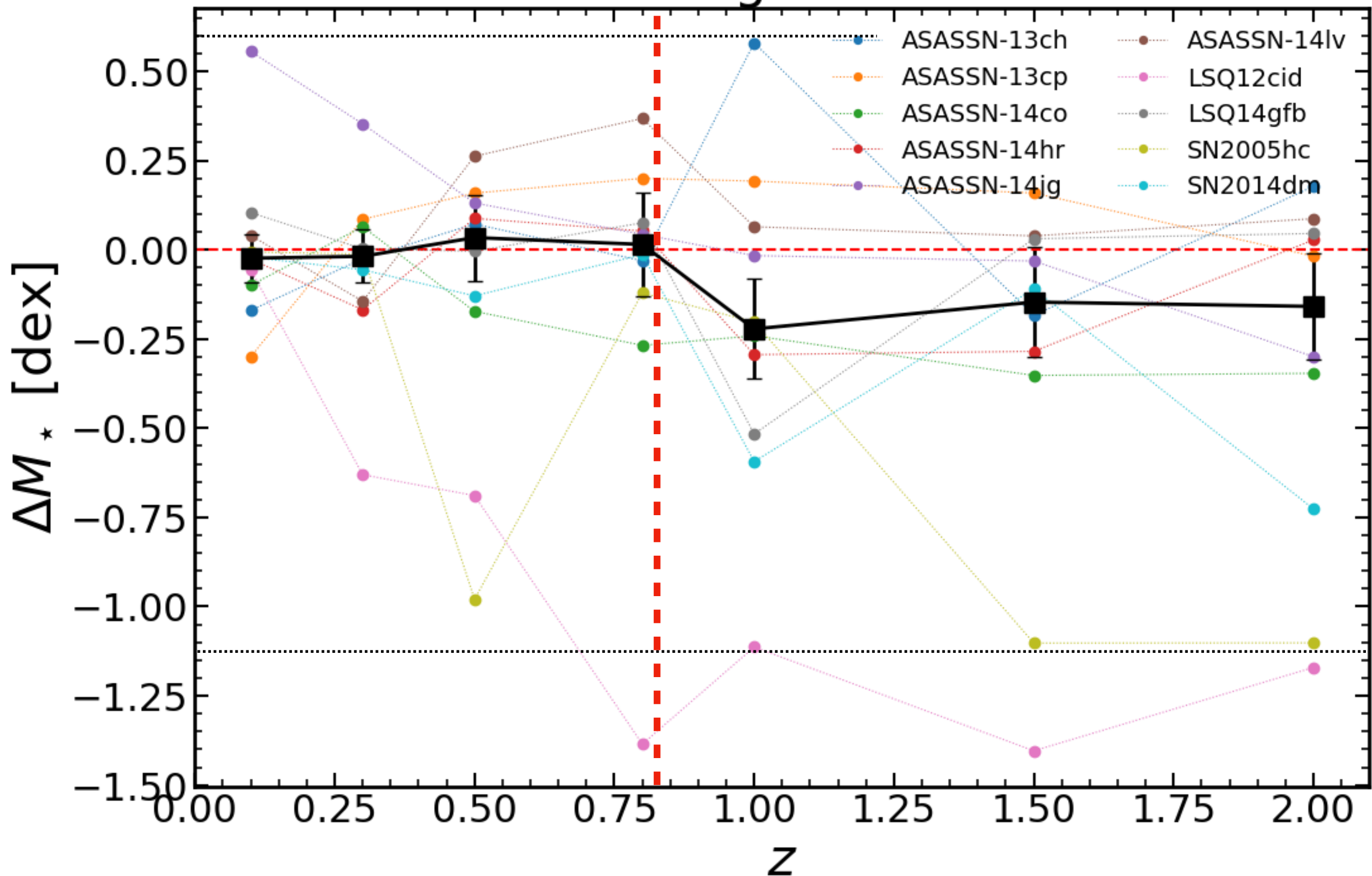
Broad Band Photometry



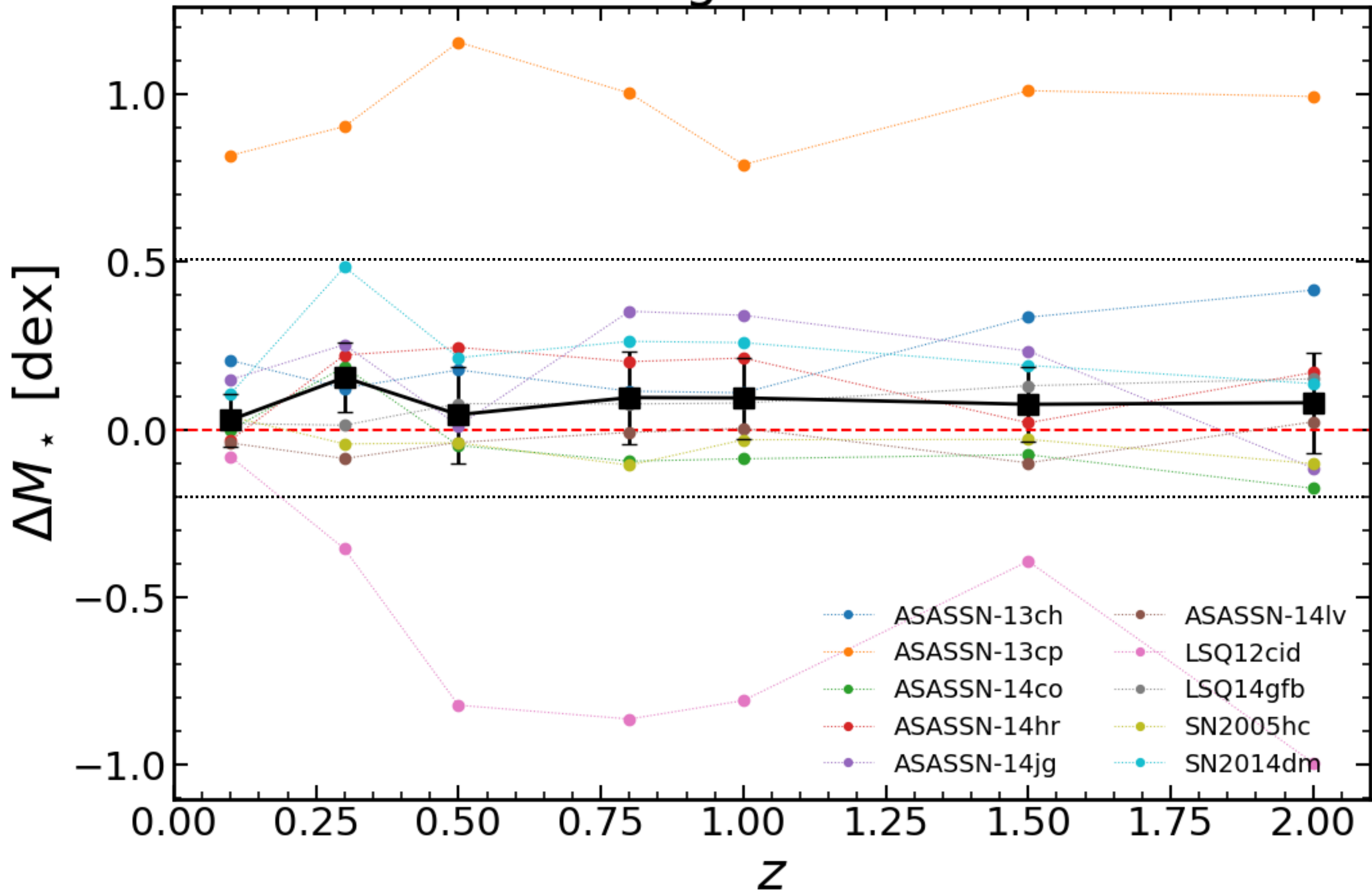
Broad Band Photometry



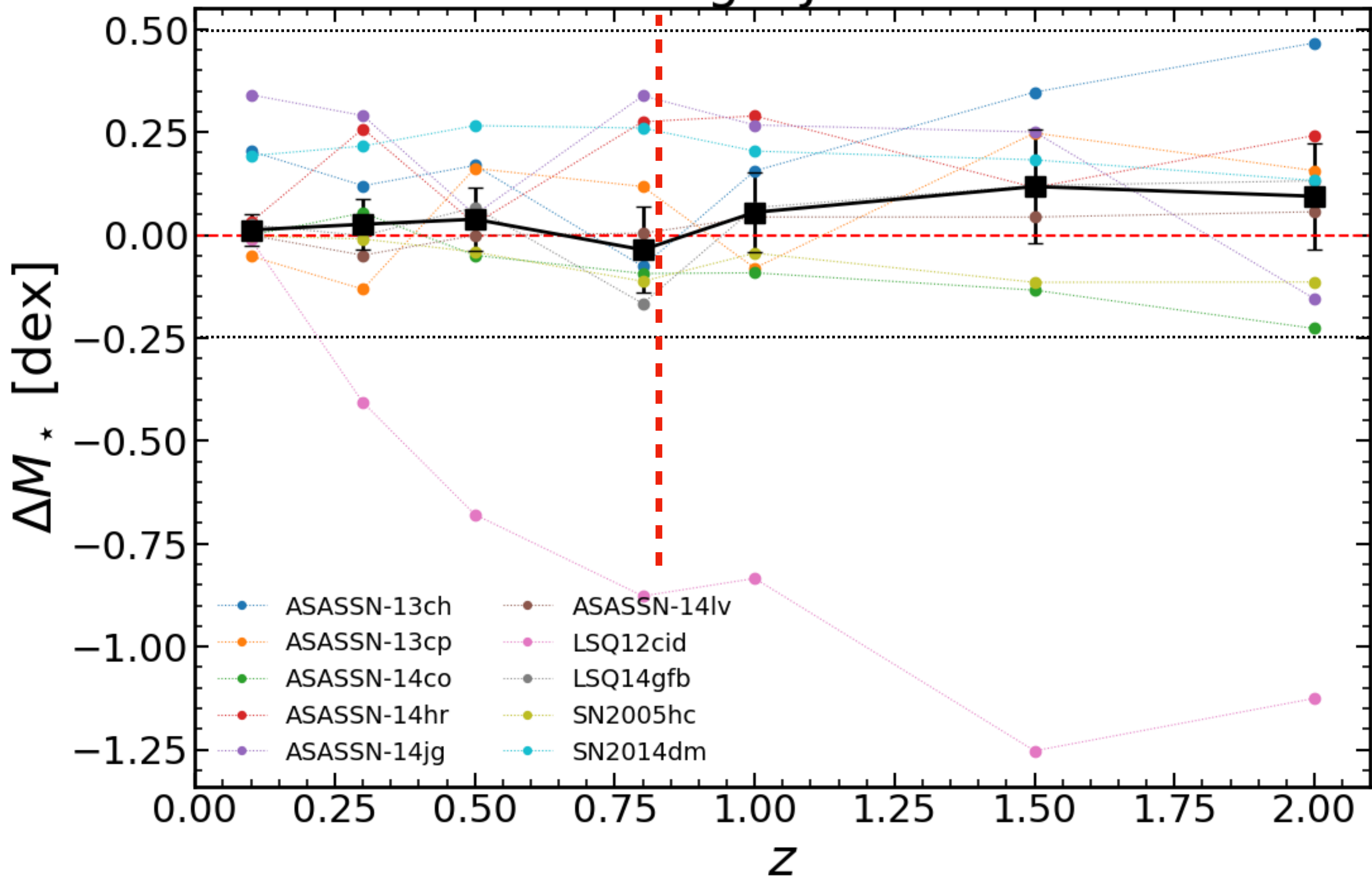
griz



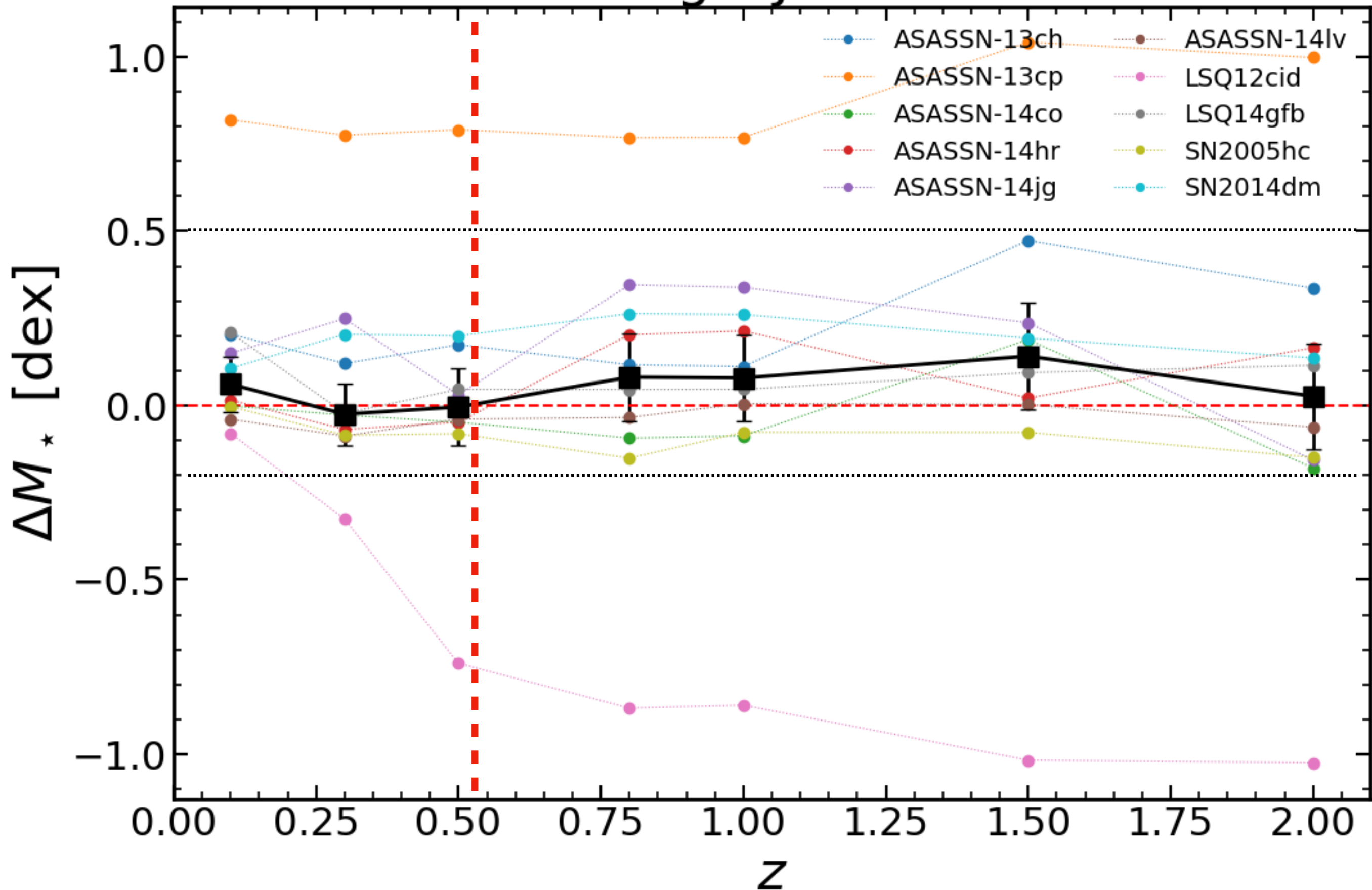
grizHK



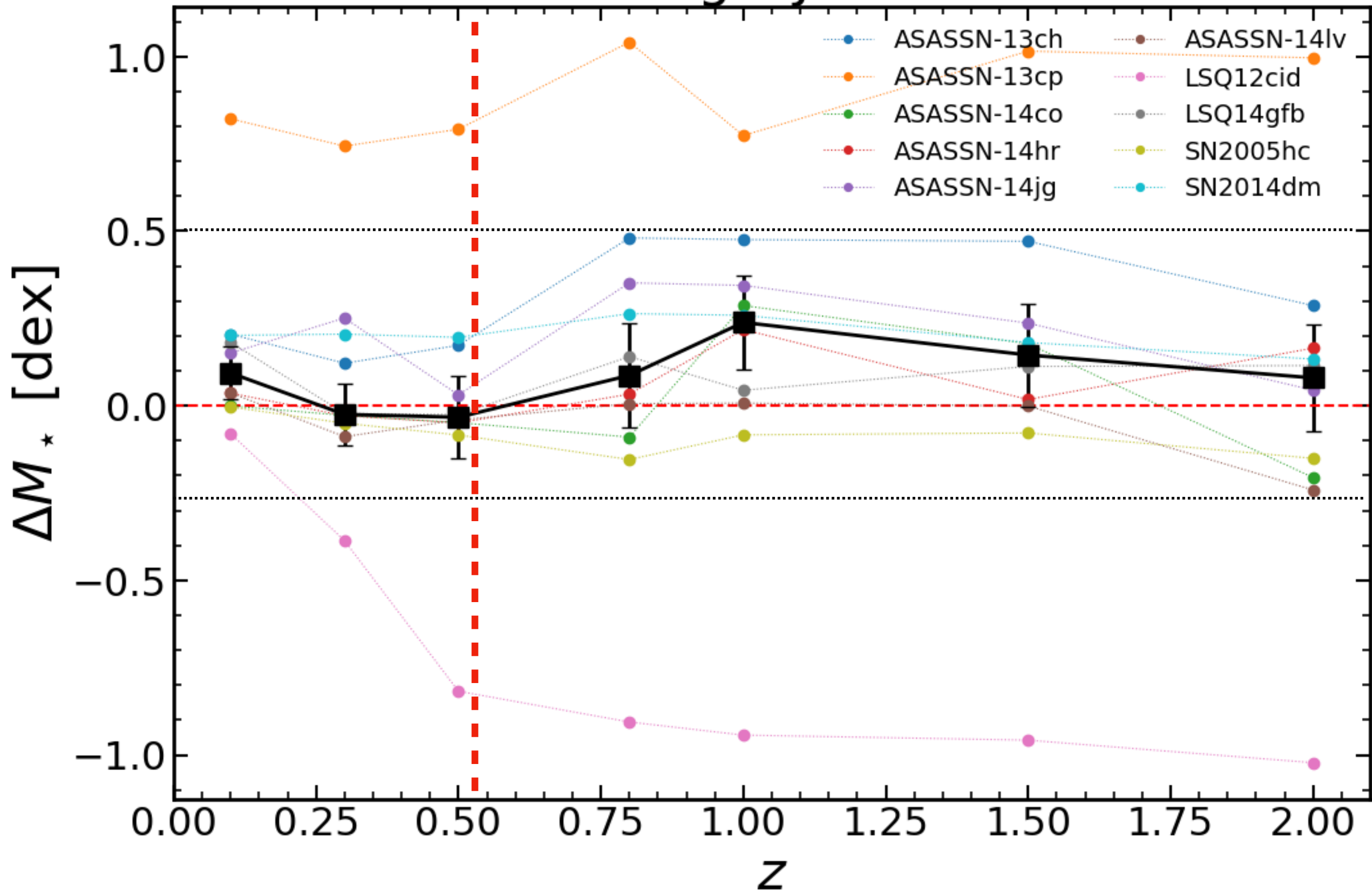
grizJH



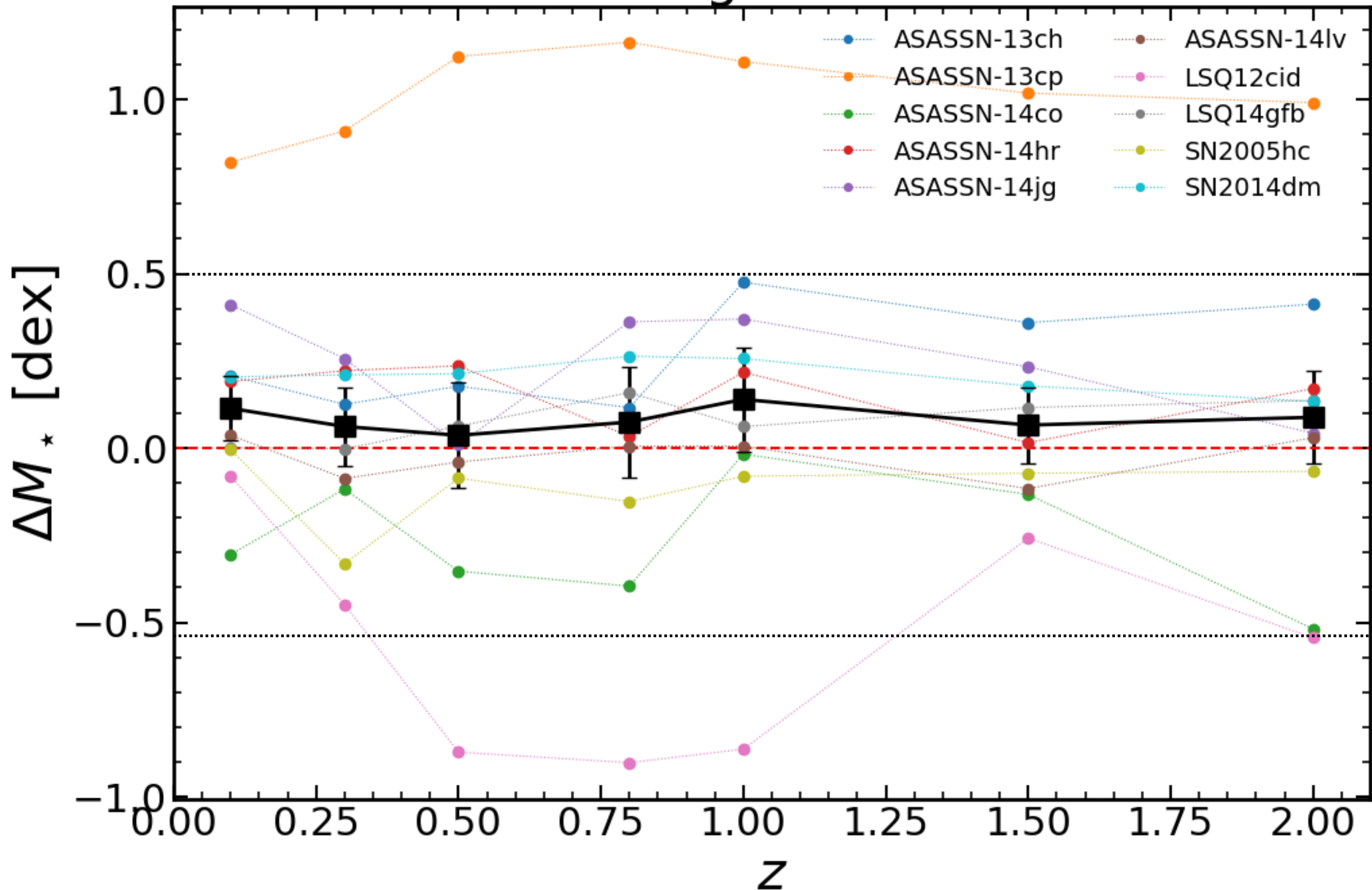
grizJHK



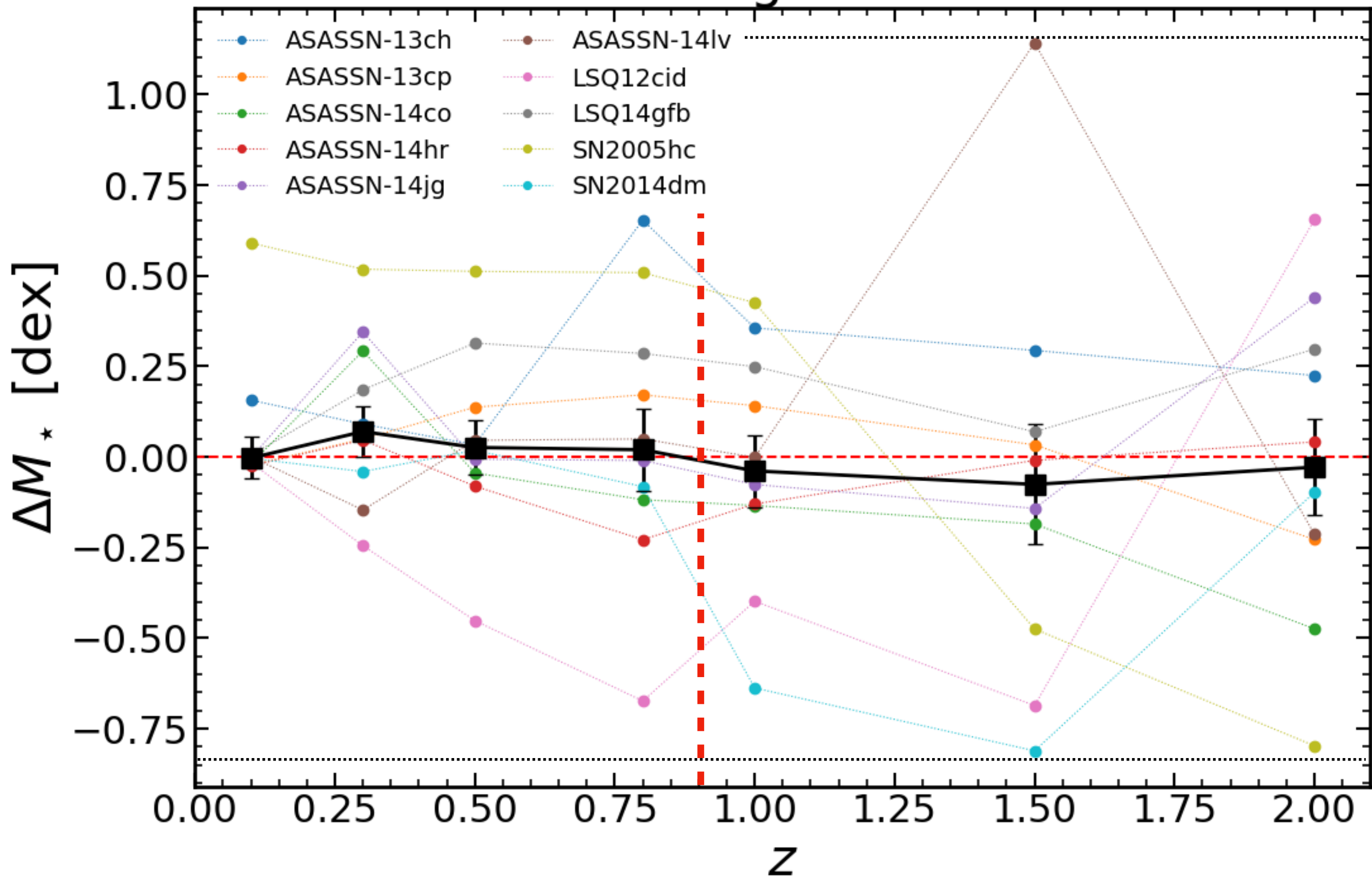
grizJK



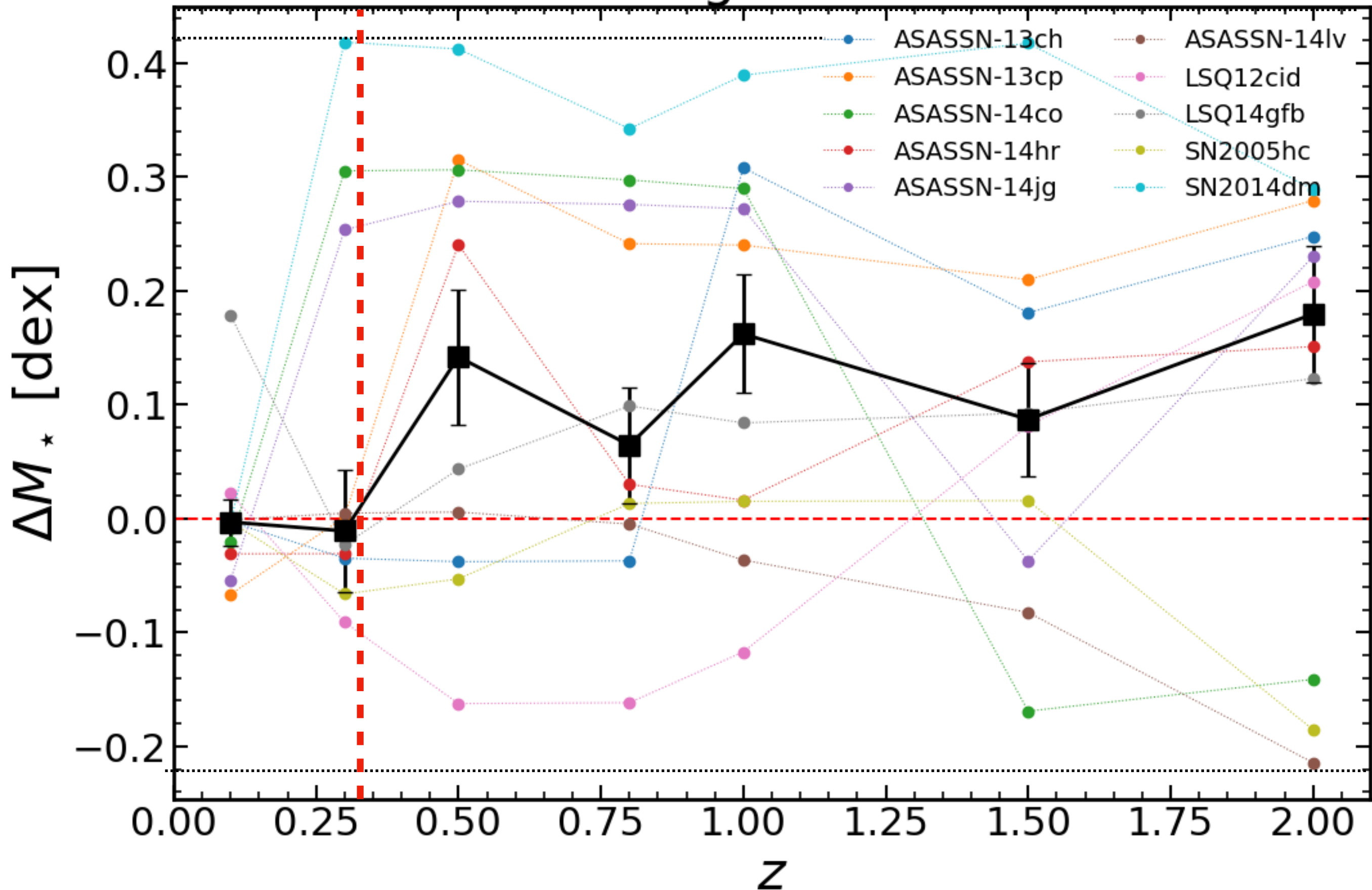
grizK



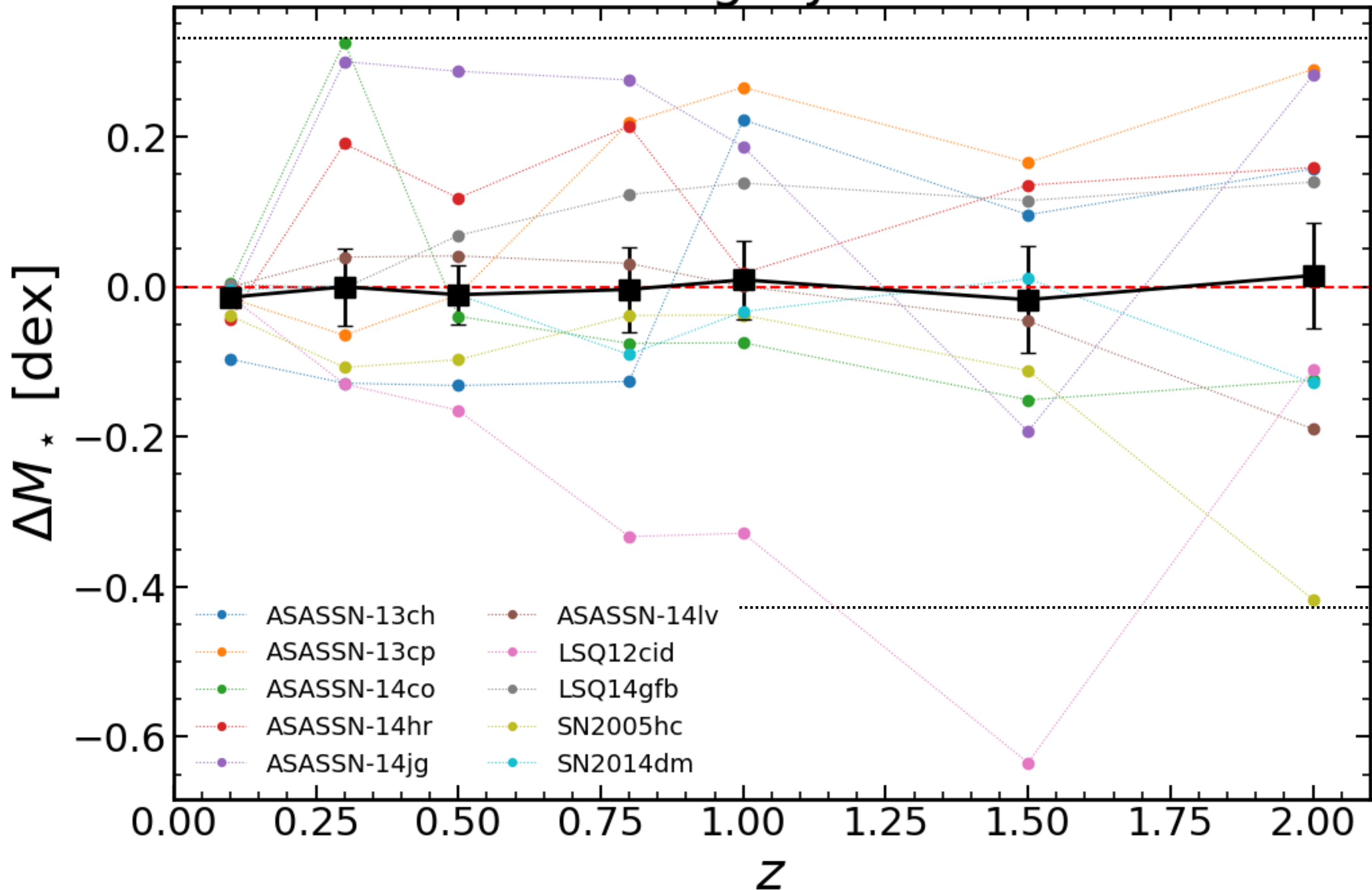
ugriz



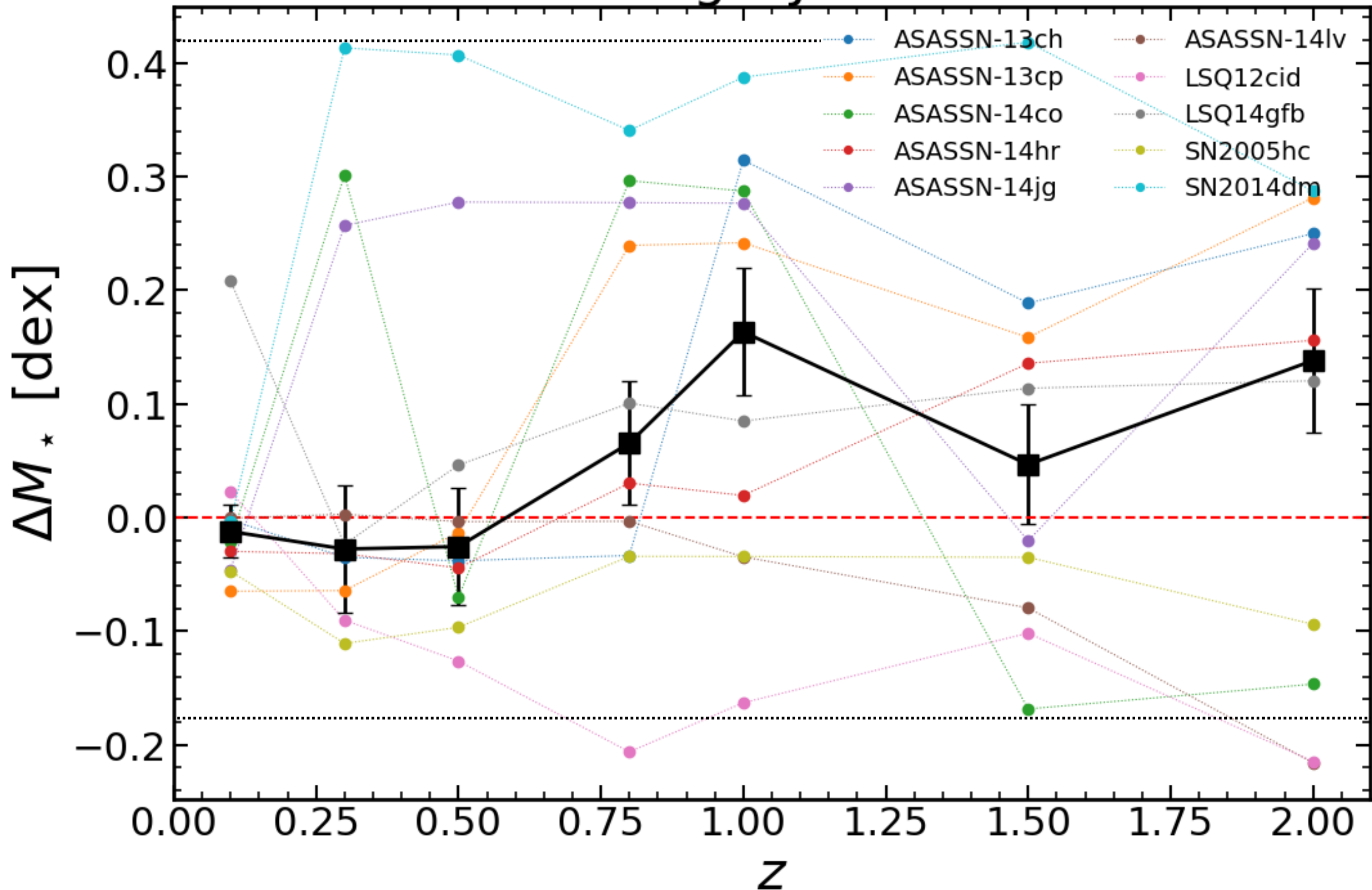
ugrizHK



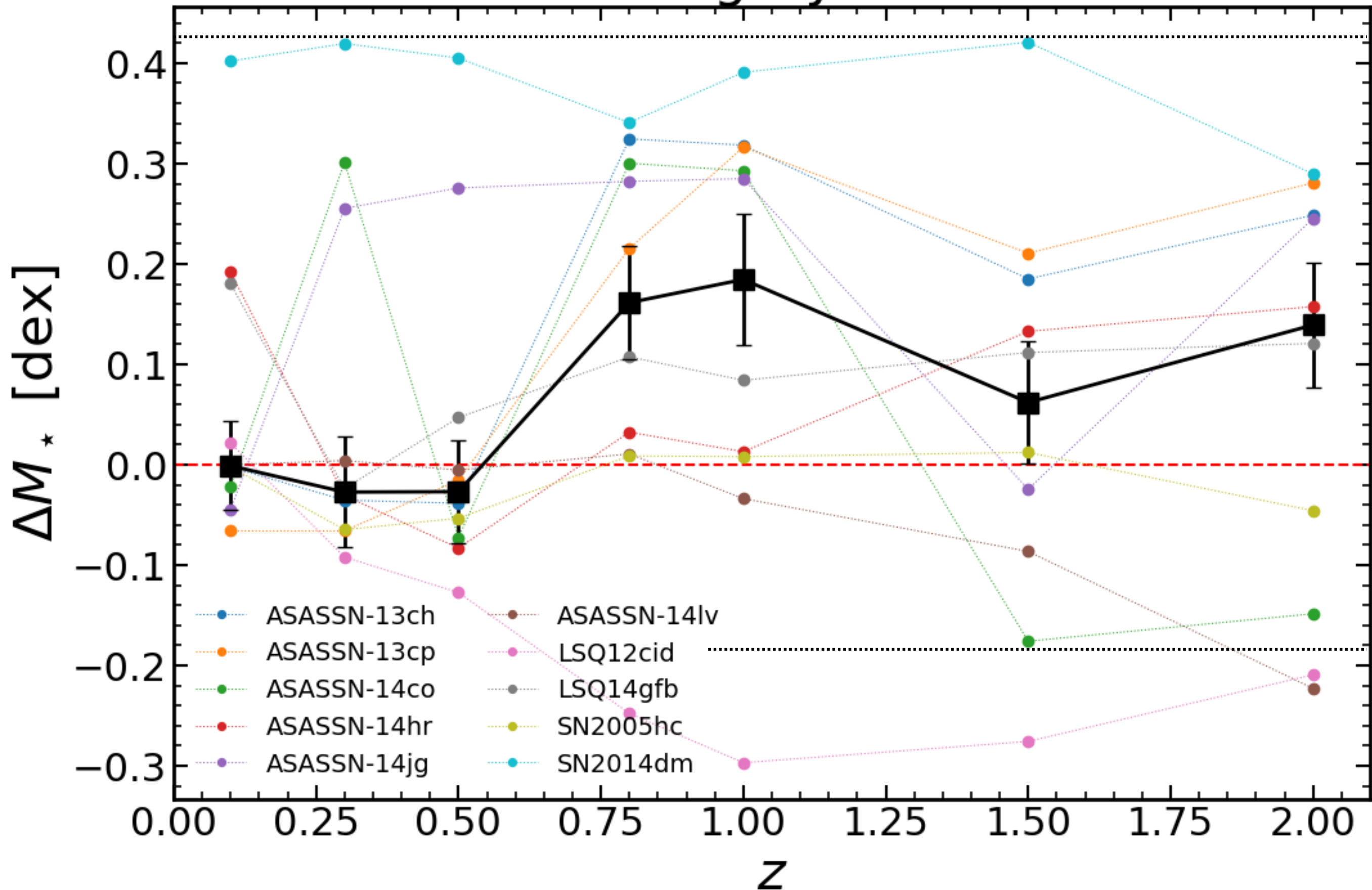
ugrizJH



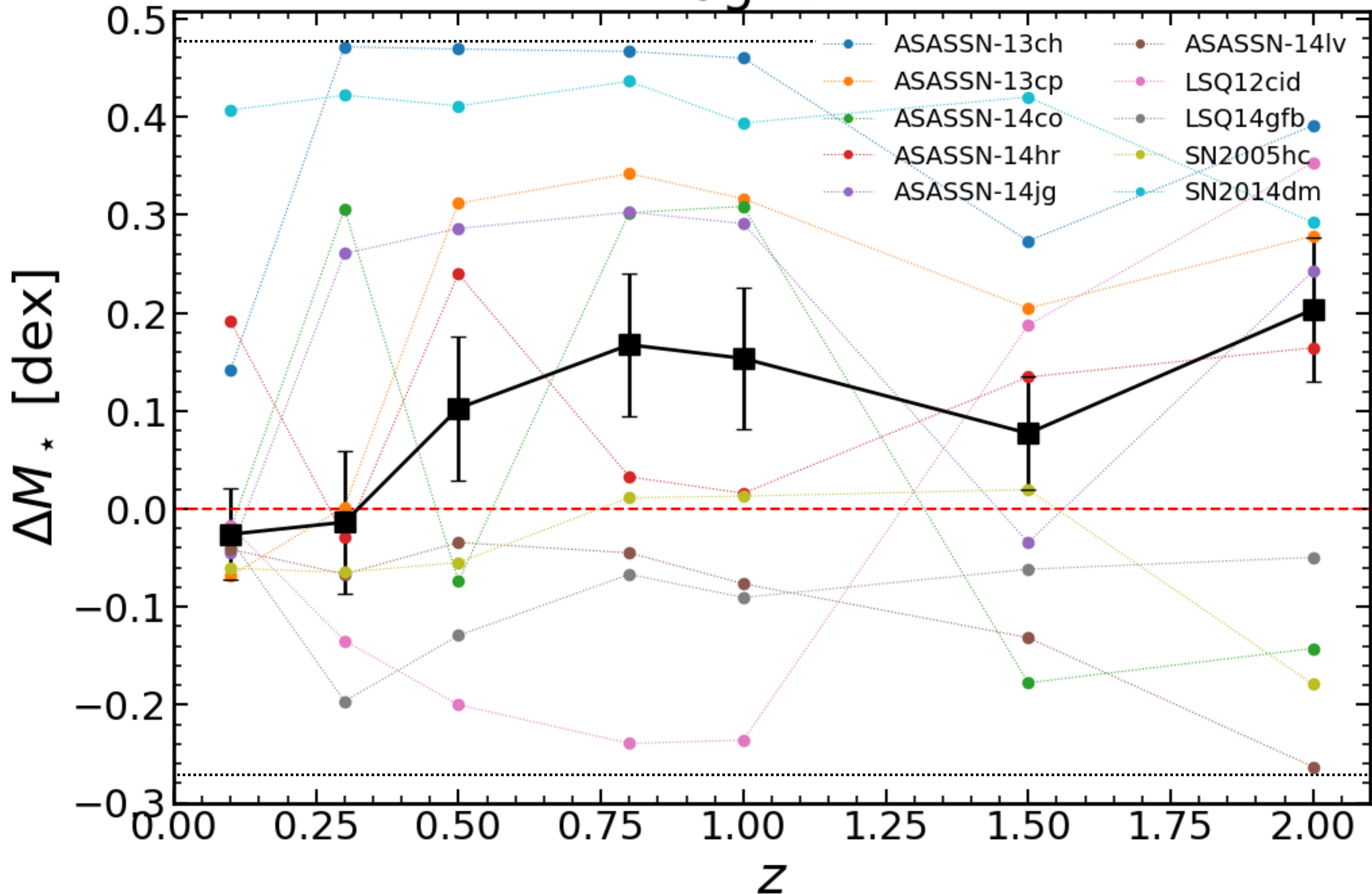
ugrizJHK

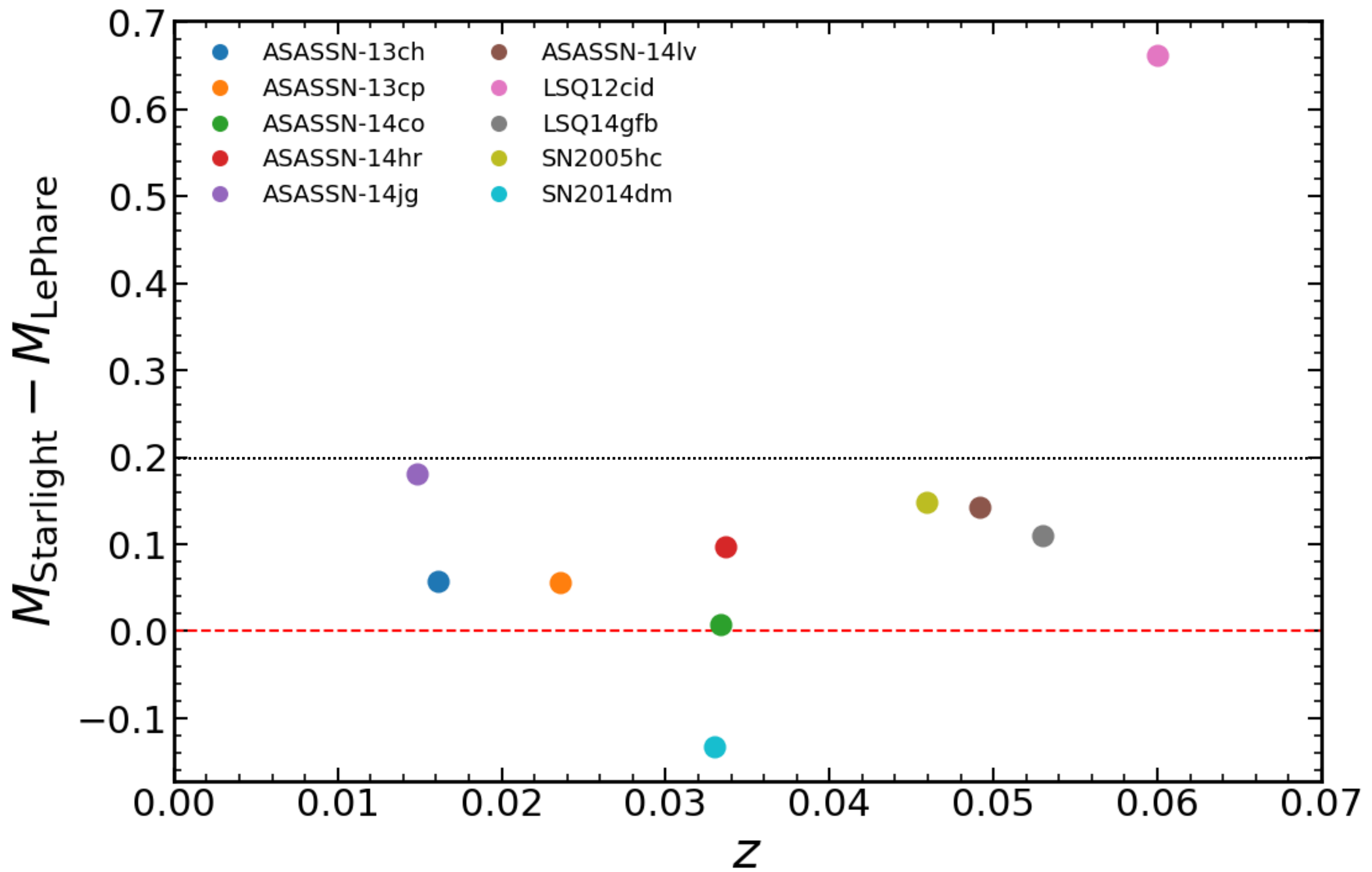


ugrizJK

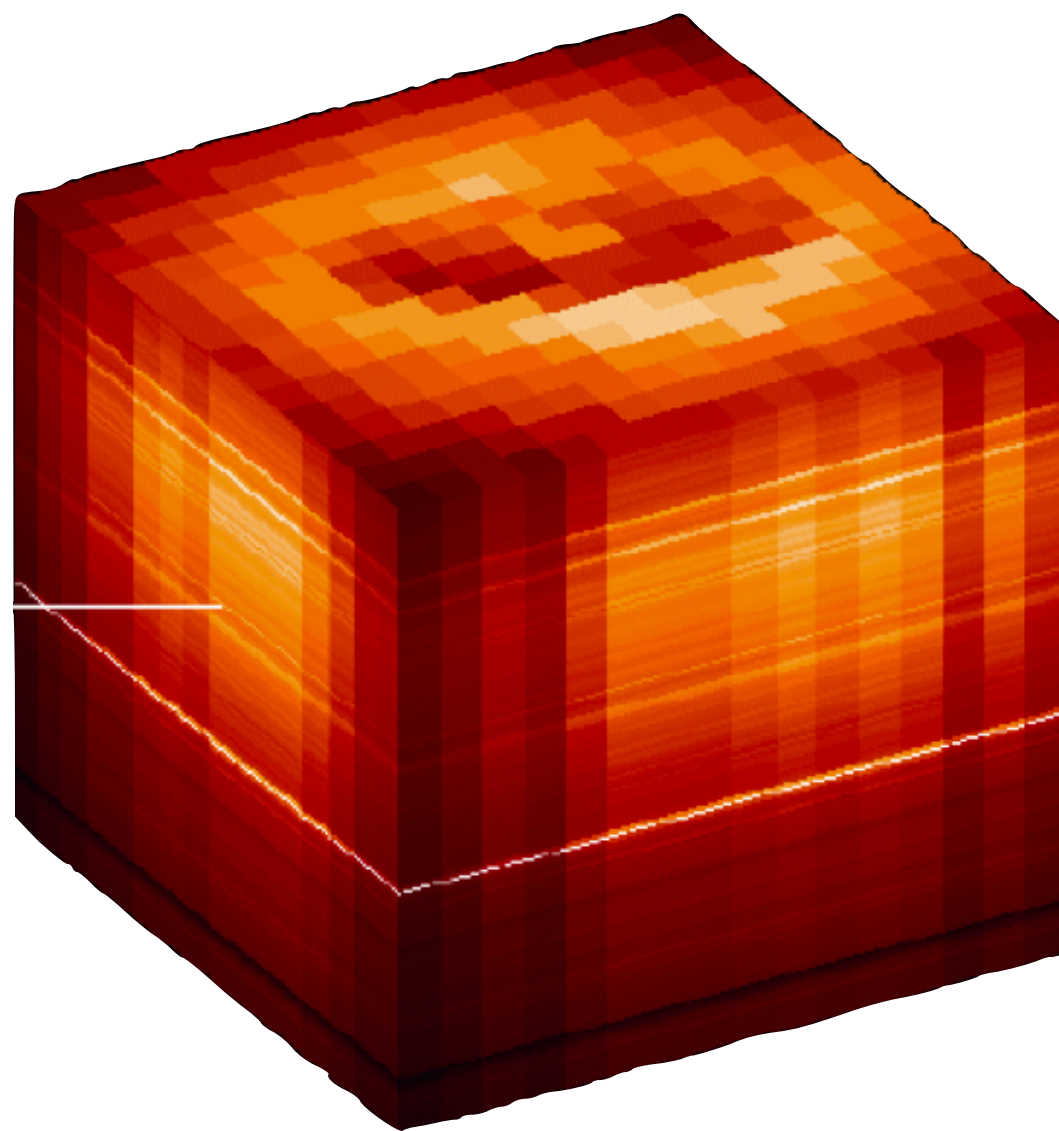
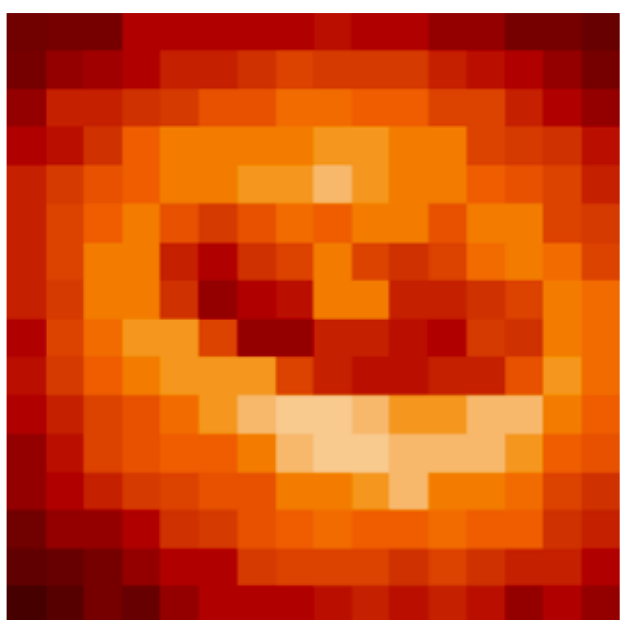


ugrizK

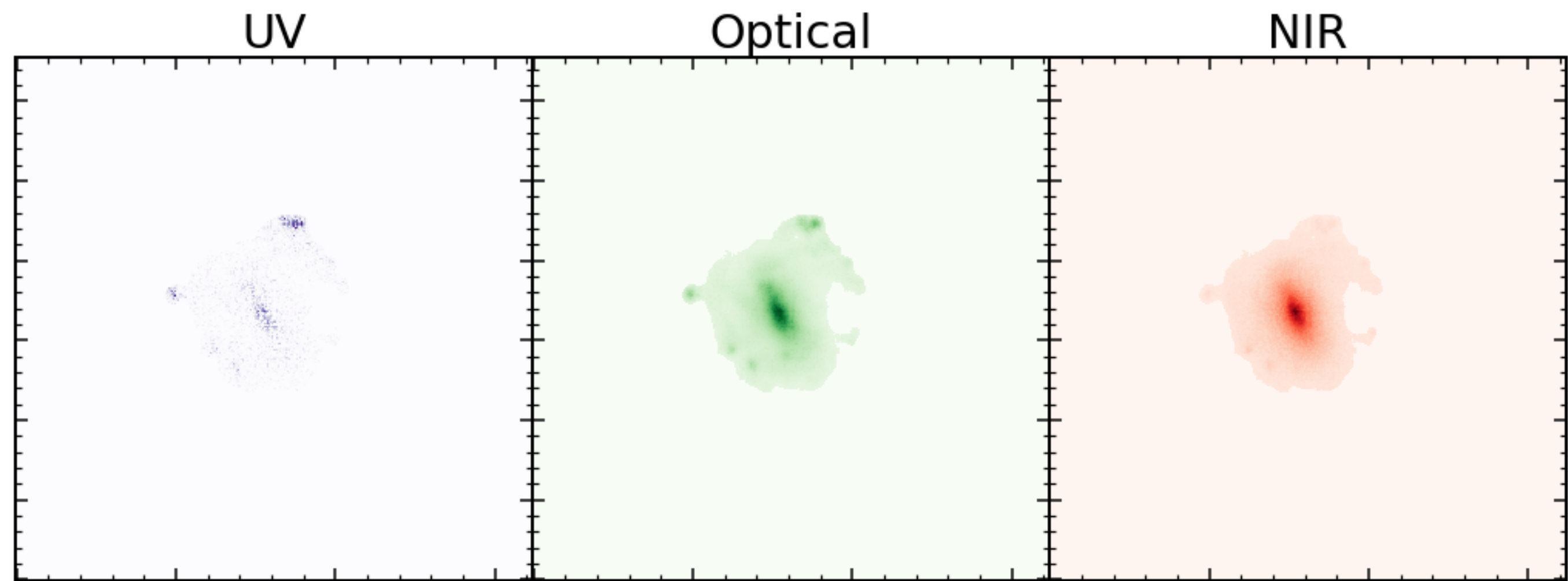




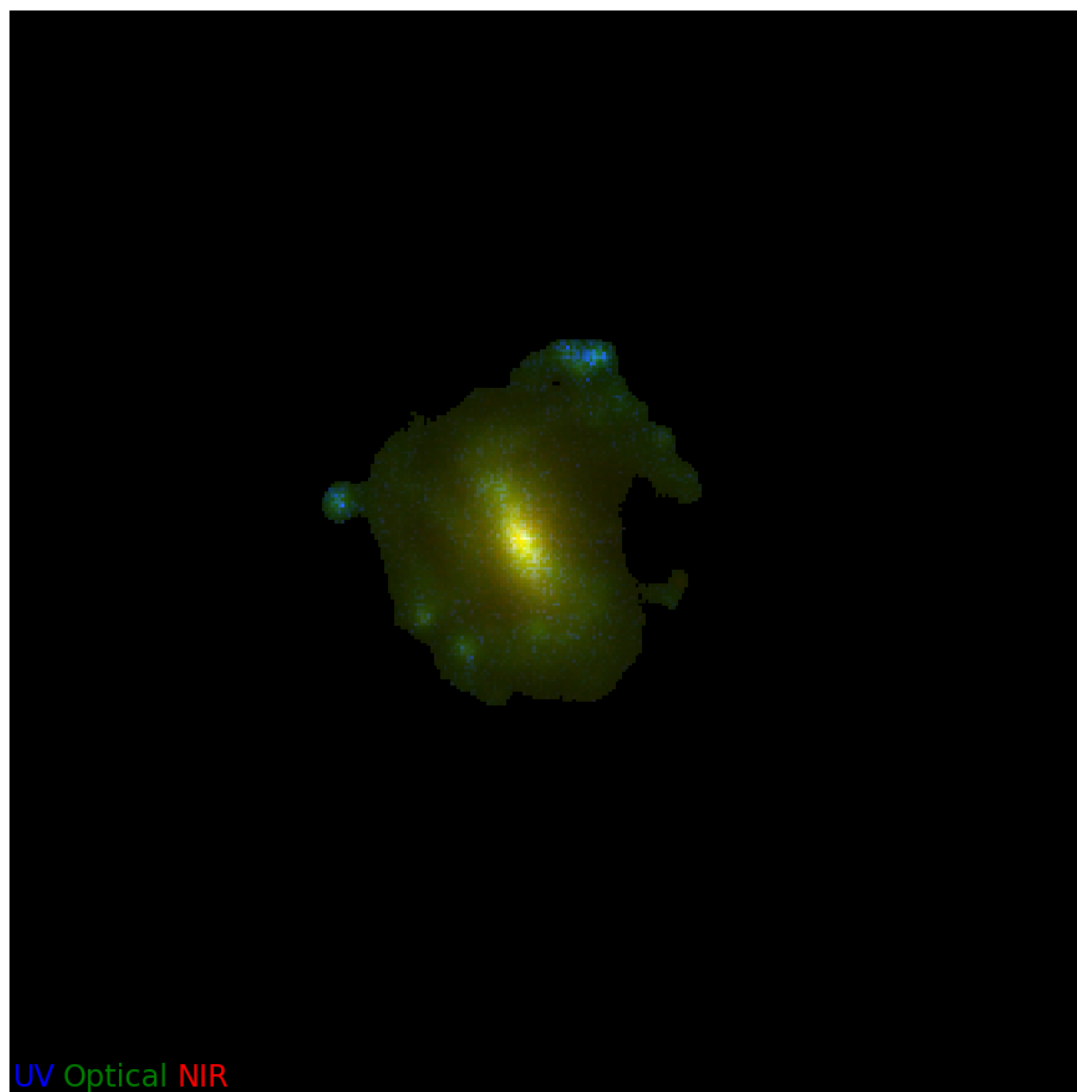
3-D approach



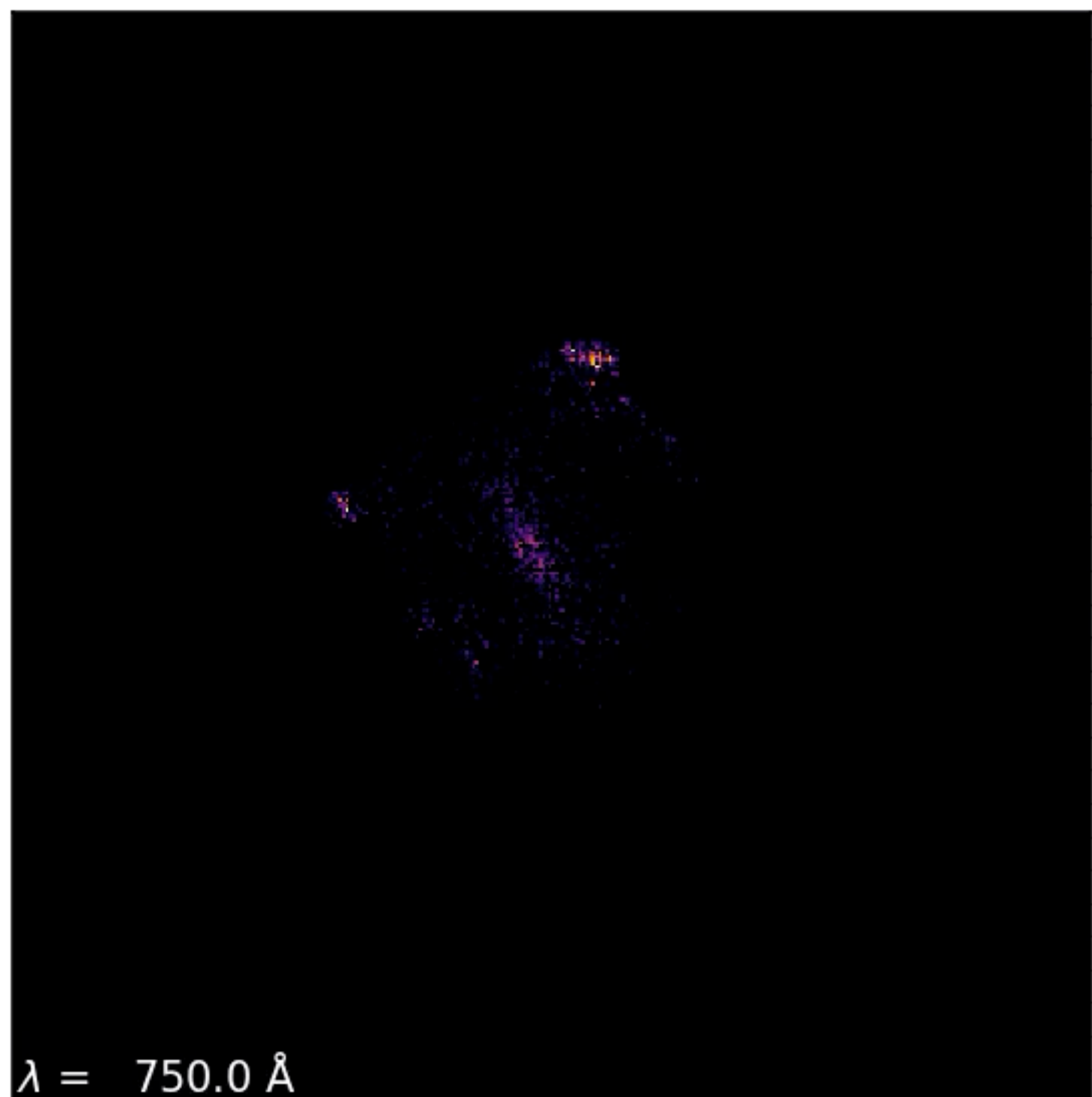
Work in progress



Work in progress

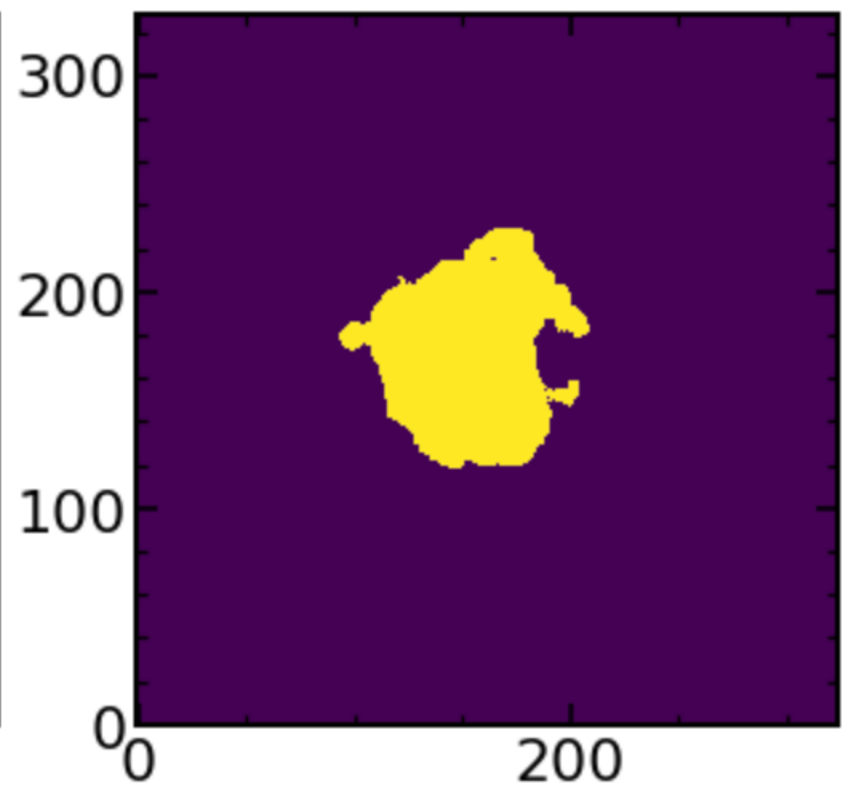
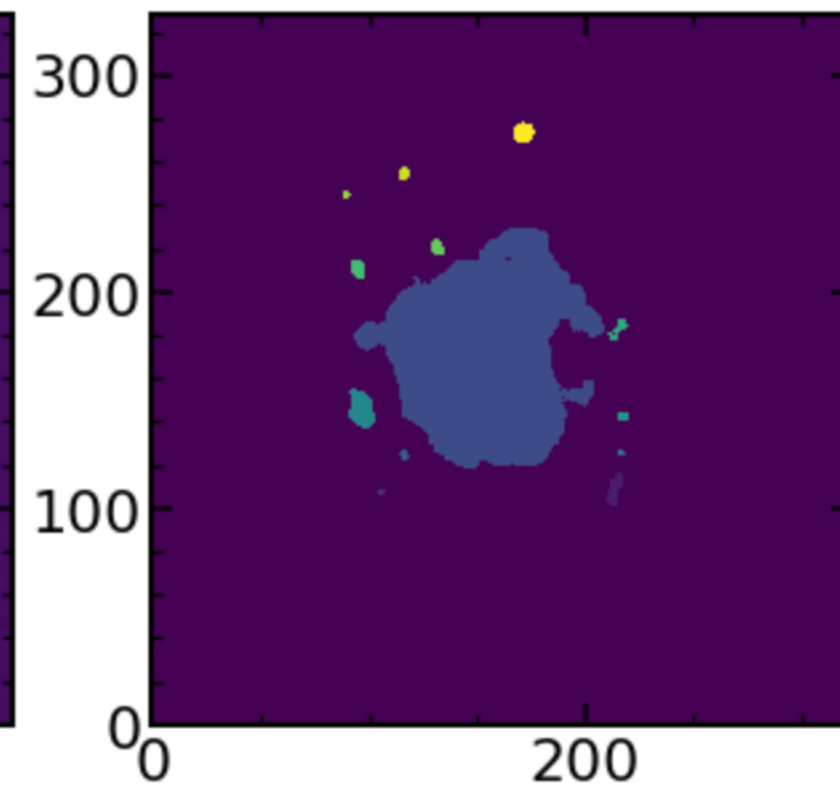
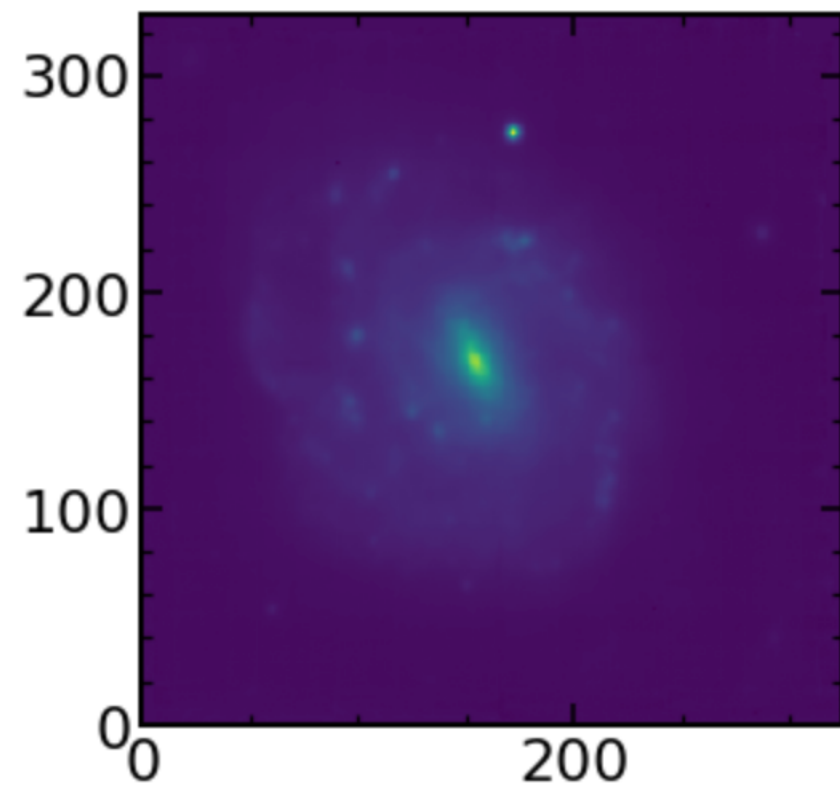


UV Optical NIR



$\lambda = 750.0 \text{ \AA}$

Work in progress



Summary

Things need to improve and feedback is needed!

Summary

- The test was successful on debugging the code for limitations within the magnitude computation as well as the filter design for each individual redshift.
- The test successfully allowed for the identification and removal of a prior that LePhare imposed on the stellar age (limiting to be younger than the age of the Universe at each redshift) that should not be used in our scenario (as we are moving galaxies of fixed age to higher redshifts, creating tension here). This is what was initially causing most of the stellar mass variations found in the initial stages of our testing.
- The test is now showing the potential limitations of using LePhare on a grid with diverse SFHs, using only 4 filters in the optical rest-frame to constrain the stellar mass. This is important to set a hard limit below which we cannot attribute any of the observed changes in stellar mass to artificial redshifting, but instead it is due only to internal limitations of the fitting code.

Future directions

Feedback is crucial before:

- ❖ move towards a more realistic scenario
 - filters
 - observational limitations
- ❖ test different SED fitting tools

Are there other tests that can be done? Are there other features that can be implemented?